RC VIII.
Human exposure to electromagnetic fields

Dragan Poljak
University of Split, FESB, Split

The course covers several aspects of human interaction with non-ionizing electromagnetic fields (EMF) including not only the undesired exposure from artificial sources, but also the biomedical applications of electromagnetic fields. The course deals with basic aspects of electromagnetic fields in environment, coupling mechanisms between humans and electromagnetic fields, established biological effects of electromagnetic fields from static to high-frequency range, international safety guidelines related to limiting human exposure to those fields, including relevant exposure limits and safety guidelines, electromagnetic-thermal dosimetry models and the related analytical/numerical solution methods.

6th European Congress on Radiation Protection
IRPA2022
30 May – 3 June 2022
Budapest, Hungary
Budapest Congress Centre

Human Exposure to electromagnetic Fields

Dragan Poljak
University of Split, Croatia

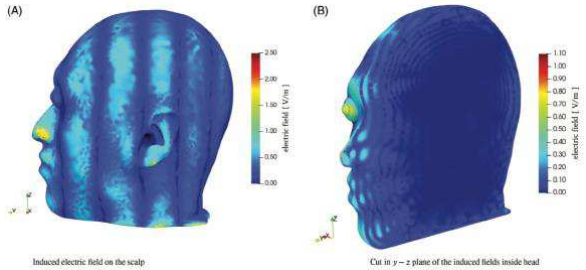

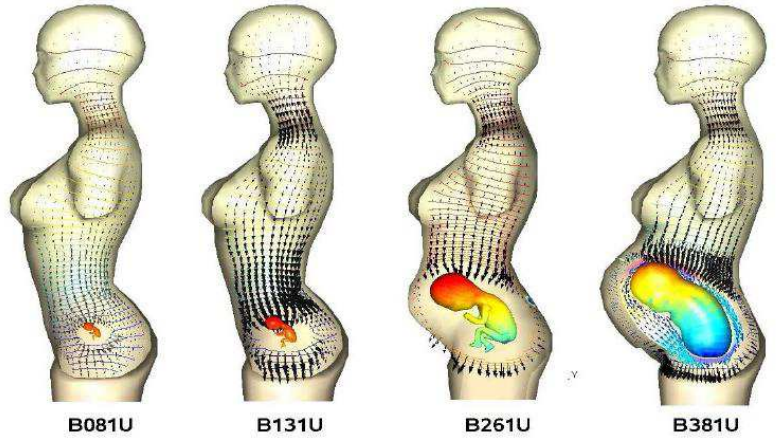

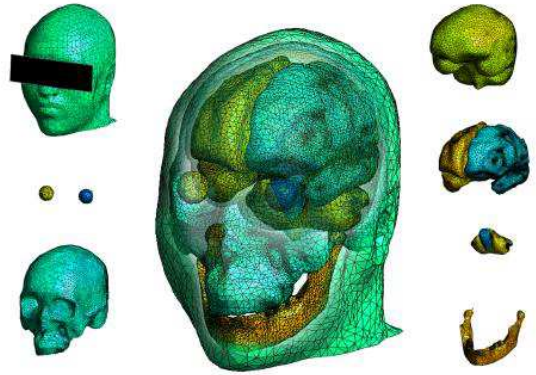

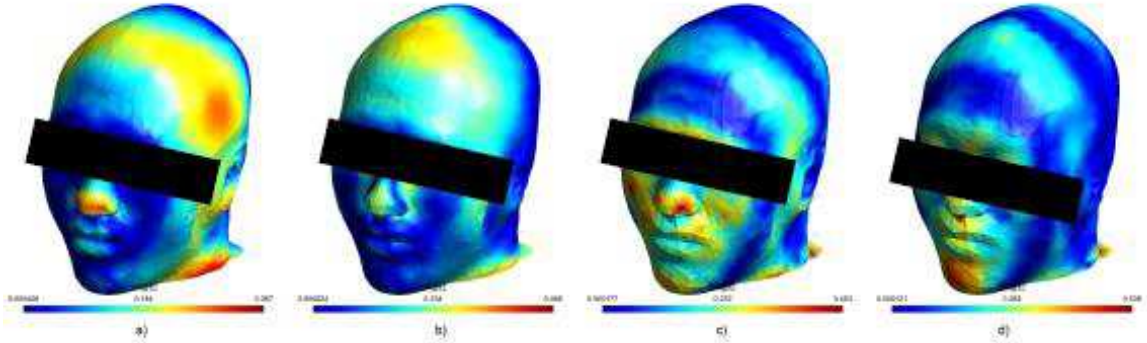

CONTENTS

INTRODUCTION: HUMAN EXPOSURE TO EM FIELDS - GENERAL ASPECTS

INCIDENT FIELD DOSIMETRY PROCEDURES – LF & HF EXPOSURES

INTERNAL FIELD DOSIMETRY PROCEDURES – LF & HF EXPOSURES

BIOMEDICAL APPLICATIONS

CONCLUSIONS

HUMAN EXPOSURE TO ELECTROMAGNTIC FIELDS – GENERAL ASPECTS

- Overview of various aspects of human interaction with electromagnetic fields (EMFs) from artificial sources.
- The coupling mechanisms between humans and static electric, static magnetic, and time-varying fields.
- The summary of the established biological effects of electromagnetic fields related to static, low-frequency and high-frequency range.
- The international safety guidelines and standards related to limiting human exposure to EMF and their legislative status in several world countries, relevant exposure limits and safety measures.

HUMAN EXPOSURE TO ELECTROMAGNTIC FIELDS – GENERAL ASPECTS

Introduction

In the 20th century, occurrence of EM fields in the environment has significantly increased.

There is also a continuing public concern associated with the possible adverse health effects due to human exposure to these fields, particularly exposure to HV power lines and radiation from cellular base stations and mobile phones.

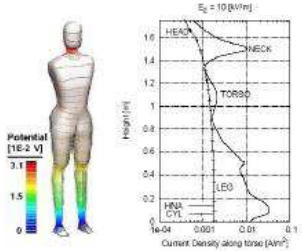

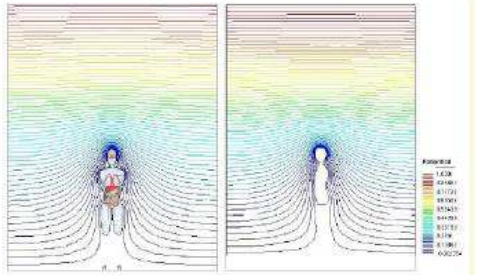

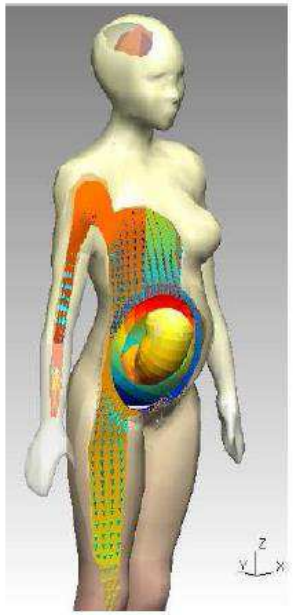

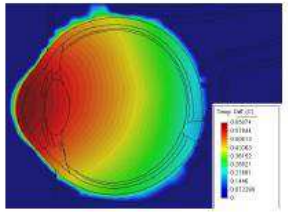

Introduction

LF fields may cause excitation of sensory, nerves and muscles.

Humans are particularly sensitive to HF fields as the body absorbs the radiated energy, and the related heating effects become dominant.

The humans absorb a great deal of energy at certain frequencies, since the body acts as an antenna if the body dimensions parts are comparable to the field wavelength.

When the body size is half the wavelength, the resonant frequency is reached and a large amount of energy is absorbed from the field at frequencies between 30 MHz and 300 MHz.

It is worth noting that children have a higher resonant frequency than adults.

HUMAN EXPOSURE TO ELECTROMAGNTIC FIELDS – GENERAL ASPECTS

COUPLING MECHANISMS AND BIOLOGICAL EFFECTS

- [**Definition**]: *A biological effect is an established effect caused by, or in response to, exposure to a biological, chemical or physical agent, including electromagnetic energy.*
- Occurs when exposure to electromagnetic field cause **any noticeable or detectable physiological response** in a biological body, such as **alterations** of the structure, metabolism, or functions of a whole organism, its organs, tissues, and cells.
- These changes are **not necessarily harmful** to individuals, and may **also** have **beneficial** consequences for a persons health or well-being.

COUPLING MECHANISMS AND BIOLOGICAL EFFECTS

- The human body has a **sophisticated mechanisms to adjust** to various influences it encounters in its surroundings.
- However, it does **not** possess adequate compensation mechanisms **for all** biological effects.
- If some biological effect is **outside the range** for the human body to compensate, it can result in **adverse health effects**.
- Therefore, biological effect in itself **may or may not** result in an adverse health effect, while an adverse health effect results in detectable health impairment of the exposed individual.

HUMAN EXPOSURE TO ELECTROMAGNTIC FIELDS – GENERAL ASPECTS

COUPLING MECHANISMS AND BIOLOGICAL EFFECTS

- The adverse health effects are often the **result of accumulated** biological effects over time and **depend on exposure dose**.
- It is established fact that electromagnetic fields above certain levels can induce biological effects.
- Experiments with healthy subjects suggest that **short-term exposure** at the levels present in the environment **do not result** in any apparent detrimental effects.
- So far, there is **currently no well-established scientific evidence** to conclude that low-level long-term exposures to electromagnetic fields at levels found in the environment are adverse to human health, and also there is no confirmed mechanism that could provide a firm basis to predict these adverse effects.

COUPLING MECHANISM

- There are three established basic coupling mechanisms with time-varying fields:
  - **Coupling to LF Electric Fields**
  - **Coupling to LF Magnetic Fields**
  - **Absorption of Energy from EM Radiation**
- Dependent on the field characteristics such as frequency, spatial uniformity, propagation and polarization direction, etc., but also on the human body characteristics such as size, morphology, and posture.

HUMAN EXPOSURE TO ELECTROMAGNTIC FIELDS – GENERAL ASPECTS

COUPLING MECHANISM

COUPLING TO TIME-VARYING FIELDS

Coupling to LF Electric Fields	Coupling to LF Magnetic Fields
• Human body significantly perturbs the spatial distribution of field. • Electric field induced inside the body will be considerably smaller. • Body is a good conductor at LF, field lines external to the body will be nearly perpendicular to the body surface. • The interaction results in electric current, formation of electrical dipoles, and the reorientation of the already presented electric dipoles in tissue. • External fields induce a shift of surface charges on the body, resulting in induced currents in the body.	• Does not significantly perturb the field. • The internal field is similar to external one. • The interaction results in induced electric fields and currents flowing in circular loops inside the body. • Proportional to the loop radius, tissue conductivity, and the rate of change and magnitude of the magnetic flux density.

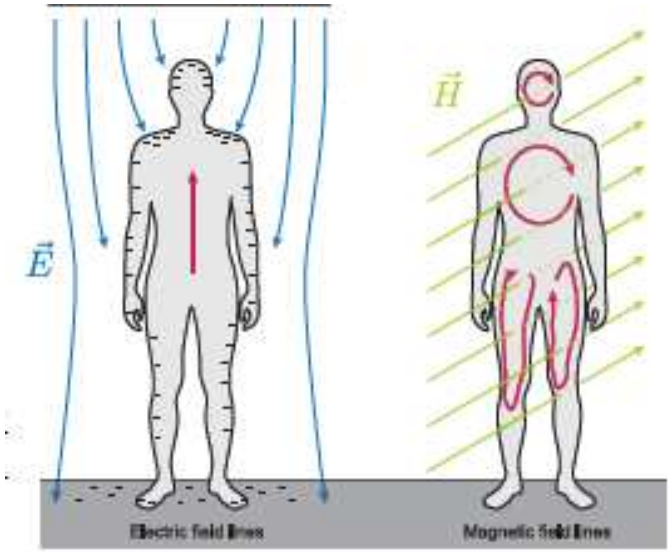

HUMAN EXPOSURE TO ELECTROMAGNTIC FIELDS – GENERAL ASPECTS

COUPLING MECHANISM

COUPLING TO TIME-VARYING FIELDS

Absorption of Energy from Electromagnetic Radiation

- Exposure to high frequency electromagnetic radiation above around 100 kHz can result in the significant absorption of energy.
- The absorbed energy excites the polarized particles in the tissue sufficiently to transform them into thermal energy resulting in consequent temperature rise.
- The electromagnetic energy absorbed by the human body is expressed in terms of specific absorption rate (SAR).
- The amount of energy absorbed will depend on: dimensions, morphology, posture of the exposed body.
- The resonant absorption frequency of not grounded human body is around 70 MHz (for taller individuals, it is lower, while for shorter adults, children, babies, and seated persons, it is around 100 MHz).
- Above 10 GHz, small penetration depth, a more appropriate dosimetric quantity is the incident power density of the field.

HUMAN EXPOSURE TO ELECTROMAGNTIC FIELDS – GENERAL ASPECTS

BIOLOGICAL EFFECTS

- The biological body response due to electromagnetic field (EMF) exposure **depends** primarily **on the frequency** of the applied field.
- All reported biological effects can be classified as either **non-thermal** (<5-10 MHz) **and thermal** (100 kHz-300 GHz).
- In the transition region between 100 kHz and 5–10 MHz, both non-thermal and thermal effects can be produced.

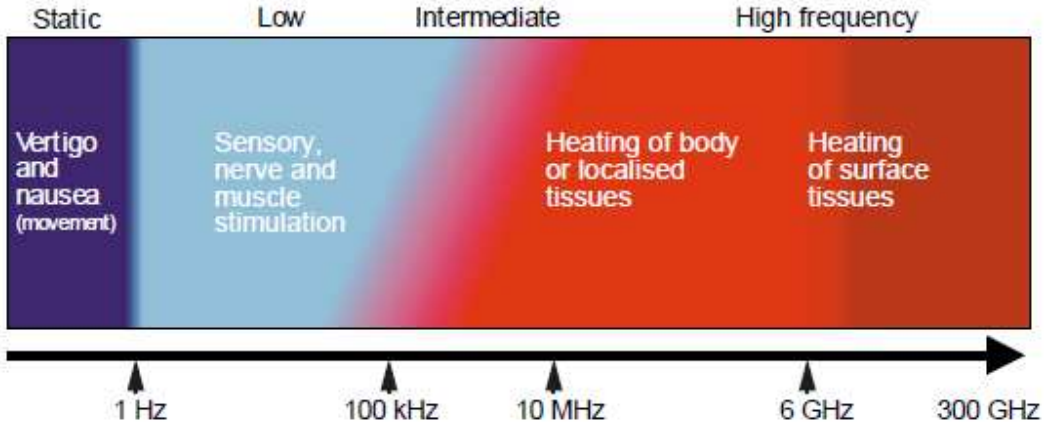

HUMAN EXPOSURE TO ELECTROMAGNTIC FIELDS – GENERAL ASPECTS

SAFETY GUIDELINES AND EXPOSURE LIMITS

- The **ultimate goal** of a health-based EMF standards - the **protection of humans** exposed to electromagnetic fields (EMF).
- Safety guidelines for the exposure to EMF rely upon a **well-established effects** based on the experimental data from biological systems, on epidemiological and human studies, as well as on understanding of the various interaction mechanisms.
- The **safety or the exposure limit** is considered as that threshold below which exposure can be considered safe according to the available scientific knowledge. Nevertheless, the **safety limit does not represent an exact boundary** between safety and hazard.
- For efficient protection against the harmful effects, the regulatory agencies, in addition to setting safety limits, **need to incorporate a safety margin** to allow for the uncertainty.

SAFETY GUIDELINES AND EXPOSURE LIMITS

- **EMF STANDARDS**: The standards related to personal protection generally referring to maximum levels to which complete or partial body exposure is permitted from any EMF emitting devices represent the exposure standards.
- Developed by the International Commission on Non-Ionizing Radiation Protection (**ICNIRP**), the Institute of Electrical and Electronic Engineers International Committee on Electromagnetic Safety (**IEEE ICES**) and various national authorities.
- The exposure standards typically include some safety factors and provide the basic guide for limiting personal exposure.
- Currently, **no internationally** mandated standards for EMF, each country sets its own national standard - in most cases based on **ICNIRP guidelines**.

HUMAN EXPOSURE TO ELECTROMAGNTIC FIELDS – GENERAL ASPECTS

ICNIRP GUIDELINES

Table: Basic restrictions for human exposure to high-frequency EMF according to the 1998 ICNIRP Guidelines.

Exposure characteristic	Frequency range	Whole body average SAR [W/kg]	Localized SAR (head and trunk) [W/kg]	Localized SAR (limbs) [W/kg]	Power density [W/m²]
Occupational exposure	10 MHz - 10 GHz	0.4	10	20	-
	10-300 GHz	-	-	-	50
General public exposure	10 MHz - 10 GHz	0.08	2	4	-
	10-300 GHz	-	-	-	10

Notes:
1. All SAR values are to be averaged over any 6-min period.
2. Localized SAR averaging mass is any 10 g of contiguous tissue; the maximum SAR so obtained should be the value used for the estimation of exposure.
3. For pulses of duration tp the equivalent frequency to apply in the basic restrictions should be calculated as f = 1/(2tp). Additionally, for pulsed exposures in the frequency range 0.3 to 10 GHz and for localized exposure of the head, in order to limit or avoid auditory effects caused by thermoelastic expansion, an additional basic restriction is recommended. This is that the SA should not exceed 10 mJ/kg for workers and 2 mJ/kg for the general public, averaged over 10 g tissue.
4. Power densities are to be averaged over any 20 cm2 of exposed area and any 68/ f 1.05 -min period (where f is in GHz) to compensate for progressively shorter penetration depth as the frequency increases.
5. Spatial maximum power densities, averaged over 1 cm2, should not exceed 20 times the values above.

ICNIRP GUIDELINES

- The fundamental quest in protection of humans exposed to electromagnetic radiation is to satisfy the given basic restrictions.
- When it is not practical to calculate or measure quantities associated with the basic restrictions (usually the case in many realistic exposure scenarios) - **the comparison with reference levels** can be used to estimate if the basic restrictions will be exceeded.
- These reference levels correspond to basic restrictions **under the worst case scenario** for the following quantities: **E** [V/m], **H** [A/m], **B** [T], **S** [W/m²], $\mathbf{I_c}$ [mA], and, for pulsed fields, specific energy absorption **SA** [J/kg].
- If the reference levels are exceeded it does not necessarily mean that the basic restrictions are exceeded.
- However, **when the reference levels are exceeded it is necessary to test** compliance with the relevant basic restrictions and to determine if the additional protective measures are necessary.

HUMAN EXPOSURE TO ELECTROMAGNTIC FIELDS – GENERAL ASPECTS

ICNIRP GUIDELINES

Table: Reference levels for HF fields (in rms values) according to the 1998 ICNIRP Guidelines.

Frequency range	E [V/m]	H [A/m]	B [uT]	S_{eq} [W/m²]
Occupational exposure				
10 MHz - 400 MHz	61	0.16	0.2	10
400 MHz - 2 GHz	3 $f^{1/2}$	0.008 $f^{1/2}$	0.01 $f^{1/2}$	f/40
2 GHz - 300 GHz	137	0.36	0.45	50
General public exposure				
10 MHz - 400 MHz	28	0.073	0.092	2
400 MHz - 2 GHz	1.375 $f^{1/2}$	0.0037 $f^{1/2}$	0.0046 $f^{1/2}$	f/200
2 GHz - 300 GHz	61	0.16	0.20	10

Notes:
1. f as indicated in the frequency range column.
2. Provided that basic restrictions are met and adverse indirect effects can be excluded, field strength values can be exceeded.
3. For frequencies between 100 kHz and 10 GHz, S_{eq}, E^2, H^2, and B^2 are to be averaged over any 6-min period. 4. For frequencies exceeding 10 MHz it is suggested that the peak equivalent plane wave power density, as averaged over the pulse width, does not exceed 1,000 times the S_{eq} restrictions, or that the field strength does not exceed 32 times the field strength exposure levels given in the table.
5. For frequencies exceeding 10 GHz, S_{eq}, E^2, H^2, and B^2 are to be averaged over any $68/f^{1.05}$-min period (f in GHz).

HUMAN EXPOSURE TO ELECTROMAGNTIC FIELDS – GENERAL ASPECTS

2019/2020 STANDARDS/GUIDELINES

- Previous:

C95.6- 2002	IEEE Std 'Safety Levels, exposure to EMF,	0 – 3 kHz'
C95.1-2005	IEEE 'Safety Levels, exposure to RF-EMF,	3 kHz – 300 GHz'
C95.1-2019	IEEE 'Safety Levels, exposure to EMF,	0 Hz – 300 GHz'
ICNIRP 1998	Guidelines for limiting exposure to EMF	up to 300 GHZ
ICNIRP 2010	Guidelines for limiting exposure to EMF	1 Hz –100 kHz

- New: C95.1-2019 Std **revises & combines** Std.s C95.1-2005 & C95.6-2002 into a single standard; **changes on exposure above 6 GHz/10 GHz**
- **Purpose**: *to provide science-based exposure criteria to protect against established adverse health effects in humans associated with exposure to EMF; induced and contact currents; and contact voltages, over the* ***frequency range of 0 Hz to 300 GHz***

2019/2020 STANDARDS/GUIDELINES

- For exposures **above 6 GHz, the energy is absorbed close to the body surface**
- The energy penetration depth into the skin at 6 GHz is ~4 mm, and the penetration decreases with increasing frequency. At 300 GHz, the energy penetration depth is ~0.12 mm
- Due to different biological effects of exposure to particular frequencies, the standard addresses **three bands**: 0 Hz-100 kHz, 100 kHz-6 GHz, and 6-300 GHz
- IEEE and ICNIRP agree that **thermal effects continue to be the appropriate basis for protection** against RF exposure at frequencies above 100 kHz

HUMAN EXPOSURE TO ELECTROMAGNTIC FIELDS – GENERAL ASPECTS

2019/2020 STANDARDS/GUIDELINES

- Updated IEEE C95.1-2019 reference levels: **Safety factors applying 100 kHz- 6 GHz Thermal Effects**

1. Whole body averaged (WBA)

Behavioral effects in animals over many frequencies, threshold at 4 W/kg

10x - 0.4 W/kg for upper tier (controlled environment)

50x - 0.08 W/kg for lower tier (general public)

2. Localized exposure (averaged in 10 g)

Cataract observed in rabbits, threshold at 100 W/kg

10x - 10 W/kg for upper tier

50x - 2 W/kg for lower tier

3. SAR is averaged over 30 min for WBA exposure and 6 min for local exposure

4. Epithelial power density through body surface is averaged over 6 min

2019/2020 STANDARDS/GUIDELINES

Table: IEEE C95.1-2019 Table 5—DRLs (**100 kHz to 6 GHz**) Thermal Effects

Conditions	Persons in unrestricted environments SAR (W/kg)	Persons permitted in restricted environments SAR (W/kg)
Whole-body exposure	0.08	0.4
Local exposure (head and torso)	2	10
Local exposure (limbs and pinnae)	4	20

DRL: Dosimetric Reference Limits

Table: IEEE C95.1-2019 Table 6—DRLs (**6 GHz to 300 GHz**) Thermal Effects

Conditions	Epithelial power density (W/m2)	
	Persons in unrestricted environments SAR (W/kg)	Persons permitted in restricted environments SAR (W/kg)
Body surface	20	100

DRL: Dosimetric Reference Limits

HUMAN EXPOSURE TO ELECTROMAGNTIC FIELDS – GENERAL ASPECTS

2019/2020 STANDARDS/GUIDELINES

- **Main differences** in IEEE C95.1-2019:

1. Upper RF boundary for whole body average (WBA) SAR has been changed from **3 GHz to 6 GHz** because of improved measurement capabilities and **to harmonize with** the revised **ICNIRP** guidelines

2. Term 'extremities' is changed to 'limbs' involving the whole arms and legs, instead of portions distal to the elbows and knees. This change is **to harmonize** with C95.6-2002 and the **ICNIRP** guidelines

3. Local exposure ERL is now **frequency dependent**, instead of being a fixed factor of 20 times the whole-body ERL, regardless of frequency

4. **Averaging time** is 30 minutes for **whole body** RF exposure and 6 minutes for **local** exposure

2019/2020 STANDARDS/GUIDELINES

- **Main differences** in IEEE C95.1-2019 (cont.):

1. Local exposure limits **between 6 GHz and 300 GHz** have changed: the dosimetric reference limit (DRL) is the **epithelial power density** inside the body surface, and exposure reference levels (ERLs) is the **incident power density** outside the body. For smaller areas, relaxed limits are allowed

2. Averaging power density area is defined as a **4cm2 square**

3. Small exposed areas **above 30 GHz**: the epithelial power density is allowed to exceed the DRL or ERL by a factor of 2, with an averaging area of **1cm2**

4. Peak DRL and ERL limits for local exposures to pulsed RF fields are defined, and **new fluence limits for single RF-modulated pulses above 30 GHz** are introduced. The averaging area for single pulse fluence is 1 cm2 square

HUMAN EXPOSURE TO ELECTROMAGNTIC FIELDS – GENERAL ASPECTS

About dosimetry…

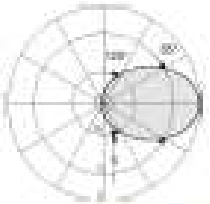
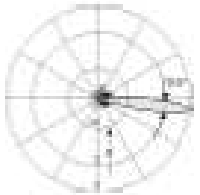

- Dosimetry methods for human exposure to EM fields from ELF range to HF radiation involve the assessment of:
  - ✓ the external fields generated by EMI source at a given frequency (**incident field dosimetry**),
  - ✓ the fields induced inside the body (**internal field dosimetry**),
  - ✓ the related temperature rise due to the exposure to EM fields (**thermal dosimetry**)
- Several methods are used in theoretical and experimental dosimetry.
- EMI sources: power lines, transformer substations, PLC systems, RFID antennas, GSM base station antenna systems, etc.
- The results obtained from calculation and/or measurement procedures are to be compared to the exposure limits proposed by safety guidelines.

HUMAN EXPOSURE TO ELECTROMAGNTIC FIELDS – GENERAL ASPECTS

About dosimetry...

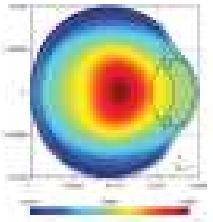

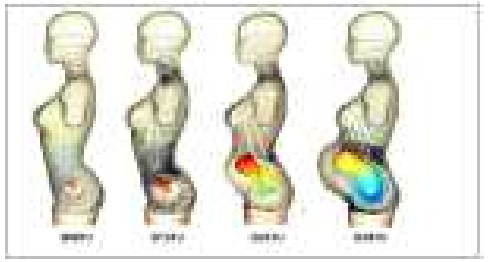

- Sophisticated numerical modeling is required to predict distribution of internal fields.
- Today realistic computational models comprising of cubical cells are mostly related to application of Finite Difference Time Domain (FDTD) methods.
- In certain studies, the Finite Element Method (FEM) is considered to be a more accurate method than the FDTD, and a more sophisticated tool for the treatment of irregular or curved shape domains.
- Some studies have demonstrated that the use of Boundary Element Method (BEM), fast multipole techniques and wavelet techniques to reduce the computational cost.

INCIDENT FIELD DOSIMETRY PROCEDURES – LF &HF EXPOSURES

- Dosimetry techniques to determine external electric and magnetic fields due to low frequency (LF) and high frequency (HF) sources
- Theoretical and experimental procedures described
- LF electromagnetic interference (EMI) sources related to power line communication (PLC) systems, RFID loop antennas and radio base stations
- Examples given for: power lines, transformer substations, PLC systems and base station antenna systems

Incident Field Dosimetry Procedures – LF Exposures

Assessment of E and H field from overhead power lines

- The amplitudes of the three currents:

$$|I_1(x)| = |I_2(x)| = |I_3(x)|$$

- Phase differences:

$$I_2(x) = I_1(x)\, e^{j2\pi/3}, \quad I_3(x) = I_1(x)\, e^{-j2\pi/3}$$

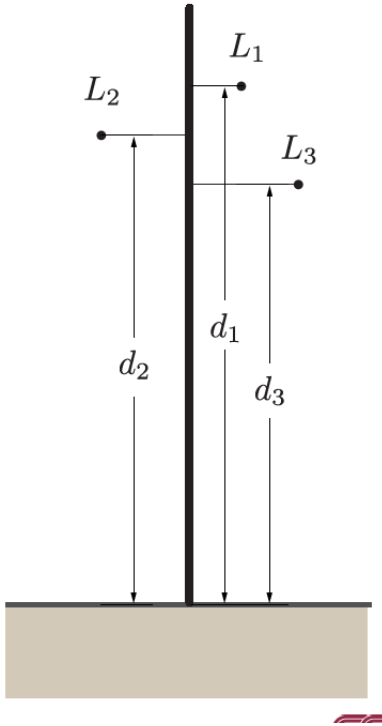

FIG: Configuration of high voltage, three-phase, three-wire power line.

Assessment of E and H field from overhead power lines

The electric field

- Analytical approach, based on thin wire antenna theory is used.
- The *E* field is expressed in terms of Hertz vector potential:

$$\vec{E} = \nabla\nabla\vec{\Pi} + k^2\vec{\Pi}$$

$$\Pi_{0x} = \frac{e^{-jk_0r_1}}{r_1} - \frac{e^{-jk_0r_2}}{r_2} + 2\int_0^\infty \frac{J_0(\lambda\rho)e^{-\gamma_0(z+h)}}{\gamma_0+\gamma_1}\lambda\, d\lambda \qquad \Pi_{0z} = \frac{2}{k_0^2}\cos\varphi\frac{\partial}{\partial\rho}\left\{\int_0^\infty J_0(\lambda\rho)e^{-\gamma_0(z+h)}\frac{\gamma_0-\gamma_1}{n^2\gamma_0+\gamma_1}\lambda\, d\lambda\right\}$$

$$[E_{0x}(0,y,z)]_t \sim \frac{j\omega\mu_0 I}{\pi\beta_1^2}(\beta_0 d)\left\{\frac{(z+d_1)^2-(y-L_1)^2}{\left[(z+d_1)^2+(y-L_1)^2\right]^2} + e^{j2\pi/3}\left[\frac{(z+d_2)^2-(y+L_2)^2}{\left[(z+d_2)^2+(y+L_2)^2\right]^2}\right] + e^{-j2\pi/3}\left[\frac{(z+d_3)^2-(y-L_3)^2}{\left[(z+d_3)^2+(y-L_3)^2\right]^2}\right]\right\}$$

$$[E_{0y}(0,y,z)]_t \sim \frac{\omega\mu_0 I}{2\pi\beta_0}\left\{(y-L_1)\left[\frac{1}{(z-d_1)^2+(y-L_1)^2}-\frac{1-2\beta_0^2/\beta_1^2}{(z+d_1)^2+(y-L_1)^2}\right] + e^{j2\pi/3}(y+L_2)\left[\frac{1}{(z-d_2)^2+(y+L_2)^2}-\frac{1-2\beta_0^2/\beta_1^2}{(z+d_2)^2+(y+L_2)^2}\right] + e^{-j2\pi/3}(y-L_3)\left[\frac{1}{(z-d_3)^2+(y-L_3)^2}-\frac{1-2\beta_0^2/\beta_1^2}{(z+d_3)^2+(y-L_3)^2}\right]\right\}$$

$$[E_{0z}(0,y,z)]_t \sim \frac{\omega\mu_0 I}{2\pi\beta_0}\left\{\frac{z-d_1}{(z-d_1)^2+(y-L_1)^2}-\frac{z+d_1}{(z+d_1)^2+(y-L_1)^2} + e^{j2\pi/3}\left[\frac{z-d_2}{(z-d_2)^2+(y+L_2)^2}-\frac{z+d_2}{(z+d_2)^2+(y+L_2)^2}\right] + e^{-j2\pi/3}\left[\frac{z-d_3}{(z-d_3)^2+(y-L_3)^2}-\frac{z+d_3}{(z+d_3)^2+(y-L_3)^2}\right]\right\}$$

Incident Field Dosimetry Procedures – LF Exposures

Assessment of E and H field from overhead power lines

The magnetic field

- The magnetic field components are given by: $\nabla \times \vec{E} = -\frac{\partial \vec{B}}{\partial t}$

i.e. it follows:

$$[B_{0x}(0,y,z)]_t = \frac{2j\mu_0 I k_0}{\pi k_1^2}\left\{\frac{(y-L_1)(z+d_1)}{\left[(z+d_1)^2+(y-L_1)^2\right]^2}+e^{j2\pi/3}\left[\frac{(y+L_2)(z+d_2)}{\left[(z+d_2)^2+(y+L_2)^2\right]^2}\right]+ +e^{-j2\pi/3}\left[\frac{(y-L_3)(z+d_3)}{\left[(z+d_3)^2+(y-L_3)^2\right]^2}\right]\right\}$$

$$[B_{0y}(0,y,z)]_t = \frac{\mu_0 I}{2\pi}\left\{\frac{4(z+d_1)(k_0 d)}{k_1^2\left[(z+d_1)^2+(y-L_1)^2\right]^2}\left[1-\frac{2\left[(z+d_1)^2-(y-L_1)^2\right]}{(z+d_1)^2+(y-L_1)^2}\right]- -\frac{(z-d_1)}{(z-d_1)^2+(y-L_1)^2}+\frac{(z+d_1)}{(z+d_1)^2+(y-L_1)^2}+ +e^{j2\pi/3}\left\{\frac{4(z+d_2)(k_0 d)}{k_1^2\left[(z+d_2)^2+(y+L_2)^2\right]^2}\times\left[1-\frac{2\left[(z+d_2)^2-(y-L_2)^2\right]}{(z+d_2)^2+(y-L_2)^2}\right]- -\frac{(z-d_2)}{(z-d_2)^2+(y-L_2)^2}+\frac{(z+d_2)}{(z+d_2)^2+(y-L_2)^2}+ +e^{-j2\pi/3}\left\{\frac{4(z+d_3)(k_0 d)}{k_1^2\left[(z+d_3)^2+(y+L_3)^2\right]^2}\times\left[1-\frac{2\left[(z+d_3)^2-(y-L_3)^2\right]}{(z+d_3)^2+(y-L_3)^2}\right]- -\frac{(z-d_3)}{(z-d_3)^2+(y-L_3)^2}+\frac{(z+d_3)}{(z+d_3)^2+(y-L_3)^2}\right\}$$

$$[B_{0z}(0,y,z)]_t = \frac{\mu_0 I}{2\pi}\left\{\frac{y-L_1}{(z-d_1)^2+(y-L_1)^2}-\frac{(y-L_1)(1-2k_0^2/k_1^2)}{(z+d_1)^2+(y-L_1)^2}+ +\frac{4(y-L_1)(k_0 d)}{k_1^2\left[(z+d_1)^2+(y-L_1)^2\right]}\left[1+\frac{2\left[(z+d_1)^2-(y-L_1)^2\right]}{(z+d_1)^2+(y-L_1)^2}\right]+ +e^{j2\pi/3}\left\{\frac{y+L_2}{(z-d_2)^2+(y+L_2)^2}-\frac{(y+L_2)(1-2k_0^2/k_1^2)}{(z+d_2)^2+(y+L_2)^2}+ +\frac{4(y+L_2)(k_0 d)}{k_1^2\left[(z+d_2)^2+(y+L_2)^2\right]^2}\times\left[1+\frac{2\left[(z+d_2)^2-(y+L_2)^2\right]}{(z+d_2)^2+(y+L_2)^2}\right]\right\}+ +e^{-j2\pi/3}\left\{\frac{y-L_3}{(z-d_3)^2+(y-L_3)^2}-\frac{(y-L_3)(1-2k_0^2/k_1^2)}{(z+d_3)^2+(y-L_3)^2}+ +\frac{4(y-L_3)(k_0 d)}{k_1^2\left[(z+d_3)^2+(y-L_3)^2\right]^2}\left[1+\frac{2\left[(z+d_3)^2-(y-L_3)^2\right]}{(z+d_3)^2+(y-L_3)^2}\right]\right\}\right\}$$

Computational results for *E*-field

- An illustrative computational example is related to the 3-phase power line with: mean distance between two towers ls=300m, line current I=90 A, U=110 kV.

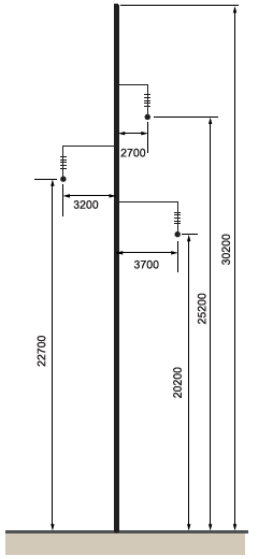

FIG: Three-wire, three-phase 110 kV power line.

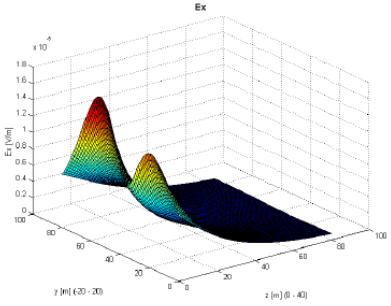

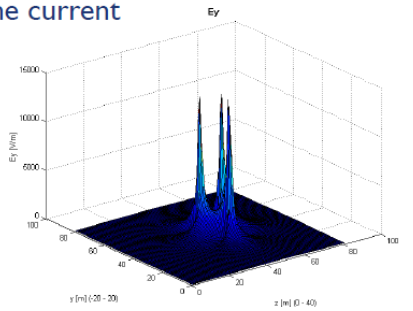

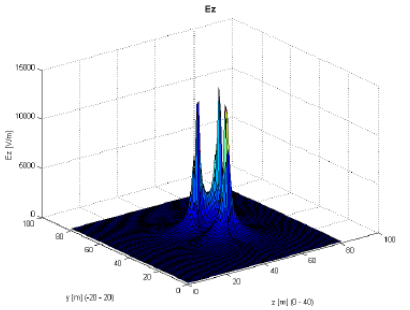

FIG: Spatial distribution of the electric field components in x = 0 plane, where y coordinate takes values from -20 m to 20 m

Incident Field Dosimetry Procedures – LF Exposures

Computational results for *E*-field

Table: Comparison to Safety Standards	
Safety standards	E [V/m]
ICNIRP guidelines for occupational exposure	10000
ICNIRP guidelines for general public exposure	5000
Croatian law for professional exposure areas	5000
Croatian law for increased sensitivity areas	2000
E_x component	$<2x10^{-5}$
E_y component	~3000
E_z component	3570

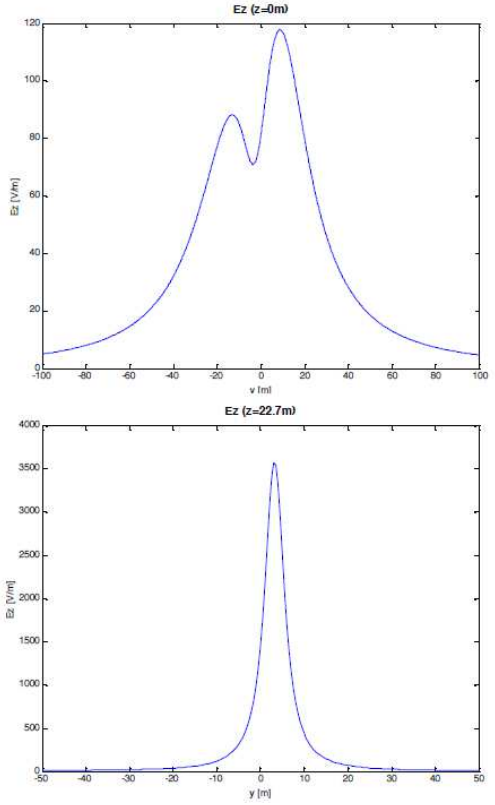

FIG: E_z component of the electric field on the ground level (top) and on the level of the middle conductor (bottom).

Analytical results for *H*-field

- Measured and analytically calculated values of magnetic flux density *B* from the three-phase power line 11m above the ground

Table: Measured and calculated values at I=90 A

Distance from y axis [m]	Measured		Analytical	
	B[uT] z=1m	B[uT] z=2m	B[uT] z=1m	B[uT] z=2m
-30	0.08	0.08	0.129	0.132
-20	0.15	0.15	0.243	0.254
-15	0.22	0.23	0.353	0.377
-10	0.33	0.37	0.522	0.575
-5	0.54	0.61	0.736	0.842
0	0.76	0.95	0.890	1.046
5	0.77	0.94	0.832	0.973
10	0.56	0.60	0.608	0.680
15	0.35	0.37	0.405	0.435
20	0.22	0.23	0.273	0.287
30	0.10	0.11	0.140	0.144

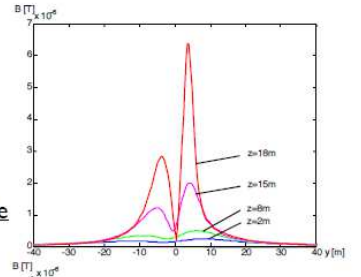

FIG: B_y component of the magnetic flux density.

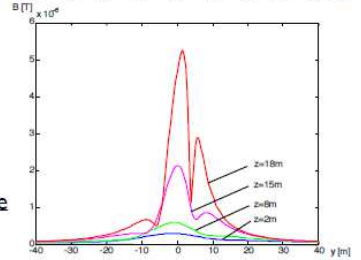

FIG: B_z component of the magnetic flux density.

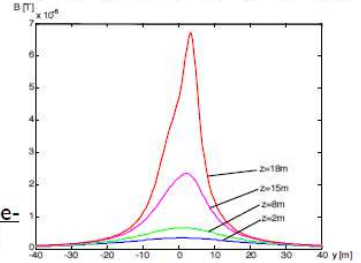

FIG: Total magnetic flux density B due to the three-wire, three-phase 110 kV power line.

Incident Field Dosimetry Procedures – LF Exposures

Analytical results for *H*-field

- Magnetic field measurement:

Table: Comparison of the results with safety standards

Method or Standard	B [uT]		H [A/m]	
	z=2m	z=24m	z=2m	z=24m
Analytical, h=20.2m	0.330	10.340	0.263	8.228
Numerical, h=20.2m	0.327	10.342	0.260	8.230
Analytical, h=11m	1.046	-	0.832	-
Experimental, h=7m	1.84	-	1.464	-
Experimental, h=11m	0.95	-	0.756	-
ICNIRP	100		80	
Croatian EMF protection regulation	40		32	

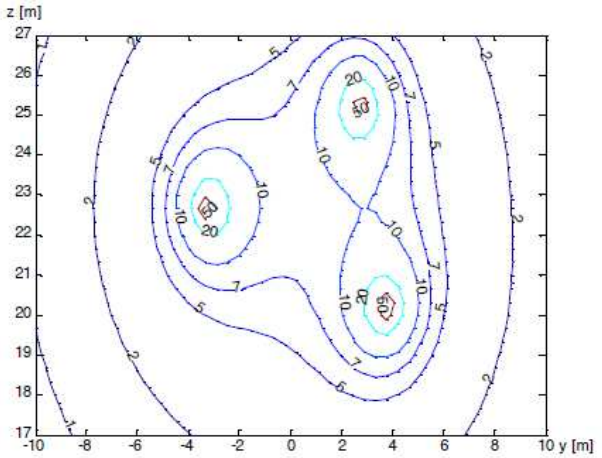

FIG: Magnetic field H [A/m] in the vicinity of a three-phase power line.

Incident Field Dosimetry Procedures – LF Exposures

Assessment of E and H field from power substation

The electric field

- When the potential along the wire is known one deals with the Scalar Potential Integral Equation (SPIE):

$$\varphi(x,z) = \frac{1}{4\pi\varepsilon}\int_{-L}^{+L}\frac{\rho_l(x')\,dx'}{R}$$

- Substation conductors are divided into a number of segments. SPIE transforms into a system of equations for unknown charges along the each segment:

$$\begin{bmatrix} P_{11} & P_{12} & \cdots & P_{1n} \\ P_{21} & P_{22} & \cdots & P_{2n} \\ \cdot & \cdot & & \\ \cdot & \cdot & & \\ \cdot & \cdot & & \\ P_{n1} & P_{n2} & \cdots & P_{nn} \end{bmatrix} \cdot \begin{bmatrix} q_1 \\ q_2 \\ \cdot \\ \cdot \\ \cdot \\ q_n \end{bmatrix} = \begin{bmatrix} \varphi_1 \\ \varphi_2 \\ \cdot \\ \cdot \\ \cdot \\ \varphi_n \end{bmatrix}$$

- $\varphi_1,\ldots,\varphi_n$ - the boundary element potentials,
- $q_1,\ldots,q_n$ - the boundary element charges,
- $P_{11}, P_{12}\ldots, P_{nn}$ - the Maxwell coefficients

- Field components at an point (x,y,z), generated by a boundary element, can be computed, as follows:

$$W^2 = y^2 + z^2$$

$$E_{xi} = -\frac{\partial\varphi}{\partial x} = \frac{q_i}{4\pi\varepsilon_0 L_i}\left[\frac{1}{\sqrt{(L_i-x)^2+W^2}} - \frac{1}{\sqrt{x^2+W^2}}\right]$$

$$E_{yi} = -\frac{\partial\varphi}{\partial y} = \frac{q_i}{4\pi\varepsilon_0 L_i}\frac{y}{W^2}\left[\frac{L_i-x}{\sqrt{(L_i-x)^2+W^2}} + \frac{x}{\sqrt{x^2+W^2}}\right]$$

$$E_{zi} = -\frac{\partial\varphi}{\partial z} = \frac{q_i}{4\pi\varepsilon_0 L_i}\frac{z}{W^2}\left[\frac{L_i-x}{\sqrt{(L_i-x)^2+W^2}} + \frac{x}{\sqrt{x^2+W^2}}\right]$$

The magnetic field

- The magnetic induction due to a straight current element is determined by the Biot-Savart law:

$$d\vec{B} = \frac{\mu}{4\pi}\frac{i(t)\,\vec{dl}\times(\vec{r}-\vec{r}\,')}{|\vec{r}-\vec{r}\,'|^3} = \frac{\mu}{4\pi}\frac{i(t)\,\vec{dl}\times\vec{R}}{R^3}$$

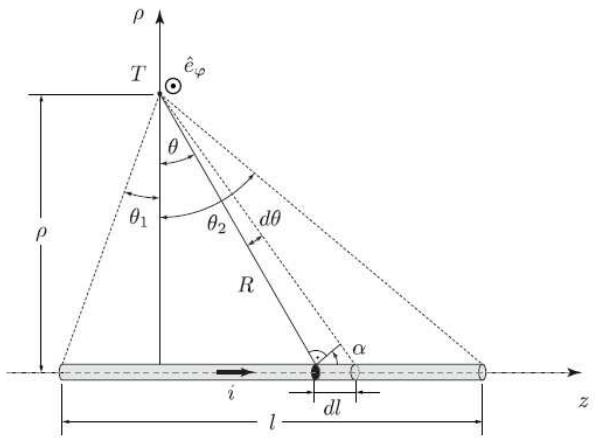

FIG: Straight current element

- Performing some mathematical manipulation and integrating the contributions along the entire length of a conductor it follows:

$$\vec{B} = \hat{e}_\varphi\frac{\mu\,i(t)}{4\pi\rho}\int_{\theta_1}^{\theta_2}\cos\theta d\theta = \hat{e}_\varphi\frac{\mu\,i(t)}{4\pi\rho}(\sin\theta_1+\sin\theta_2)$$

- The total value of the magnetic flux density in a point of space can be expressed as:

$$B(t) = \sqrt{\left(\sum_{i=1}^{N}B_{x,i}(t)\right)^2 + \left(\sum_{i=1}^{N}B_{y,i}(t)\right)^2 + \left(\sum_{i=1}^{N}B_{z,i}(t)\right)^2}$$

Incident Field Dosimetry Procedures – LF Exposures

Assessment of E and H field from power substation

The electric field

- Numerical approach, based on quasistatic approximation is used.
- The electric field is expressed in terms of scalar potential.
- The scalar potential is obtained by solving the Scalar Potential Integral Equation (SPIE) via Boundary Element Method (BEM).

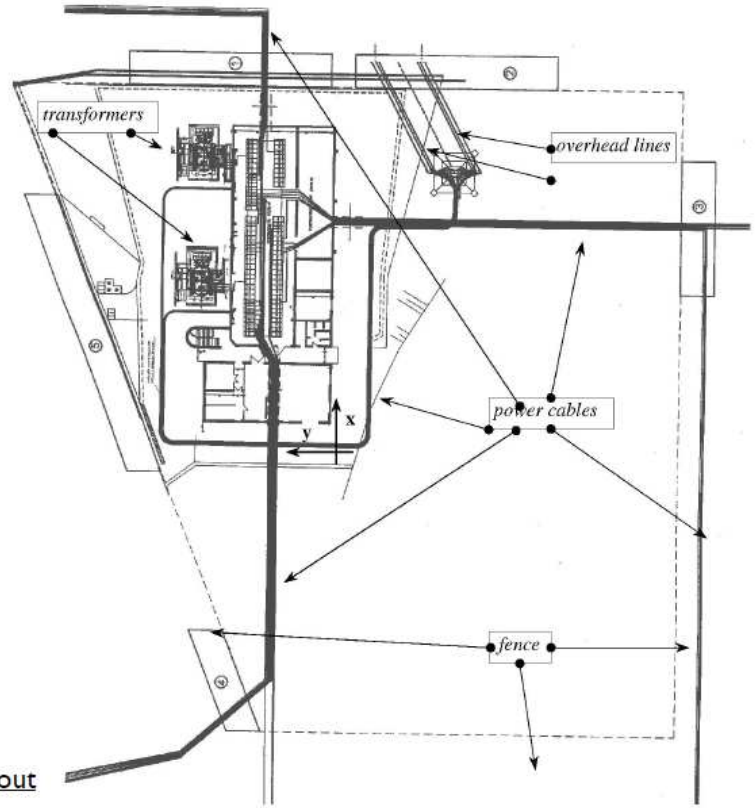

FIG: Substation layout

Incident Field Dosimetry Procedures – LF Exposures

Computational results for *E*-field

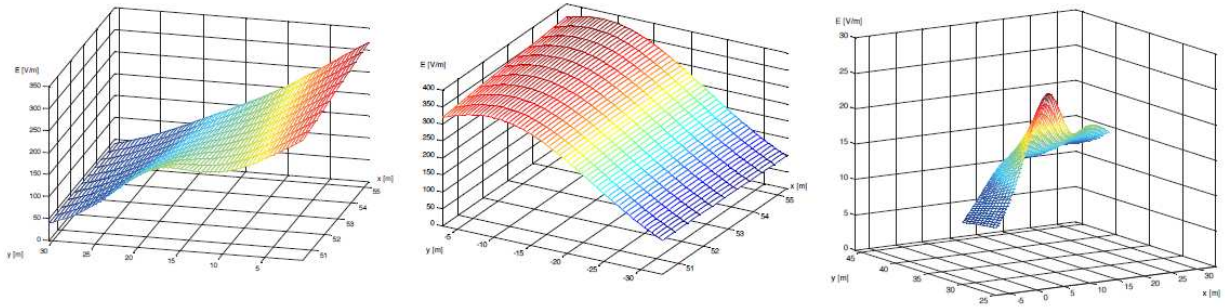

Domain No. 1 Domain No. 2 Domain No. 5

FIG: Spatial distribution of the electric field

Table: Comparison to Safety Standards		
Electric field [kV/m]	Workers [kV/m]	Public [kV/m]
0.381	10 (5)	5 (2)

Computational results for *H*-field

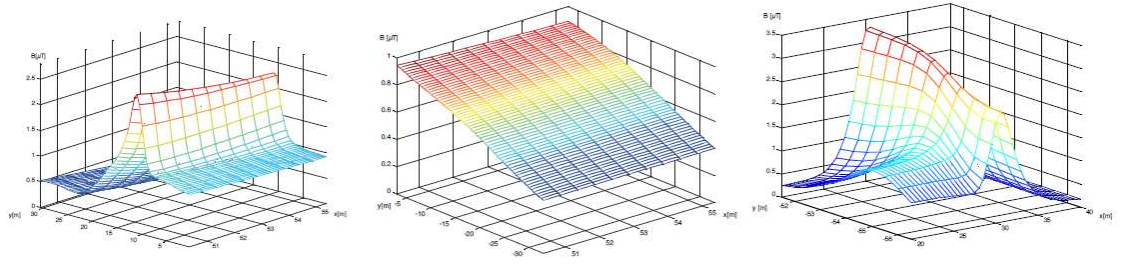

Domain No. 1 Domain No. 2 Domain No. 3

FIG: Spatial distribution of the magnetic field

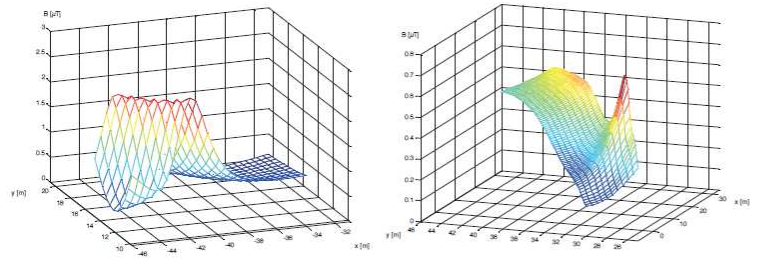

Domain No. 4 Domain No. 5

Table: Comparison to Safety Standards		
Magnetic flux density [uT]	Workers [uT]	Public [uT]
3.344	500 (100)	100 (40)

Incident Field Dosimetry Procedures – LF Exposures

Assessment of E and H field from power substation

Measurement results for *H*-field

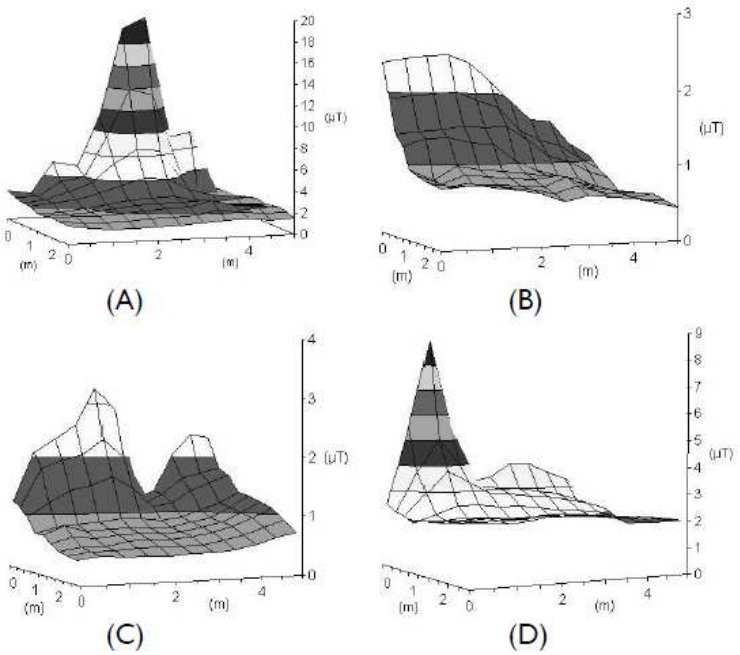

FIG: TS 10/0,4 kV substation 1: (A) southern side, (B) eastern side, (C) northern side, and (D) western side.

- Nominal power 630 kVA

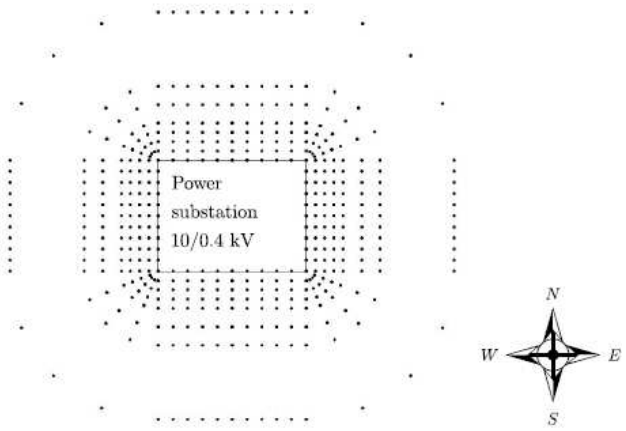

FIG: Measurement points

Table: Comparison to Safety Standards

Magnetic flux density [uT]	Workers [uT]	Public [uT]
18.3	500 (100)	100 (40)

Incident Field Dosimetry Procedures – HF Exposures

Incident Field Dosimetry Procedures – HF Exposures

Assessment of human exposure to PLC system

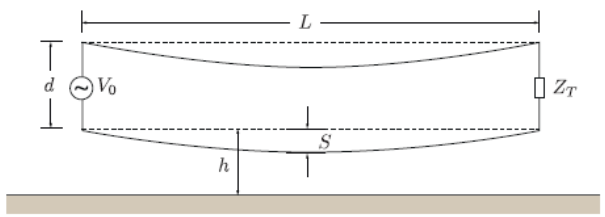

FIG: Simple PLC system

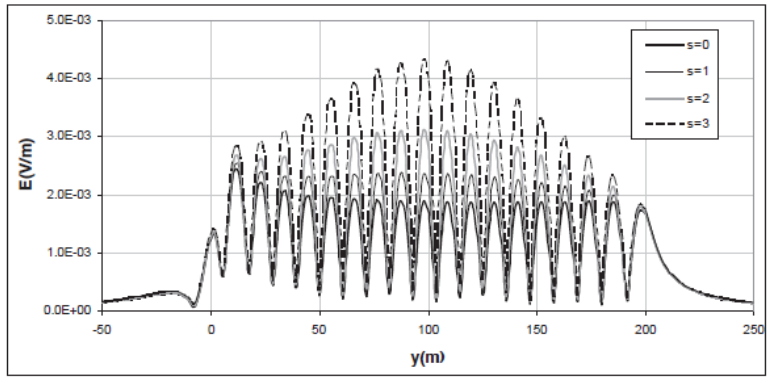

FIG: E_z component of the radiated electric field under the line for different values of conductor sag (x=0m, z=1.5m, σ=0.005S/m, ε_r=13)

- E-field values for f up to 10 MHz are added to asses the cumulative effect:

(general public)

$$\sum_{i>1\ \mathrm{MHz}}^{10\ \mathrm{MHz}} \frac{E_i}{a} + \sum_{i>10\ \mathrm{MHz}}^{30\ \mathrm{MHz}} \left(\frac{E_i}{E_{L,i}}\right)^2 = 1.15 \cdot 10^{-3}$$

(workers)

$$\sum_{i>1\ \mathrm{MHz}}^{10\ \mathrm{MHz}} \frac{E_i}{a} + \sum_{i>10\ \mathrm{MHz}}^{30\ \mathrm{MHz}} \left(\frac{E_i}{E_{L,i}}\right)^2 = 4.03 \cdot 10^{-4}$$

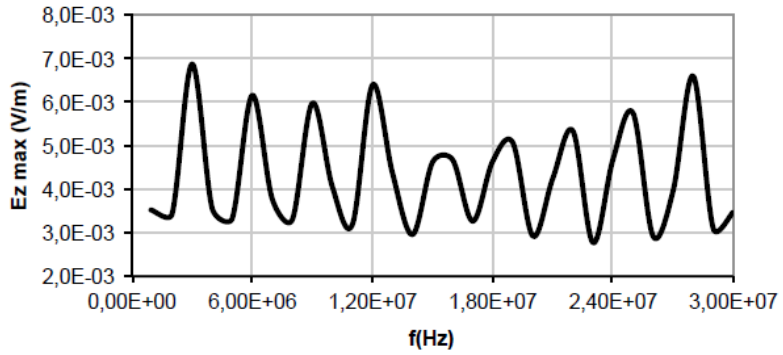

FIG: Maximal value of E_z component below the conductor (z=1.75m)

Incident Field Dosimetry Procedures – HF Exposures

Incident Field Dosimetry Procedures – HF Exposures

Assessment of human exposure to RFID loop antenna

- The input power is P=50mW per loop antenna. The wire radius is 0.9 mm, while the side length of the wire square loop is 46.5 cm.
- Fig shows the measured H field distribution along the vertical line from z = 0 to z = 2 m, corresponding to a human standing beside the system, at a diagonal distance of approx. 1.8 m from the center of the antenna system (x = 1.3 m, y = 1.3 m), thus representing an employee exposure to the anti-theft gate for a longer period.

FIG: Anti-theft store protection gate

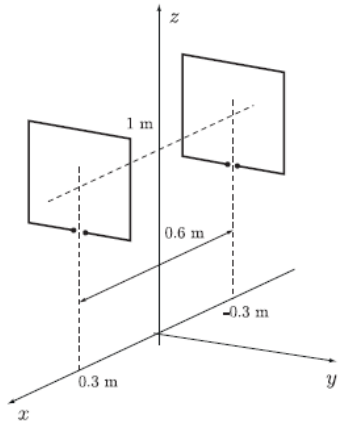

FIG: Gate antenna system used measurement

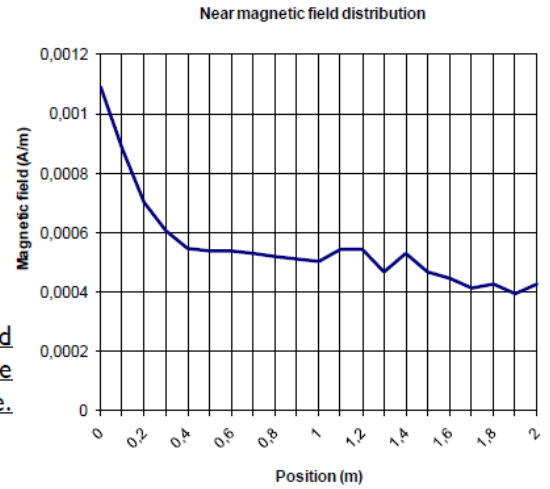

FIG: Magnetic field intensity along the vertical line.

- The measured field value of 1.1mA/m² is significantly below ICNIRP reference levels (160mA/m² for workers and 73mA/m² for general population.

Incident Field Dosimetry Procedures – HF Exposures

Radiation From a Base Station Antennas

- The levels of public exposure to EM energy from any base stations vary depending on antenna type, location and distance from the base station.
- The base station antennas are most commonly used in a sectorial arrangement and produce a so-called pie-shaped beam.
- This beam is wide in the horizontal direction and narrow in its vertical direction.

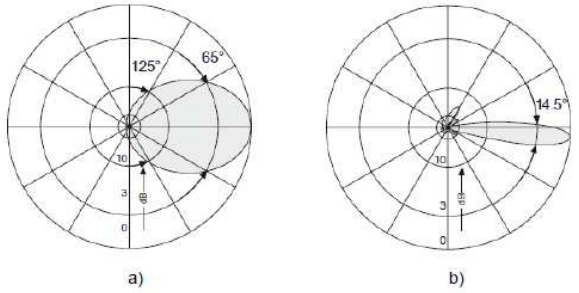

FIG: a) Horizontal pattern of GSM antenna ,B) Vertical pattern of GSM antenna

- The exposure can be determined by calculations and/or measurement.
- It should be noted that the presence of reflecting and scattering structures can have influence on both the exposure and power deposition inside the human body.

Radio base stations: Analytical and numerical approach to the radiated field assessment

- *EIRP* (equivalent isotropic radiated power) is an important concept to express the capabilities of RF transmission.
- The power density of an isotropic point radiator: $\bar{P}_d = \frac{P_t}{4\pi r^2}$
- P_t is the power input to the antenna
- For directional antenna, the power density is defined as: $\bar{P}_d = \frac{P_t G_t}{4\pi r^2}$
- G_t is the gain ratio of the transmitting antenna based on an isotropic radiator.
- *EIRP* is then given by the product: $\mathrm{EIRP} = P_t \cdot G_t$ G_t is a numeric gain.
- *EIRP* can also be written in decibel expression: $\mathrm{EIRP} = [P_t] + [G_t]$
- If the attenuation of the system are taken into account then it follows:

$$\mathrm{EIRP}\ [dBm] = P_t\ [dB] + G_t\ [dBi] - L\ [dB] \qquad \mathrm{EIRP} = \frac{P_t \cdot G_t}{L}$$

- *L* represents the ohmic losses.

Incident Field Dosimetry Procedures – HF Exposures

Near Field Analysis: Assessment of Power Density

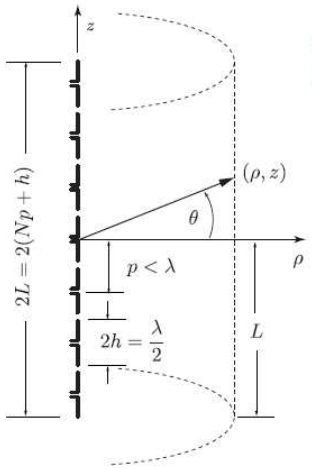

FIG: Base station antennas can be represented by an colinear array of resonant dipoles

The total average power radiated by an axial array (N-number of carriers, channels, rho-distance):

$$P_{\text{tot}} = N P_{\text{rad}} = \oint_S \vec{S}\, d\vec{A} = \int_0^{2\pi} \int_{-L}^{+L} S \cdot \hat{e}_\theta^* \, \rho \, d\phi \, dz \cdot \hat{e}_\rho$$

$$= S \cdot 2\pi\rho \cdot 2L, \qquad (3.59)$$

The average power density: $$S = \frac{N P_{\text{rad}}}{2\pi\rho 2L}. \qquad (3.60)$$

Taking into account sectorial coverage: $$S = \frac{N P_{\text{rad}}}{\pi\rho 2L} \frac{180}{\bar{\phi}}, \qquad (3.61)$$

Far Field Analysis: Calculation of Power Density and Electric Field

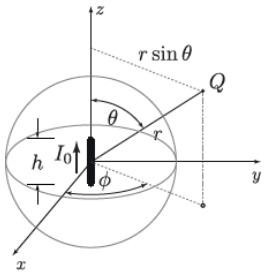

FIG: In case of observation point in far field, the base station antenna represents a point radiation source (Hertz dipole).

Using a concept of effective isotropic radiated power (EIRP) the total field and power density can be written, as follows:

$$E = 2\frac{\sqrt{30N \cdot \text{EIRP}}}{R} F(\phi, \theta),$$

$$S = \frac{N \cdot \text{EIRP}}{\pi R^2} F^2(\phi, \theta).$$

where a factor 2 represents the worst case scenario of the reflection of the plane wave from the PEC ground.

Incident Field Dosimetry Procedures – HF Exposures

Radio base stations: Measurements

Mesurement has been performed by using following equipment:

•Holaday Industries HI4455 + HI4460, isotropic probe calibrated for broadband measurement;

•Calibrated electric dipole + Hewlett-Packard HP 8590B spectrum analyzer for narrow-band measurement

Electric dipole is calibrated in a way to provide the information about the incident electric field directly from the measured power from spectrum analyzer. The attenuation of the cable is taken into account, as well.

The frequency selective measurement is performed using the spectrum analyzer as a measuring equipment.

The broadband measurement enables one to determine whether the total RF field is within the reference levels.

On the other hand, the narrow-band measurement is frequency selective and serves as a test for particular source, i.e. to determine whether its field is in accordance to the reference levels.

Incident Field Dosimetry Procedures – HF Exposures

Radio base stations: Measurements

Measurement example No1:

FIG: Antenna system of GSM base station mounted on a roof top at the altitude of approximately 17m above ground.

Table: Parameters of the roof-top GSM base station.

Operating frequency	GSM downlink band; 935 - 960 MHz
Number of sectors	3
Direction of main lobes	Sector A, 0°; Sector B, 120°; Sector C, 230°
Elevation of main lobes	Sector A, 0°; Sector B, 0°; Sector C, 3°
Antenna types	Sector A/B/C; Celwave APXV 906514, 2 antennas (per sector)
Number of channels	Sector A/B/C; 3
Maximal permissible EIRP per channel	Sector A/B/C; 58 dBm

Table: Location 1

Measured total field E [V/m]	Reference level E [V/m]
2.33	42.00

Radio base stations: Measurements

Measurement example No2:

FIG: Example with roof-top antenna system in sectorial arrangement mounted at a height of 48 m above ground.
A view to the 2 sector of base station antenna system.
The radiated power per channel is P=955 W at 935 MHz.

Table: Parameters of the roof-top GSM base station.

Operating frequency	GSM downlink band; 935 - 960 MHz
Number of sectors	3
Direction of main lobes	Sector A, 30°; Sector B, 150°; Sector C, 270°
Elevation of main lobes	Sector A, 0°; Sector B, 0°; Sector C, 3°
Antenna types	Sector A/B/C; Celwave APXV 906514, 2 antennas (per sector)
Number of channels	Sector A/B, 4; Sector C, 3
Maximal permissible EIRP per channel	Sector A/B/C; 59.8 dBm

Table: Location 2 (Flat at the 15th floor below antenna system at an approximated distance of 8 m from) radiation source)

Measured total field E [V/m]	Reference level E [V/m]
0.23	42.00

Measured field values are within the internationally proposed reference levels.

Incident Field Dosimetry Procedures – HF Exposures

Radio base stations: Measurements results

Measurement example No3:

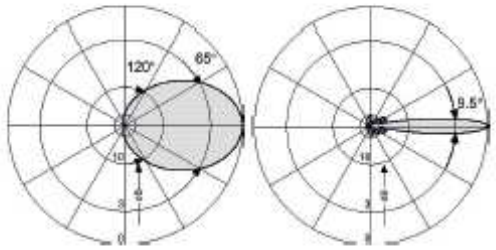

FIG: **Kathrein 739 623:** Horizontal (left) and vertical (right) pattern

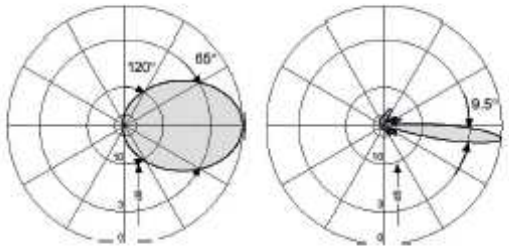

FIG: **Kathrein 739 634:** Horizontal (left) and vertical (right) pattern

Table: Parameters of the Kathrein 739 623 antenna	
Antenna gain	17 dBi
EIRP per channel	Cca. 430 W
Front-to-back ratio	> 30 dB

Table: Parameters of the Kathrein 739 634 antenna	
Antenna gain	17 dBi
EIRP per channel	Cca. 430 W
Front-to-back ratio	> 30 dB
Electrical tilt	-6°

Radio base stations: Measurements results

Measurement example No3:

The measurement locations:

- Loc. 1: balcony of the third floor of the house, in the vicinity of the source;
- Loc. 2: balcony on the second floor of the house, in the vicinity of the source;
- Loc. 3: balcony on the third floor, in the vicinity of the source.

FIG: A veiw to the radiaton source from which the domain 1 is seen. The domain 3 can be noticed down and left

Table: Location 1	
Measured total field E [V/m]	Reference level E [V/m]
1.76	42.00
Broadband measurement: 1.9 V/m	

Table: Location 2	
Measured total field E [V/m]	Reference level E [V/m]
1.23	42.00
Broadband measurement: 1.9 V/m	

Table: Location 3	
Measured total field E [V/m]	Reference level E [V/m]
2.08	42.00
Broadband measurement: 3.5 V/m	

Incident Field Dosimetry Procedures – HF Exposures

Far Field Analysis: Presence of a Lossy Ground and Layered Medium

Simple analytical relations for the incident field dosimetry (antenna radiating in the presence of inhomogeneous media)

6 different approximation schemes for the assessment of BS antenna:

- Antenna insulated in free space (FS)
- Antenna above perfect ground (PG)
- Antenna above lossy half space
  - Using Fresnel reflection coeff.
  - Using modified image theory (MIT) approximation
- Model of a layered medium featuring MIT appr.
- Compared to results obtained by NEC

All calculations carried out for the far field zone.

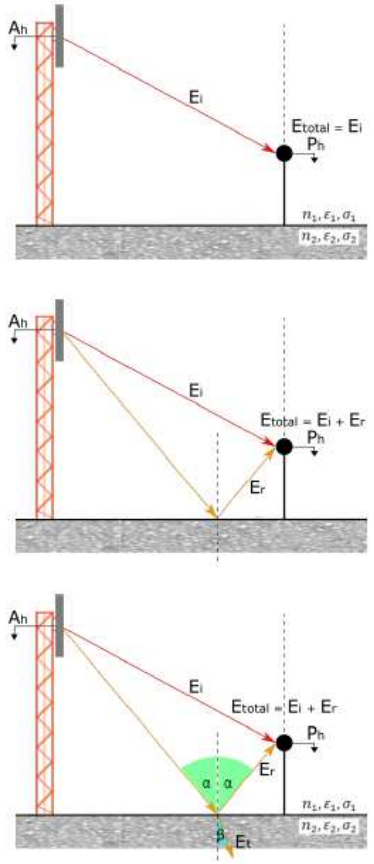

FIG: Top too bottom: a) Free space approx., b) Perfect ground approx., c) Antenna above lossy half space

Incident Field Dosimetry Procedures – HF Exposures

Far Field Analysis: Presence of a Lossy Ground and Layered Medium

- **Free space approximation**:
  - used by some dosimetry guidelines
  - neglects effects due to reflection and scattering
  - takes into account only incident field

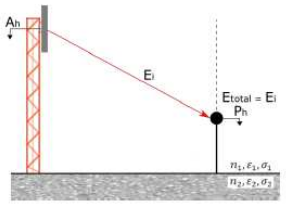

FIG: Free space approximation

Total electric field in the far field:

$$E^{tot} = E^{inc} = \frac{\sqrt{30N \cdot \mathrm{EIRP}}}{R}$$

- **Perfect ground approximation**:
  - account the effect of reflected wave
  - assumption if perfectly conducting ground

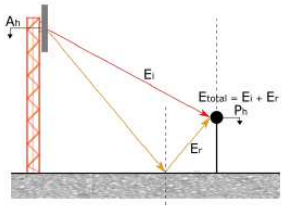

FIG: Perfect ground approximatio

$$E^{tot} = E^{inc} + E^{ref}$$

$$E^{ref} = \frac{\sqrt{30N \cdot \mathrm{EIRP}}}{R^*}$$

R* - distance from the image antenna to calculation point above PEC ground

Far Field Analysis: Presence of a Lossy Ground and Layered Medium

- **Antenna above a lossy half space**:
  - Using Fresnel reflection coeff.
  - Using modified image theory (MIT) approximation

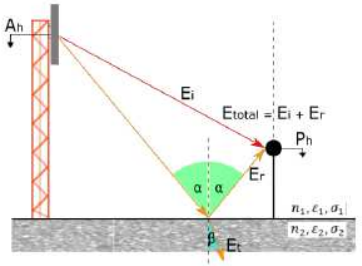

$$E^{ref} = \Gamma^{Fr} \cdot \frac{\sqrt{30N \cdot \mathrm{EIRP}}}{R^*}$$

$$\Gamma^{Fr} = \frac{Z_1 \cos\alpha - Z_2 \cos\beta}{Z_1 \cos\alpha + Z_2 \cos\beta} \qquad Z_2 = \frac{j\omega\mu}{\gamma}$$

$$E^{ref} = \Gamma^{MIT} \cdot \frac{\sqrt{30N \cdot \mathrm{EIRP}}}{R^*}$$

$$\Gamma^{MIT} = \frac{\varepsilon_{eff} - \varepsilon_0}{\varepsilon_{eff} + \varepsilon_0}$$

$$\varepsilon_{eff} = \varepsilon_r \varepsilon_0 - j\frac{\sigma}{\omega}$$

Incident Field Dosimetry Procedures – HF Exposures

Far Field Analysis: Presence of a Lossy Ground and Layered Medium

- **Computational example 1:** 2m antenna consisting of 8 dipoles and metal grid with total radiated power P=100 W/channel. f = 936.8 MHz; Ph= 2 m

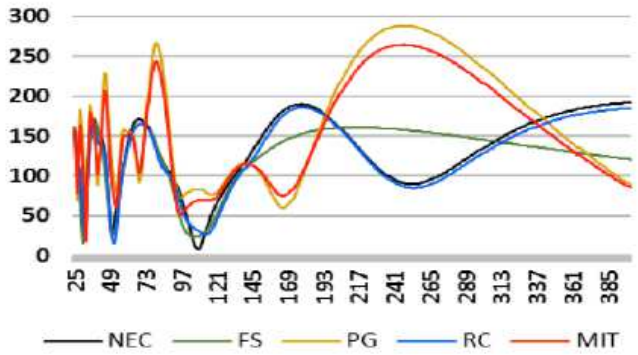

FIG: a) Electric field (mV/m) via different approaches compared to NEC at specific distance from antenna (sigma=0.01 S/m, **epsilon_2 = 10, A_h = 20 m**)

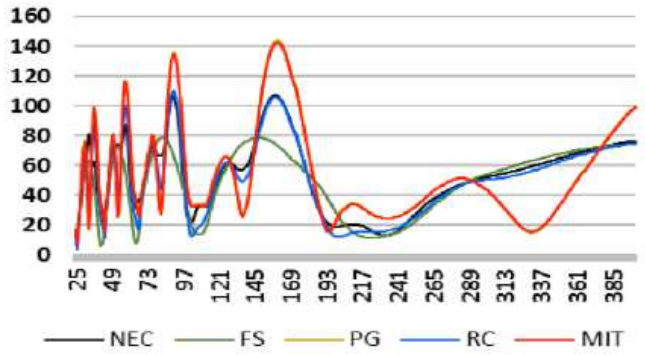

FIG: b) Electric field (mV/m) via different approaches compared to NEC at specific distance from antenna (sigma=0.01 S/m, **epsilon_2 = 110, A_h = 40 m**)

Incident Field Dosimetry Procedures – HF Exposures

Far Field Analysis: Presence of a Lossy Ground and Layered Medium

- **Computational example 2:** Assessment of field radiated by BS antenna over a two-layered ground:
- Reflected field from air-multilayer interface given by:

$$E^{ref} = \Gamma_{ml}^{MIT} \cdot \frac{\sqrt{30N \cdot \mathrm{EIRP}}}{R^*}$$

$$\Gamma_{ml}^{MIT} = \frac{R_{01} + R_{02}e^{-2\gamma l}}{1 + R_{01} \cdot R_{02}e^{-2\gamma l}}$$

$$\Gamma^{Fr} = \frac{\varepsilon_{eff,m} - \varepsilon_{eff,n}}{\varepsilon_{eff,m} + \varepsilon_{eff,n}}$$

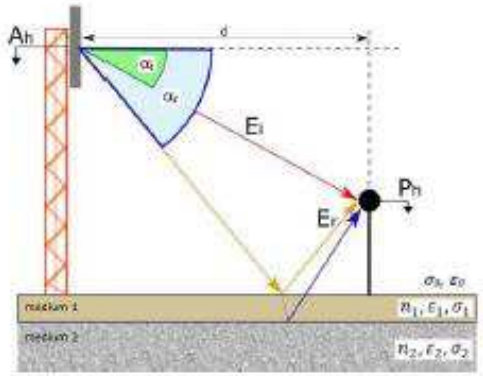

FIG: The total electric field above a multilayered medium composed of incident and reflected fields

Far Field Analysis: Presence of a Lossy Ground and Layered Medium

- **Computational example 2:** antenna power P=100 W, f = 936.8 MHz (one active channel); antenna mounted 25 m above ground

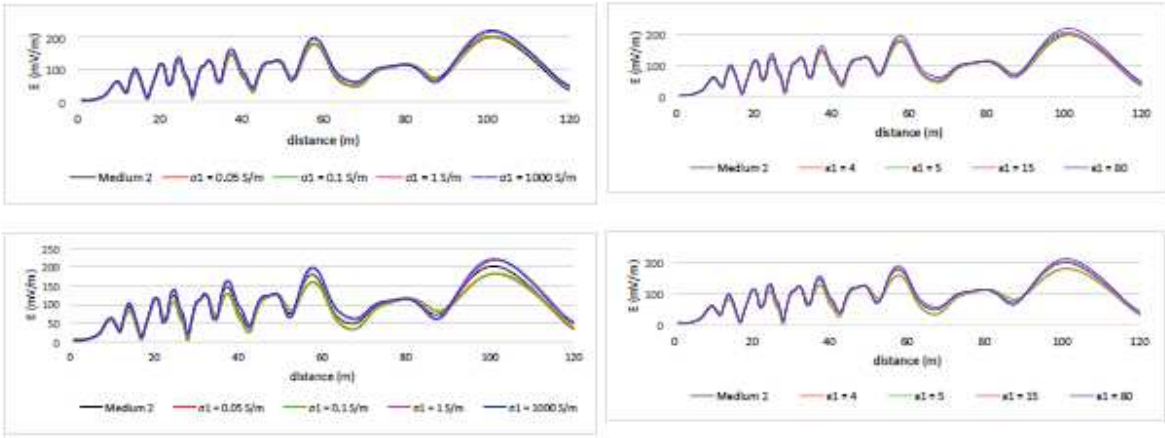

FIG: Electric field for different values of sigma 1 and epsilon 1 with medium 1 thickness: a) and c) 1 cm, b) and d) 25 cm

Incident Field Dosimetry Procedures – HF Exposures

Accurate numerical modeling of base station antenna systems

- The formulation is based on the set of the coupled Pocklington integro-differential equations for induced currents along the wires.
- This set of equations is numerically solved via the Galerkin-Bubnov indirect Boundary Element Method (GB-IBEM).
- Knowing the currents induced along the array the radiated electric field is calculated and compared with results calculated via widely used analytical relations for the far field.

A vertical antenna array of M dipoles of placed in front of a PEC reflector is considered.

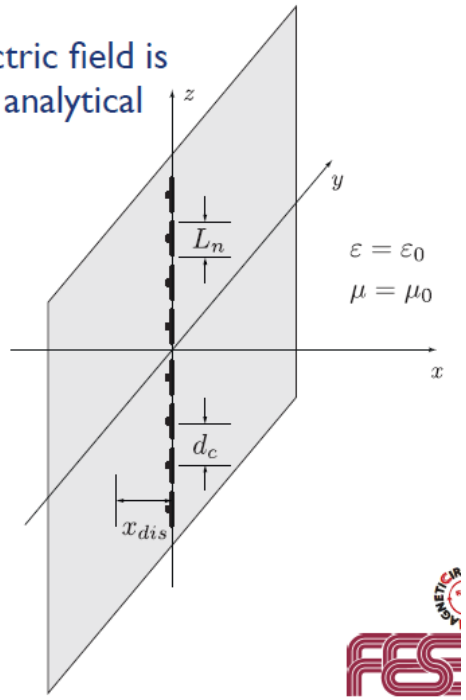

FIG: **GSM antenna model:** Antenna array in front of reflector

Incident Field Dosimetry Procedures – HF Exposures

Accurate numerical modeling of base station antenna systems

The current distribution

The currents induced along the antenna elements are governed by the set of coupled Pocklington integro-differential equations:

$$E_{zm}^{inc} = \frac{1}{j4\pi\omega\varepsilon_0}\sum_{n=1}^{M}\left[\frac{\partial^2}{\partial z^2}+k^2\right]\int_{-L/2}^{+L/2} I_n(z')\,G_{mn}(z,z')\,dz', \quad m=1,2,\ldots,M$$

where $I_n(z)$ is the current distribution along the n-th wire, and G_{mn} is the Green's function given by:

$$G_{mn}(z,z') = g_{0mn}(z,z') - g_{imn}(z,z')$$

$$g_{0mn}(z,z') = \frac{e^{-jkR_{mn}}}{R_{mn}}$$

$$g_{imn}(z,z') = \frac{e^{-jkR^*_{mn}}}{R^*_{mn}}$$

The numerical solution: The Galerkin-Bubnov scheme of the Indirect Boundary Element Method

Accurate numerical modeling of base station antenna systems

The radiated field

The components of the electric field radiated by the vertical array:

$$E_x = \frac{1}{j4\pi\omega\varepsilon_0}\sum_{n=1}^{M}\frac{\partial^2}{\partial x\partial z}\int_{-L/2}^{+L/2} G_{mn}(x,z')\,I_n(z')\,dz' = \frac{1}{j4\pi\omega\varepsilon_0}\sum_{n=1}^{M}\int_{-L/2}^{+L/2}\frac{\partial I_n(z')}{\partial z'}\frac{\partial G_{mn}(x,z')}{\partial x}dz'$$

$$E_y = \frac{1}{j4\pi\omega\varepsilon_0}\sum_{n=1}^{M}\frac{\partial^2}{\partial x\partial z}\int_{-L/2}^{+L/2} G_{mn}(y,z')\,I_n(z')\,dz' = \frac{1}{j4\pi\omega\varepsilon_0}\sum_{n=1}^{M}\int_{-L/2}^{+L/2}\frac{\partial I_n(z')}{\partial z'}\frac{\partial G_{mn}(y,z')}{\partial y}dz'$$

$$E_z = \frac{1}{j4\pi\omega\varepsilon_0}\sum_{n=1}^{M}\left[\frac{\partial^2}{\partial z^2}+k_1^2\right]\int_{-L/2}^{+L/2} G_{mn}(z,z')\,I_n(z')\,dz' =$$

$$= \frac{1}{j4\pi\omega\varepsilon_0}\sum_{n=1}^{M}\left[\int_{-L/2}^{+L/2}\frac{\partial G_{mn}(z,z')}{\partial z}\frac{\partial I_n(z')}{\partial z'}dz' + k^2\int_{-L/2}^{+L/2} I_n(z')\,G_{mn}(z,z')\,dz'\right]$$

Incident Field Dosimetry Procedures – HF Exposures

Accurate numerical modeling of base station antenna systems

NUMERICAL RESULTS

- The computational example: the GSM sector antenna consisting of 8 half-wave dipole antennas spaced by 0.75λ, with radius of 0.004λ.
- This array is distanced from reflector at x=-0.176λ. The reflector is modeled as an infinite, perfectly conducting plane.
- All dipoles are driven by the voltage generator placed at the centre of each dipole.
- The total input power of all sources is chosen to be 30W per GSM channel.
- The horizontal and vertical radiation pattern is shown below.

The horizontal and vertical radiation pattern are computed.

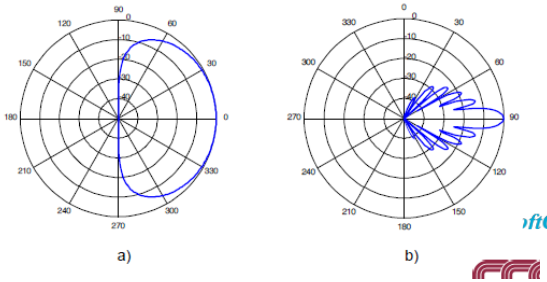

FIG: Horizontal (a) and vertical (b) pattern.

Accurate numerical modeling of base station antennas

Comparison of the results obtained via the different methods:

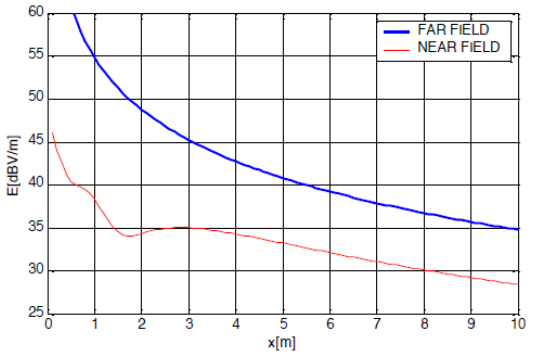

FIG: Calculated electric field ϕ=0°, z=0m

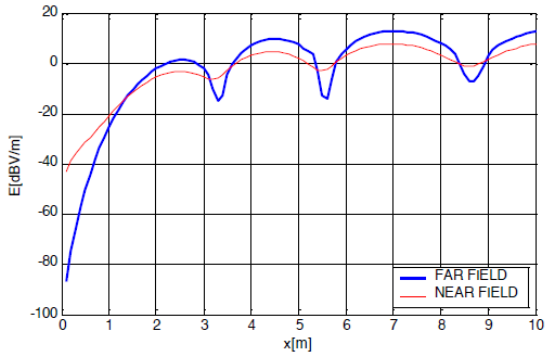

FIG: Calculated electric field ϕ=0°, z=-5m

The use of analytical relations for the calculation of the radiated electric field in the near zone results in significant overestimation (7-15 dB) only in the main lobe e.g. for z=0.

Beneath the main lobe, near field values could be higher than the value obtained by the far field pattern, particularly visible for the nulls of the radiation pattern (underestimation up to level of 12 dB).

Incident Field Dosimetry Procedures – HF Exposures

Radiation from WPT Systems

- ❑ Nowadays many devices rely on wireless charging.
- ❑ Sometimes the human body can be located in the vicinity of WPT transmitter and it is of interest to carry out the exposure assessment via incident/internal dosimetry procedures, based on analytical/numerical approach.
- ❑ While the main feature of the realistic human body models is accuracy, the simplified models ensure rapid estimation of the phenomena.

- Curved wire antennas, (e.g. loops or helical antennas), have a number of applications in communication systems.
- Two principal modes of helical antennas - the normal (broadside) and axial (endfire) modes.
- *The normal mode;* radiation occurs when the helical antenna diameter is much smaller than wavelength.
- *The axial mode* occurs when the helix circumference is one wavelength and ensures maximum radiation along the helical antenna axis.
- The helix axial mode is often of most importance and it is used in wide range of applications.

Incident Field Dosimetry Procedures – HF Exposures

Radiation from WPT Systems

Formulation: Single wire in free space

- The field generated by curved wire configurations is determined by integrating the current distribution along the wire.

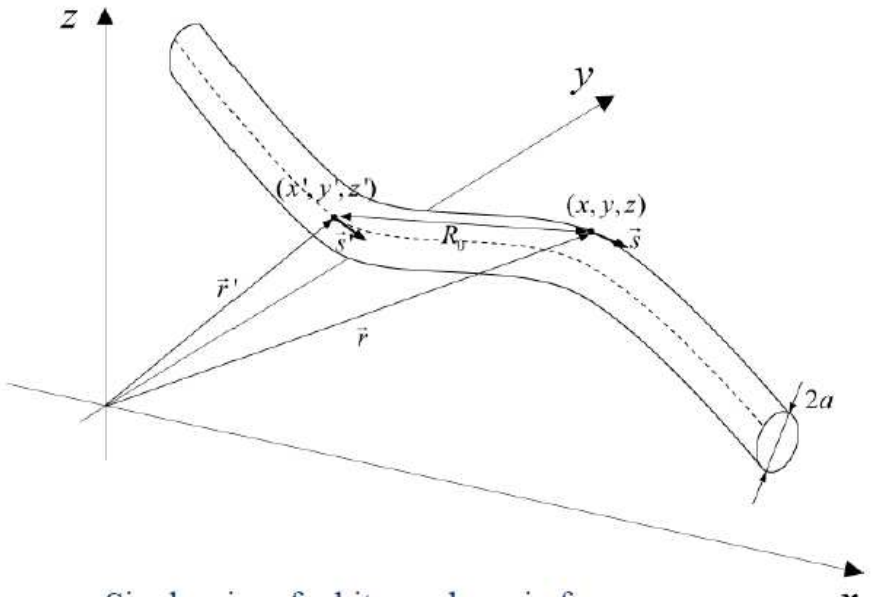

Single wire of arbitrary shape in free space

- The current distribution is obtained by solving the corresponding Pocklington equation via GB-IBEM.

Incident Field Dosimetry Procedures – HF Exposures

Radiation from WPT Systems

Formulation: Single wire in free space

- Curved wire integral equation can be derived by satisfying the continuity conditions for tangential field components.

$$\vec{e}_x \cdot \left(\vec{E}^{exc} + \vec{E}^{sct} \right) = 0$$

- From the 1st Maxwell equation:

$$\nabla \times \vec{E} = -\frac{\partial \vec{B}}{\partial t}$$

and Lorentz gauge

$$\nabla \vec{A} = -j\omega\mu\varepsilon\varphi$$

it follows

$$\vec{E}^{sct} = -j\omega\vec{A} + \frac{1}{j\omega\mu\varepsilon}\nabla(\nabla\vec{A})$$

Formulation: Single wire in free space

- Magnetic vector potential is defined by the particular integral:

$$\vec{A}(\vec{r}) = \frac{\mu}{4\pi}\iint_V \vec{J}(\vec{r}\,')\frac{e^{-jk|\vec{r}-\vec{r}\,'|}}{|\vec{r}-\vec{r}\,'|}dV(\vec{r}\,')$$

where: J - volume current density, μ - medium permeability.

- For the case of curved PEC wires volume current density is replaced by the axial current:

$$\vec{A}(s) = \frac{\mu}{4\pi}\int_C I(s')g_0(s,s',s^*)\vec{s}\,'ds' \qquad g_0(s,s') = \frac{e^{-jkR}}{R}$$

- Satisfying the continuity conditions the Pocklington integro-differential equation (IDE) is obtained:

$$E^{inc}(s) = -\frac{1}{j4\pi\omega\varepsilon_0}\int_0^L \left[k_1^2 \vec{e}_s \vec{e}_{s'} - \frac{\partial^2}{\partial s \partial s'} \right] g_0(s,s')I(s')ds'$$

Incident Field Dosimetry Procedures – HF Exposures

Radiation from WPT Systems

Formulation: Single wire in free space

- Once the current distribution is determined the *E*-field and *H*-field field radiated by a curved wire structure are given by following expressions:

$$\vec{E} = \frac{1}{j4\pi\omega\varepsilon_0}\left[k^2\int_0^L \vec{e}_{s'} I(s')g_0(\vec{r},\vec{r}')ds' + \int_0^L \frac{\partial I(s')}{\partial s'}\nabla g_0(\vec{r},\vec{r}')ds'\right]$$

$$\vec{H}_S = -\frac{1}{4\pi}\int_0^L I(s')\vec{e}_{s'}\times\nabla g_0(\vec{r},\vec{r}')ds'$$

Numerical solution: Single wire in free space

- The Pocklington IDE for curved wires is handled via the GB-IBEM.
- Performing certain mathematical manipulation Pocklington IDE is transformed into the following matrix equation:

$$\sum_{m=1}^{M}\sum_{i=1}^{n_e}[Z]_{ji}^{m}\{I\}_i^m = \{V\}_j^m, \quad j = 1,2,\ldots n_e$$

$$[Z]_{ij}^m = -\int_{-1}^{1}\int_{-1}^{1}\{D\}_j\{D'\}_i^T g_0(s,s')\frac{ds'}{d\xi'}d\xi'\frac{ds}{d\xi}d\xi + k^2\vec{e}_s\vec{e}_{s'}\int_{-1}^{1}\int_{-1}^{1}\{f\}_j\{f'\}_i^T g_0(s,s')\frac{ds'}{d\xi'}d\xi'\frac{ds}{d\xi}d\xi$$

$$\{V\}_j^m = -j4\pi\omega\varepsilon_0\int_{-1}^{1}E_s^{inc}(s)f_j(s)\frac{ds}{d\xi}d\xi$$

Incident Field Dosimetry Procedures – HF Exposures

Radiation from WPT Systems

Numerical solution: Single wire in free space

- The total *E*-field and *H*-field field are obtained by contributing all wire segments:

$$\vec{E}^m = \frac{1}{j4\pi\omega\varepsilon_0}\sum_{m=1}^{M}\sum_{i=1}^{n_e}\left[k^2\int_{-1}^{1}\vec{e}_{s'}I_i^m f_i(\xi)g_0(\vec{r},\vec{r}')\frac{ds'}{d\xi}d\xi+\int_{-1}^{1}I_i^m\frac{\partial f_i(\xi)}{\partial\xi}\nabla g_0(\vec{r},\vec{r}')\frac{ds'}{d\xi}d\xi\right]$$

$$\vec{H}^m = -\frac{1}{4\pi}\sum_{m=1}^{M}\sum_{i=1}^{n_e}\int_{-1}^{1}I_i^m f_i(\xi)\vec{e}_{s'}\times\nabla g_0(\vec{r},\vec{r}')\frac{ds'}{d\xi}d\xi$$

- where *N* and *n* stands for the actual number of elements and local nodes, respectively.

Formulation: Multiple wires in free space

- The currents induced along curved wires located above a lossy ground are governed by the set of Pocklington IEs:

$$E_{sm}^{exc}(s_m) = \frac{j}{4\pi\omega\varepsilon_0}\sum_{n=1}^{N_w}\int_0^{L_n}\left\{\left[k^2\vec{e}_{s_m}\vec{e}_{s_n}-\frac{\partial^2}{\partial s_m\partial s_n'}\right]g_{0n}(s_m,s_n')+R_{TM}\left[k^2\vec{e}_{s_m}\vec{e}_{s_n^*}-\frac{\partial^2}{\partial s_m\partial s_n^*}\right]g_{in}(s_m,s_n^*)+\right.$$
$$\left.(R_{TE}-R_{TM})\vec{e}_{s_m}\vec{e}_p\cdot\left[k^2\vec{e}_p\vec{e}_{s^*}-\frac{\partial^2}{\partial p\partial s^*}\right]g_i(s_m,s_n^*)\right\}I(s_n')ds'+Z_{Lm}I(s_m),\qquad m=1,2,\ldots N_w$$

- Green functions

$$g_{0mn}(s_m,s_n') = \frac{e^{-jk\,R_{1mn}}}{R_{1mn}}\qquad \underline{n}=\frac{\varepsilon_{eff}}{\varepsilon_0}\qquad \varepsilon_{eff}=\varepsilon_r\varepsilon_0-j\frac{\sigma}{\omega}$$

Incident Field Dosimetry Procedures – HF Exposures

Radiation from WPT Systems

Formulation: Multiple wires in free space

- The total *E* - field and *H* – field irradiated by a configuration of arbitrarily shaped wires is given by:

$$\vec{E} = \sum_{n=1}^{N_w} \left[k_1^2 \int_0^{L_n} \vec{e}_{s_n} I(s_n') g_{0n}(\vec{r},\vec{r}') ds_n' + \int_0^{L_n} \frac{\partial I(s_n')}{\partial s_n'} \nabla g_{0n}(\vec{r},\vec{r}') ds_n' \right]$$

$$\vec{H} = \sum_{n=1}^{N} \int_0^{L_n} I(s_n') \vec{e}_{sn'} \times \nabla g_{0n}(\vec{r},\vec{r}') ds_n'$$

Numerical solution: Multiple wires in free space

- The set of Pocklington IEs is handled via the GB-IBEM featuring isoparametric elements.
- The unknown current along the *n*-th wire segment:

$$I_n^e(\zeta) = \sum_{i=1}^{n} I_{ni} f_{ni}(\zeta) = \{f\}_n^T \{I\}_n$$

Incident Field Dosimetry Procedures – HF Exposures

Radiation from WPT Systems

Numerical solution: Multiple wires in free space

- ...the weighted residual approach + GB procedure - the set of coupled IEs is transformed into the matrix equation:

$$\sum_{n=1}^{N_w}\sum_{i=1}^{N_n}[Z]^{e}_{ji}\{I\}^{e}_{i}=\{V\}^{e}_{j},\ m=1,2,...,N_w;\qquad j=1,2,...,N_m$$

where:

$$[Z]^{e}_{ij}=-\int_{-1}^{1}\int_{-1}^{1}\{D\}_j\{D'\}^T_i\,g_{0nm}(s_n,s_m')\frac{ds_m'}{d\xi'}d\xi',\frac{ds_n}{d\xi}d\xi+$$

$$+k_1^2\vec{e}_{s_n}\vec{e}_{s_m}\int_{-1}^{1}\int_{-1}^{1}\{f\}_j\{f'\}^T_i\,g_{0nm}(s_n,s_m')\frac{ds_m'}{d\xi'}d\xi',\frac{ds_n}{d\xi}d\xi-$$

$$+\frac{j}{4\pi\omega\varepsilon_0}\int_{-1}^{1}Z_T'\{f\}_j\{f'\}^T_j\frac{ds_n}{d\xi}d\xi$$

$$\{V\}^{n}_{j}=-j4\pi\omega\varepsilon_0\int_{-1}^{1}E^{exc}_{s_n}(s_n)\{f\}_j\frac{ds_n}{d\xi}d\xi_n$$

Numerical solution: Multiple wires in free space

- The total E- field and H-field are given by:

$$\vec{E}=\sum_{k=1}^{N}\vec{E}^{e}_{Sk}\qquad\vec{H}=\sum_{k=1}^{N}\left[\vec{H}^{e}_{Sk}\right]$$

where:

$$\vec{E}^{e}_{Sk}=\frac{1}{j4\pi\omega\varepsilon_0}\sum_{i=1}^{n}\left[k^2\int_{-1}^{1}\vec{e}_{ks}I^{e}_{ik}f_i(\xi)g_{0k}(\vec{r},\vec{r}')\frac{ds_k'}{d\xi}d\xi+\int_{-1}^{1}I^{e}_{ik}\frac{\partial f_i(\xi)}{\partial\xi}\nabla g_{0k}(\vec{r},\vec{r}')\frac{ds_k'}{d\xi}d\xi\right]$$

$$\vec{H}^{e}_{S}=-\frac{1}{4\pi}\sum_{i=1}^{n}\int_{-1}^{1}I_if_i(\xi)\vec{e}_{s'}\times\nabla g_0(\vec{r},\vec{r}')\frac{ds'}{d\xi}d\xi$$

Incident Field Dosimetry Procedures – HF Exposures

Radiation from WPT Systems

Computational examples

Loop antenna

- The circular loop antenna insulated in free space and excited via unit voltage source at, φ=0° is analyzed.
- The loop radius is *a*=0.0027λ and the wire radius is *b*=0.0637λ at 3GHz.

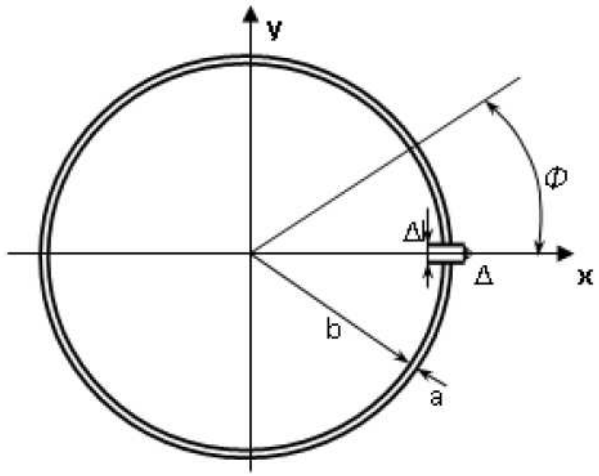

Thin wire loop antenna

Computational examples

Loop antenna

- Figs show the current distribution along the loop. All calculations are carried out by using linear elements.
- The results computed by BEM are compared to the results obtained by the Moment Method (MoM).

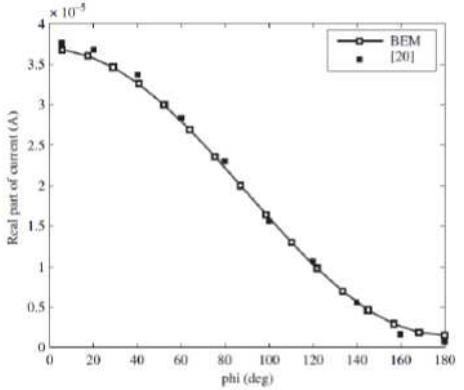

Real part of the loop current (*a*=0.0027λ, *b*=0.0637λ, *f*=3GHz)

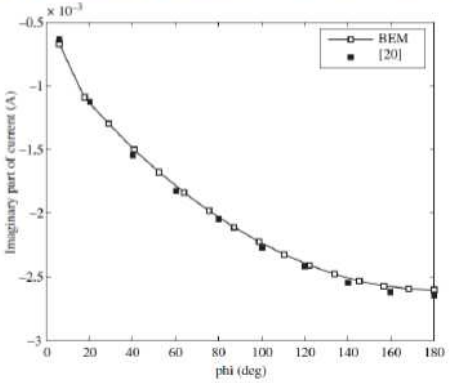

Imaginary part of loop current ((*a*=0.0027λ, *b*=0.0637λ, *f*=3GHz)

Incident Field Dosimetry Procedures – HF Exposures

Radiation from WPT Systems

Computational examples

Cylindrical helix

- The cylindrical helix consists of 6 turns, radius 5cm, pitch angle 11° and wire radius 1mm.
- Figs show the amplitude of current distribution at *f*=30MHz and *f*=750MHz.

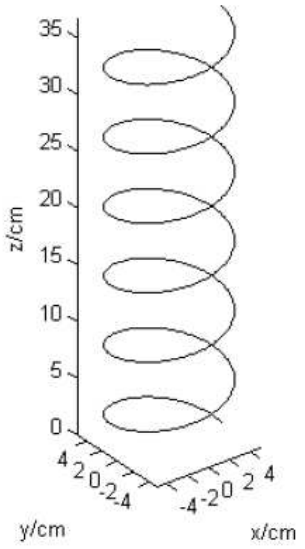

Geometry of cylindrical helix

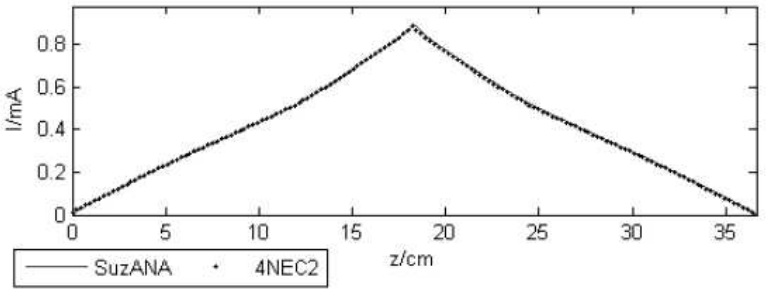

Amplitude of current distribution along cylindrical helix at *f*=30MHz

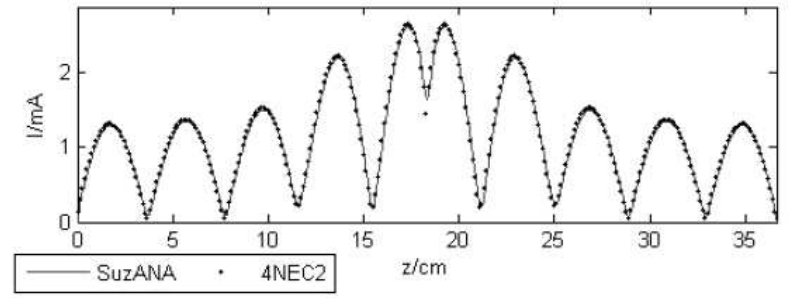

Amplitude of current distribution along cylindrical helix at *f*=750MHz

Incident Field Dosimetry Procedures – HF Exposures

Radiation from WPT Systems

Computational examples

Cylindrical helix

- Figs show the radiation pattern of cylindrical helix in horizontal and vertical plane, respectively, at *f*=30MHz.

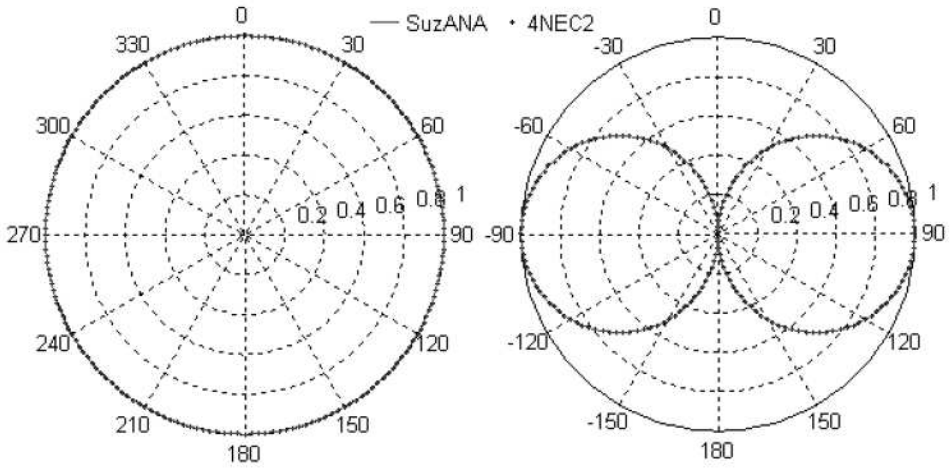

Horizontal *plane* *Vertical plane*
Radiation pattern of cylindrical helix at *f*=30MHz

Computational examples

Cylindrical helix

- Figs show the horizontal and vertical radiation pattern of cylindrical helix in horizontal and vertical plane, respectively, at *f*= 750 MHz.

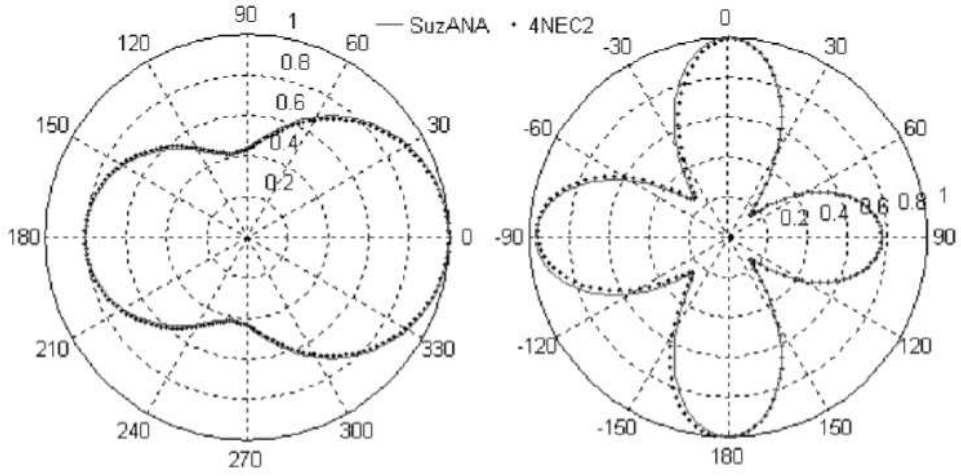

Horizontal plane Vertical plane
Radiation pattern of cylindrical helix at *f*=750MHz

Incident Field Dosimetry Procedures – HF Exposures

Radiation from WPT Systems

Computational examples

Conical helix

- The conical helix consisting of 9 turns, starting radius and pitch angle 5cm and 12° , respectively, and wire radius 1mm, is analyzed.
- Fig shows the amplitude of current distribution at *f*=1GHz.

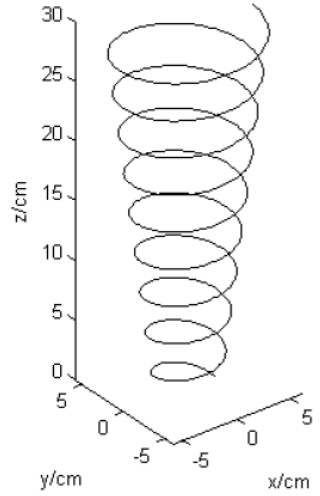

Geometry of conical helix

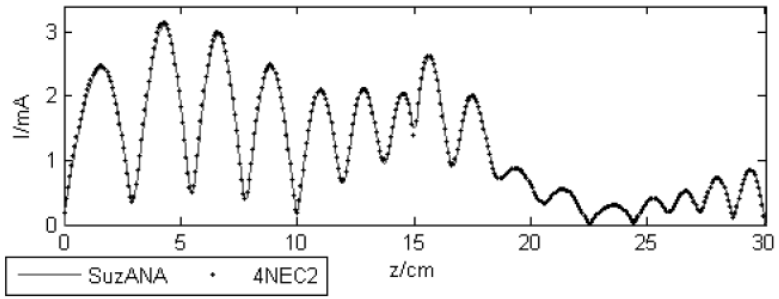

Amplitude of current distribution along conical helix at *f*=1GHz

Computational examples

Conical helix

- Fig shows the horizontal and vertical radiation pattern of the conical helix at *f*=1GHz.

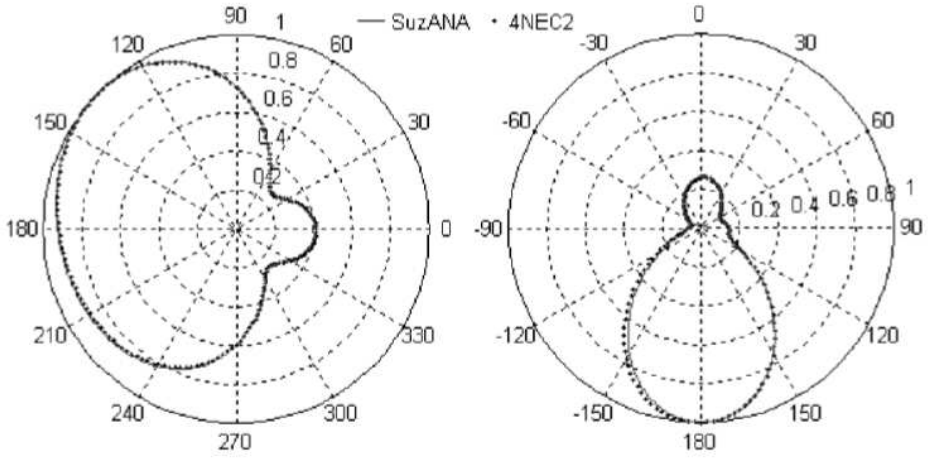

•Horizontal plane b) Vertical plane

Radiation pattern of conical helix at *f*=1GHz

Incident Field Dosimetry Procedures – HF Exposures

Radiation from WPT Systems

Computational examples

Spherical helix

- The spherical helix with helix radius 7.5cm and pitch angle 5° and the wire radius 0.2mm, is analyzed.
- Fig shows the amplitude of the current distribution at *f*=1GHz.

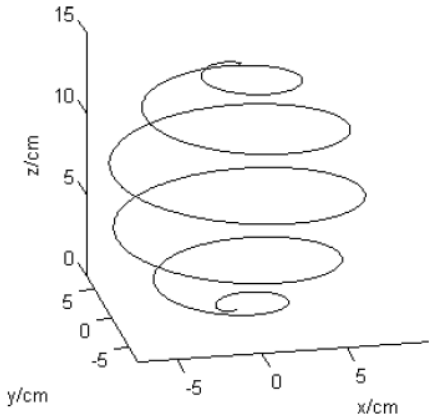

Geometry of spherical helix

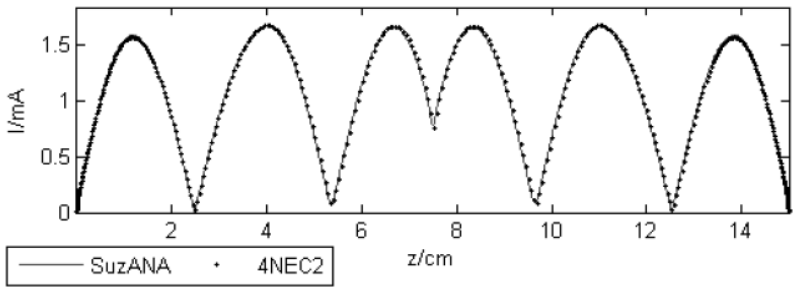

Amplitude of current distribution along the spherical helixat *f*=500MHz

Computational examples

Spherical helix

- Fig shows the horizontal and vertical radiation pattern of the spherical helix at *f*=1GHz.

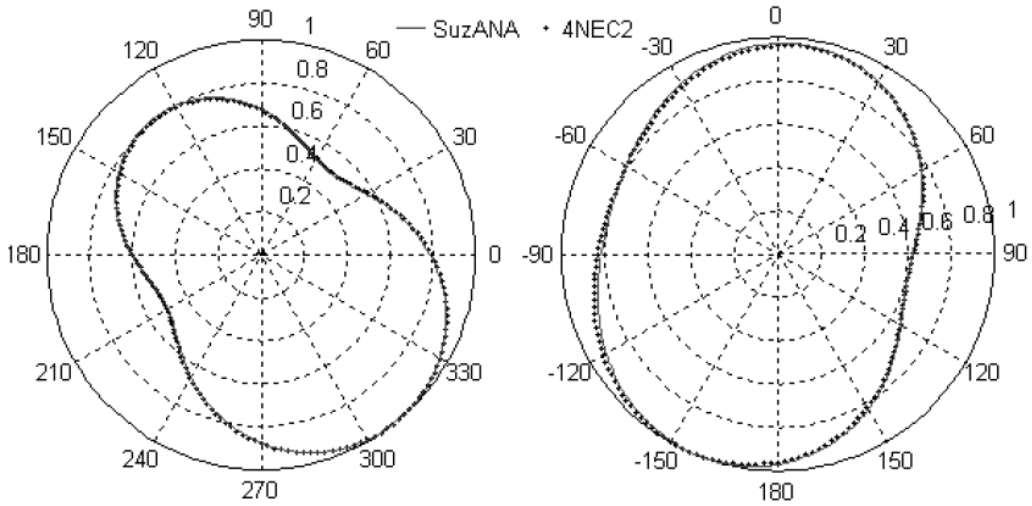

Horizontal plane Vertical plane

Radiation pattern of spherical helix at *f*=500MHz

Incident Field Dosimetry Procedures – HF Exposures

Radiation from WPT Systems

Computational examples

Spherical helix *– applications in Wireless Power Transfer (WPT) systems*

- Today's interests in Wireless Power Transfer (WPT) systems, near field communications and RFID systems have resulted in intensive research of electrically small antennas (ESAs).
- The size of ESAs is the main advantage in such systems, but at the same time leads to serious limitations.
- The most serious drawbacks of ESAs are as follows:
  - narrow bandwith,
  - small input impedance,
  - small radiation efficiency.
- Theoretical limits of e.g. WPT systems can be approached by specific design of ESA. One of the examples is spherical helix antenna design.

Radiation from WPT Systems

Computational examples

Spherical helix *– applications in Wireless Power Transfer (WPT) systems*

Advances of SHA use:

- ✓ Technique of **multiple folding** for increasing overall radiation efficiency:
  - N multiple-folded arms (assuming equal current along each arm) → radiation resistance increases with N*N and ohmic losses with N
- ✓ If **inductive feed loop** is used, by changing the distance between loop and antenna input impedance can be easily adjusted
- ✓ Spherical coil has higher radiation efficiency than cylindrical coil in the same physical volume which leads to **higher radiation efficiency**

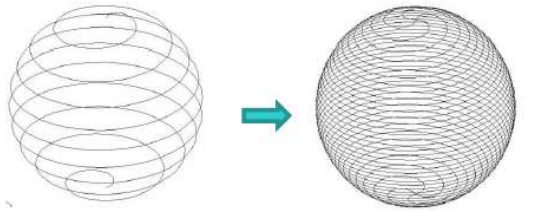

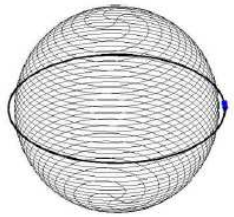

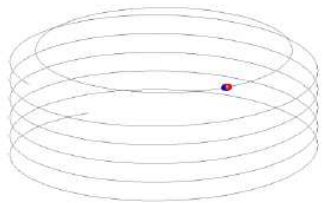

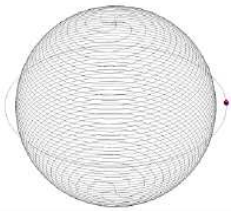

Computational examples

Spherical helix *– applications in Wireless Power Transfer (WPT) systems*

- Two examples are presented – single-arm SHA with voltage source in the middle of helix and four-arm folded SHA with indirect feed loop
- Results obtained using GB scheme of IBEM are compared with the results from FEKO
- NOTE:
  FEKO uses Method of Moments in which each segment has two nodes and base functions are linear → **linear elements!**
  GB-IBEM: each segment has three nodes with second order polynomial base functions → **curvilinear elements!**

Incident Field Dosimetry Procedures – HF Exposures

Radiation from WPT Systems

Computational examples

Spherical helix *– applications in Wireless Power Transfer (WPT) systems:* SINGLE-ARM SHA

- radius of a sphere *R = 0.208 m*
- radius of wire *r = 3 mm*
- number of turns *N=9.1*
- operating frequency *f = 13.56 MHz*
- perfect conductor
- voltage source: 1V in the middle of the helix

- Geometry of single-arm SHA is given in spherical coordinates as:

$$r = R,$$
$$\vartheta = 0 : \pi,$$
$$\varphi = (\cos\vartheta + 1)$$

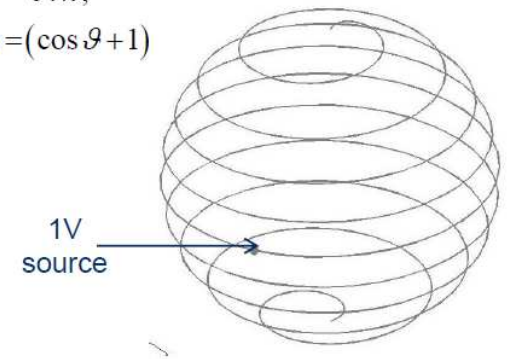

Single-arm SHA geometry

Computational examples

Spherical helix *– applications in Wireless Power Transfer (WPT) systems:* SINGLE-ARM SHA

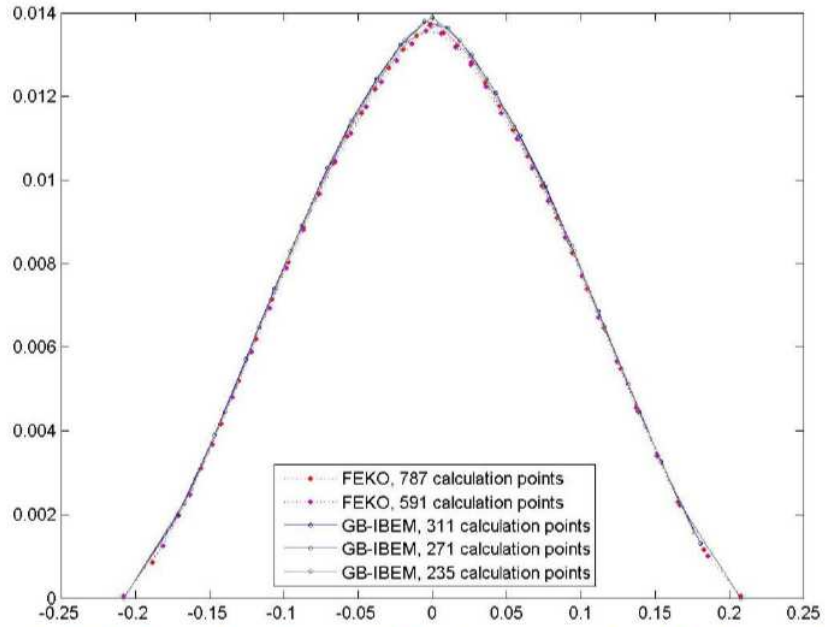

Current distribution along the z axis for given geometry of single-arm SHA

Incident Field Dosimetry Procedures – HF Exposures

Radiation from WPT Systems

Computational examples

Spherical helix *– applications in Wireless Power Transfer (WPT) systems:* 4-ARM SHA

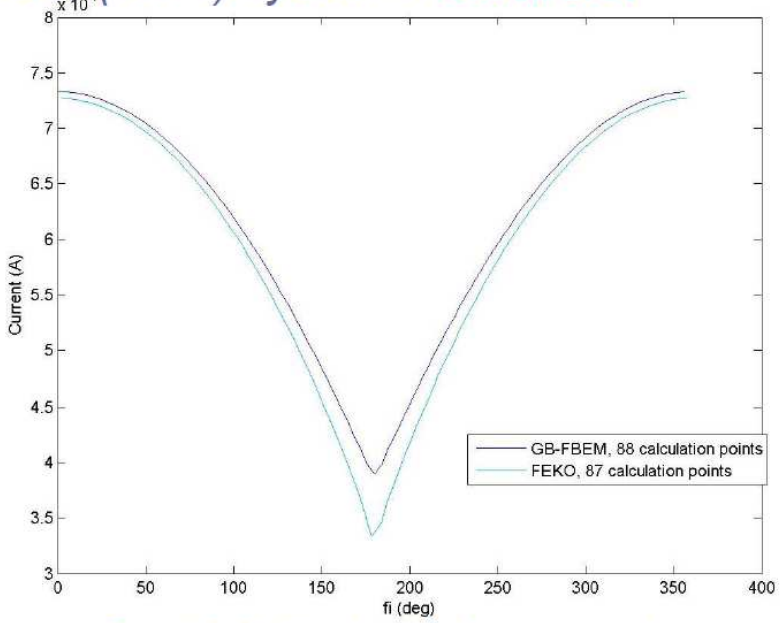

Current distribution along the loop versus angle φ

Computational examples

Spherical helix *– applications in Wireless Power Transfer (WPT) systems:* 4-ARM SHA

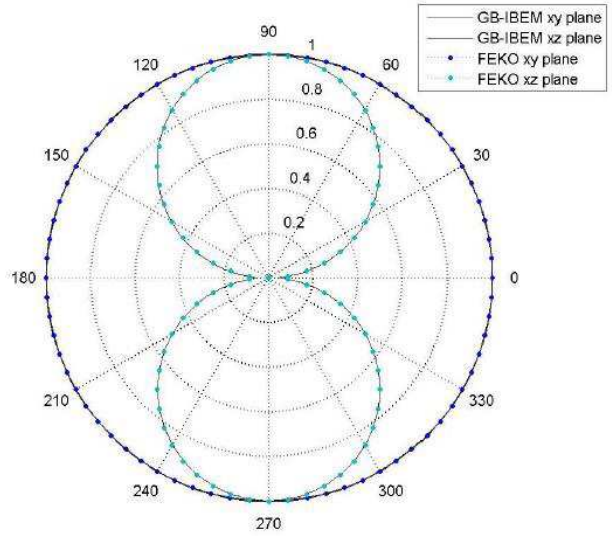

Radiation pattern: normalized directivity in horizontal (xy) and vertical (xz) planes

Radiation from WPT Systems

Incident Field Dosimetry Procedures – HF Exposures

Computational examples

Multiple helix

- The last example deals with a multiple helix configuration.
- The helix at the center of coordinate system is the active antenna. The distance between the wire axes is 0.5m

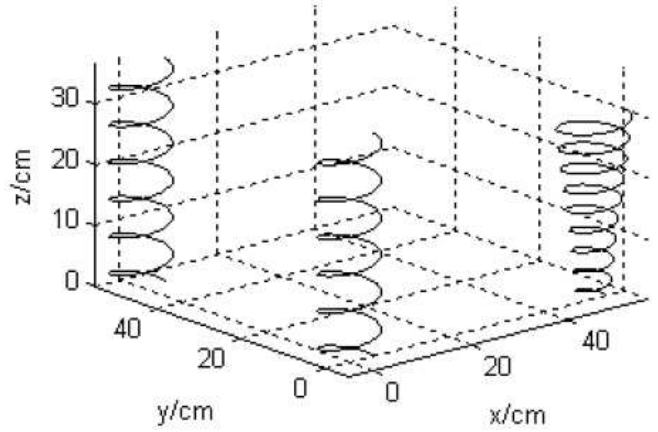

System of multiple helical antennas

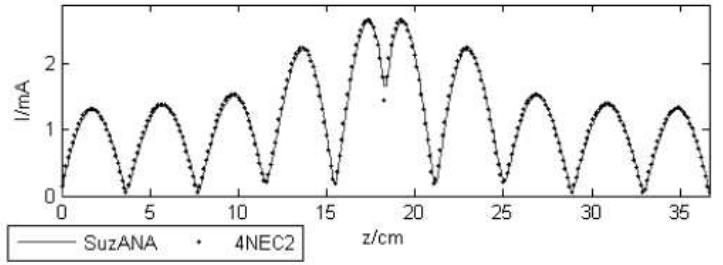

The current amplitude on active cylindrical helix at *f*=750MHz

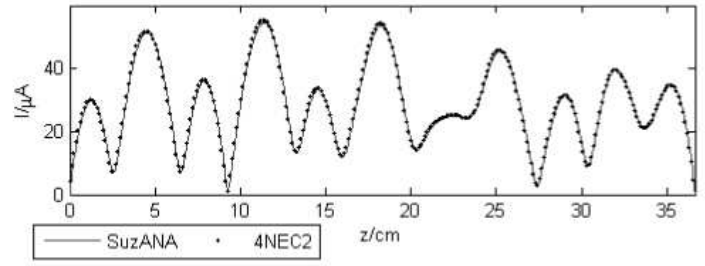

The current amplitude on passive cylindrical helix at *f*=750MHz

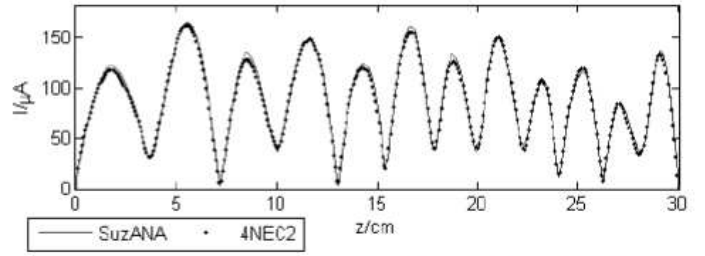

The current along passive conical helix at *f*=750MHz

INTERNAL FIELD DOSIMETRY PROCEDURES – LF &HF EXPOSURES

Simplified Models

- Simplified canonical models of the human body in the frequency and time domain, respectively.
- Frequency domain (FD) analysis involves parallelepiped body model and antenna body models, single straight thick wire body model and multiple wire representation of the body.
- Time domain (TD) analysis deals with straight thin wire antenna model of the body.
- FD antenna models are based on the Pocklington integro-differential approach while time domain formulation is based on the Hallén integral equation approach.
- Finally, transmission line body models in both FD and TD are given.

INTERNAL FIELD DOSIMETRY PROCEDURES – LF &HF EXPOSURES

Simplified Models

INTRODUCTORY REMARKS

- The starting point in the analysis of interaction of humans with time-harmonic or transient electromagnetic fields is the knowledge of the induced currents and fields inside the human body.
- A simplified approach involves the representation of the human body with a geometry with a high degree of simplification (canonical geometry), such as parallelepiped or cylinder.
- The equivalent parasitic antenna representation of the body deals with Pocklington or Hallén integral equation formulation, in either TD or FD.
- The electrical properties of the body are taken into account via the load term in the Pocklington equation for a thick cylinder.
- From the current distribution, one can readily calculate the induced current density and the electric field, the specific absorption rate, or other parameters of interest.
- This provides simple and efficient procedures for a rapid estimation of these electromagnetic phenomena.

Cylindrical models: Frequency domain analysis

At low frequencies near the power frequency f = 50 Hz, or 60 Hz the human body is a good conductor with an average conductivity of approximately 0.5 S/m.

If the body is assumed predominantly conducting the body can be represented as an equivalent cylindrical antenna model with a uniform cross section and conductivity.

Maximum current flows from the body into the ground when it is assumed that the person is standing bare footed on a good conducting ground. Under the same circumstances the cylindrical model can be extended to HF and transient exposures, respectively.

A person exposed to the EMF from ELF to GSM frequencies can be represented by an imperfectly conducting cylinder of length L and radius a.

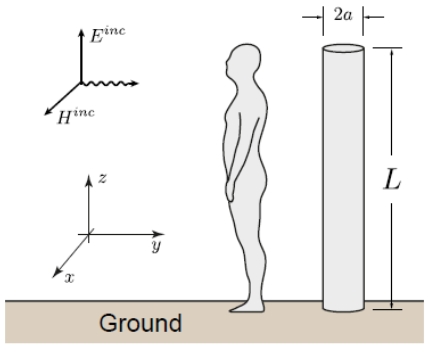

FIG: The equivalent antenna model of the human body

INTERNAL FIELD DOSIMETRY PROCEDURES – LF &HF EXPOSURES

Simplified Models

INTRODUCTORY REMARKS

- The starting point in the analysis of interaction of humans with time-harmonic or transient electromagnetic fields is the knowledge of the induced currents and fields inside the human body.
- A simplified approach involves the representation of the human body with a geometry with a high degree of simplification (canonical geometry), such as parallelepiped or cylinder.
- The equivalent parasitic antenna representation of the body deals with Pocklington or Hallén integral equation formulation, in either TD or FD.
- The electrical properties of the body are taken into account via the load term in the Pocklington equation for a thick cylinder.
- From the current distribution, one can readily calculate the induced current density and the electric field, the specific absorption rate, or other parameters of interest.
- This provides simple and efficient procedures for a rapid estimation of these electromagnetic phenomena.

Cylindrical models: Frequency domain analysis

At low frequencies near the power frequency f = 50 Hz, or 60 Hz the human body is a good conductor with an average conductivity of approximately 0.5 S/m.

If the body is assumed predominantly conducting the body can be represented as an equivalent cylindrical antenna model with a uniform cross section and conductivity.

Maximum current flows from the body into the ground when it is assumed that the person is standing bare footed on a good conducting ground. Under the same circumstances the cylindrical model can be extended to HF and transient exposures, respectively.

A person exposed to the EMF from ELF to GSM frequencies can be represented by an imperfectly conducting cylinder of length L and radius a.

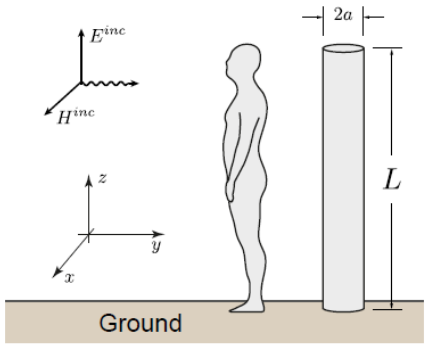

FIG: The equivalent antenna model of the human body

INTERNAL FIELD DOSIMETRY PROCEDURES – LF &HF EXPOSURES

Simplified Models

Pocklington equation formulation for LF exposures

The current distribution along the human body can be obtained as the solution of the Pocklington integro-differential equation for thick loaded straight wire.

This integro-differential equation can be derived starting from the following:

$$\vec{E} = -\nabla\varphi - j\omega\vec{A}$$

The vector and magnetic potential are coupled through the previously defined Lorentz Gauge:

$$\nabla\vec{A} = -j\omega\mu\varepsilon\varphi$$

As only axial component of the magnetic potential A_z along the cylinder exists, A_z can be represented by the integral of the axial current I(z) flowing along the equivalent dipole antenna:

$$E_z = \frac{1}{j\omega\mu\varepsilon}\left(\frac{\partial^2 A_z}{\partial z^2} + k^2 A_z\right) \qquad A_z = -\frac{\mu}{4\pi}\int_{-L}^{L}\frac{1}{2\pi}\int_{0}^{2\pi}\frac{e^{-jkR}}{R}I(z')\,dz'\,d\phi$$

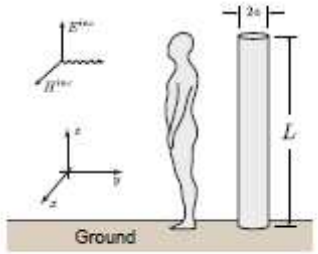

FIG: The equivalent antenna model of the human body

Pocklington equation formulation for LF exposures

Using the continuity conditions for the tangential electric field:

$$E_z^{inc} + E_z^{sct} = I(z)\,Z_L(z)$$

After some work the Pocklington integro-differential equation is obtained:

$$E_z^{inc}(z,a) = -\frac{1}{j4\pi\omega\varepsilon_0}\int_{-L}^{L}\left(\frac{\partial^2}{\partial z^2} + k^2\right)g_E(z,z')\,I(z')\,dz' + Z_L(z)\,I(z)$$

where $g_E(z,z_0)$ is given by:

$$g_E(z,z') = \frac{1}{2\pi}\int_{0}^{2\pi}\frac{e^{-jkR}}{R}\,d\phi \qquad \text{where:} \quad R = \sqrt{(z-z')^2 + 4a^2\sin^2\frac{\phi}{2}}$$

The conducting and dielectric properties of the body are taken into account by the properties of the impedance Z_L.

INTERNAL FIELD DOSIMETRY PROCEDURES – LF &HF EXPOSURES

Simplified Models

Numerical solution of the Pocklington equation

The Pocklington integral equation can be solved numerically using the boundary element formalism.

The integral equation can be written in an operator form:

$$K\,I = E$$

The unknown current is expanded:

$$I \cong I_n = \sum_{i=1}^{n} \alpha_i f_i \qquad \text{resulting in:} \quad K\,I \cong K\,I_n = \sum_{i=1}^{n} \alpha_i K f_i$$

Residual R_n can be defined as: $R_n = K\,I_n - E$

and weighted with respect to certain weighting functions W_j

$$\int_\Omega R_n W_j^*\, d\Omega = 0; \quad j = 1, 2, \ldots, n \qquad \langle R_n, W_j \rangle = \int_\Omega R_n W_j^*\, d\Omega$$

Numerical solution of the Pocklington equation

Choosing Wj = fj, the Galerkin-Bubnov procedure yields:

$$\sum_{i=1}^{n} \alpha_i \int_\Omega K(f_i) f_j\, d\Omega = \int_\Omega E\, f_j\, d\Omega; \quad j = 1, 2, \ldots, n$$

Taking into account the boundary conditions for current at the free ends of the thin wires, and after integration by parts, results in weak Galerkin formulation of the integral equation

$$\sum_{i=1}^{n} \alpha_i \frac{1}{j4\pi\omega\varepsilon} \left(-\int_{-L}^{L} \frac{df_j(z)}{dz} \int_{-L}^{L} \frac{df_i(z)}{dz'} g_E(z,z')\, dz'\, dz + k_1^2 \int_{-L}^{L} f_i(z') g_E(z,z')\, dx\, dx' \right) +$$
$$+ \int_{-L}^{L} Z_S(z) f_j(z) f_i(z)\, dz = -\int_{-L}^{L} E_z^{inc}(z) f_j(z)\, dz; \quad j = 1, 2, \ldots, n$$

The resulting matrix equation system is given by:

$$\sum_{i=1}^{M} [Z]_{ji} \{I\}_i = \{V\}_j, \quad j = 1, 2, \ldots, M$$

INTERNAL FIELD DOSIMETRY PROCEDURES – LF &HF EXPOSURES

Simplified Models

Numerical solution of the Pocklington equation

The submatrix given by:

$$[Z]_{ji} = -\frac{1}{j4\pi\omega\varepsilon}\left(\int_{\Delta l_j}\{D\}_j\int_{\Delta l_i}\{D'\}_i^T g_E(z,z')\,dz'\,dz + k^2\int_{\Delta l_j}\{f\}_j\int_{\Delta l_i}\{f\}_i^T g_E(z,z')\,dz'\,dz\right) + \int_{\Delta l_j} Z_L(z)\{f\}_j\{f\}_i^T\,dz$$

Assuming a constant incident electric field along the wire:

$$E_z^{inc} = E_0$$

the evaluation of the right-hand side vector results in:

$$V_{1j} = \int_{-\Delta l/2}^{\Delta l/2} E_0\frac{z_{j+1}-z}{\Delta l}\,dz = E_0\frac{\Delta l}{2}$$

$$V_{2j} = \int_{-\Delta l/2}^{\Delta l/2} E_0\frac{z-z_j}{\Delta l_g}\,dz = E_0\frac{\Delta l}{2}$$

Numerical solution of the Pocklington equation

In the ELF region (50/60 Hz) the cylinder representing the human body can be considered as a conducting medium whose impedance per unit length is:

$$Z_L(z) = \frac{1}{a^2\pi\sigma} + Z_c$$

where $Z_c = 1/jwC$, and C is the capacitance between the soles of the feet and their image in the earth. If the foot-soles are bare and in direct contact with the moist earth (well-grounded body) then the capacity can be neglected, i.e. $Z_c = 0$.

From the axial current the induced current density is calculated using:

$$J_z(z) = \frac{I_z(z)}{a^2\pi}$$

as well as the induced electric field:

$$E_z(z) = \frac{J_z(z)}{\sigma}$$

INTERNAL FIELD DOSIMETRY PROCEDURES – LF &HF EXPOSURES

Simplified Models

Analytical modeling of the human body - Hallen equation for LF and HF exposures

The total axial current induced in the human body when this is approximated by a parasitic cylindrical antenna with half length L, and mean radius a can be obtained by analytically solving the Hallén integral equation type

$$\int_0^z I_z(z')\frac{e^{-jkR}}{R}\,dz' = -j\frac{4\pi}{Z_0}\left[K\cos kz + \frac{1}{k}E_z^{inc} - Z_L\int_0^z I_z(s)\sin k(z-s)\,ds\right]$$

For the LF part of the electromagnetic spectrum the solution of equation is:

$$I_z(z) = j2\pi\frac{kL^2}{\psi_1 Z_0}E_z^{inc}\left[1-\left(\frac{z}{L}\right)^2\right] \qquad \text{where:} \qquad \psi_1 = 2\ln\frac{2L}{a} - 3$$

The solution for higher frequencies is:

$$I_z(z) = j2\pi\frac{kL^2}{\psi_2 Z_0}E_z^{inc}\left[1-\left(\frac{z}{L}\right)^2\right]\left[1 - j4\pi\frac{Z_L}{Z_0 k\psi_2}\right]$$

where: $$\psi_2 = \frac{1}{1-\cos kL}\left\{C_a(L,0) - C_a(L,L) - [E_a(L,0) - E_a(L,L)]\cos kL\right\}$$

Analytical modeling of the human body - Hallen equation for LF and HF exposures

The integral equation for the total current $I_{1z}(z)$ induced in a conductor with the half-length L and radius a when exposed to an incident electric field E_{inc} parallel to the cylinder is

$$\int_{-L}^{L} I_{1z}(s)\frac{e^{-jk_2 r}}{r}\,ds = -\frac{j4\pi}{\xi_0}\left(C\cos k_2 z + \frac{1}{2}V\sin k_2|z| + U^{inc} - Z^i P_z\right)$$

where: $\xi_0 = 120\pi\,\Omega$

The formula for the total axial current $I_{1z}(z)$ induced in the body when exposed to E_{inc} is

$$I_{1z}(z) = \frac{j4\pi}{\xi_0\psi_u}\frac{E_{2z}^{inc}}{k_2}\left[\frac{(\cos k_2 z - \cos k_2 L)}{\cos k_2 L} - \frac{Z_L}{(Z_0+Z_L)}\frac{(1-\cos k_2 L)}{\cos k_2 L}\frac{\sin k_2(L-z)}{\sin k_2 L}\right]$$

where: $$\psi_u = \psi_u(0) = \frac{C_a(L,0) - C_a(L,L) - (E_a(L,0) - E_a(L,L))\cos k_2 L}{1-\cos k_2 L}$$

The current density and electric field in the body are given by: $$J_{1z}(z) = \sigma_1 E_{1z}(z) = \frac{I_{1z}(z)}{A(z)}$$

INTERNAL FIELD DOSIMETRY PROCEDURES – LF &HF EXPOSURES

Simplified Models

Multiple wire model of the body

The effects of the arms being raised to various angles to the vertical body axis are modeled by attaching wires of radius a = 0.05 m and length L = 0.8 m to the cylindrical antenna.

The wires representing the arms are attached at a height of 1.4 m from the ground.

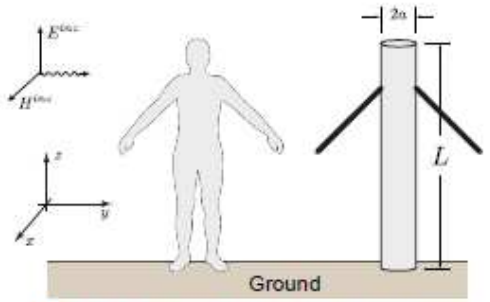

FIG: Equivalent antenna model of the body with the arms raised

$$\vec{E}_{\tan} = (j\omega\vec{A} + \nabla\varphi)_{\tan}$$

$$\vec{A}(\vec{r}) = \frac{\mu}{4\pi}\iint_S \vec{J}(\vec{r}\,')\frac{e^{-jk|\vec{r}-\vec{r}\,'|}}{|\vec{r}-\vec{r}\,'|}dS(\vec{r}\,')$$

$$\varphi(\vec{r}) = -\frac{1}{j4\pi\omega\varepsilon}\iint_S \nabla'_S\vec{J}(\vec{r}\,')\frac{e^{-jk|\vec{r}-\vec{r}\,'|}}{|\vec{r}-\vec{r}\,'|}dS(\vec{r}\,')$$

The axial current distribution is obtained by integrating the current density over the cross-section of the body.

The numerical solution can be found using the method of moments (MoM).

Computational examples: LF exposures

The first example deals with a well-grounded human body exposed to the 60 Hz overhead power line electric field.

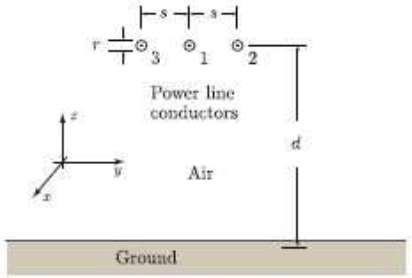

FIG: Geometry of a three-wire power line

The component of the electric field tangential to the body is assumed to be E = 10 kV/m.

The tissue conductivity varies from 0.01 S/m (bone) to 0.6 S/m (muscle).

Table: Foot current on antenna model of the human body E_{inc} = 10 kV/m, 60 Hz

Foot current	BEM	FDTD	Analytical
$I_z(0)$ [uA]	191	179	183

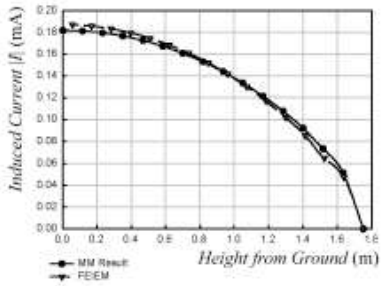

FIG: Axial current induced in the body due to the incident field (10 kV/m, 60 Hz)

INTERNAL FIELD DOSIMETRY PROCEDURES – LF &HF EXPOSURES

Simplified Models

Computational examples: LF exposures

Knowing the current distribution, one can easily determine the current density and the electric field induced in the body.

Table: ELF exposure parameters

$I_z(0)$ [uA]	$J_z(0)$ [mA/m²]	E_z [mV/m]
191	3.1	6.2

The basic restrictions for ELF exposure according to the International Commission on Non-Ionizing Radiation Protection – ICNIRP Guidelines [19] are given in terms of permissible values for the induced current density inside the body.

It has to be underlined that the obtained value of 3.1 mA/m² is less than the limit of 10 mA/m² for occupational exposure, but exceeds the limit of 2 mA/m² for general public exposure.

Computational examples: LF exposures

Next example deals with the power line with maximum current of I = 300 A at operating voltage V = 100 kV at f = 60 Hz.

The conductors are spaced horizontally at distance s = 3 m from each other and suspended at a height d = 15 m from the ground.

The person is standing at a point y = 7 m from the reference origin facing the positive y direction. The body is exposed to all 6 components of the field.

The incident field is E_{inc} = 530 V/m, 60 Hz.

Table: Foot current on antenna model of the human body E_{inc} = 530 V/m, 60 Hz

Result	MoM	BEM	Analytical
Foot current $I_z(0)$ [uA]	j9.64	j10.11	j9.8
Current density [uA/m²]	j157	j169	j163

The current density induced by the external field in individual organs inside the body can be obtained from the axial current distribution at various heights.

INTERNAL FIELD DOSIMETRY PROCEDURES – LF &HF EXPOSURES

Simplified Models

Computational examples: LF exposures

The next example the human body is exposed to electric field of 60 Hz from a power line, E_{inc} = 1081.2 V/m.

Table: Comparison of the analytical and numerical results

Physical parameter	GB-IBEM	Analytical	Discrepancy [%]
I (z=0) [uA]	7.85	8.22	4.5
J (z=0) [uA/m²]	13.08	13.7	4.5
E (z=0) [uV/m]	261.67	274.6	4.7
P (z=0) [nW/m³]	17.12	18.85	9.2

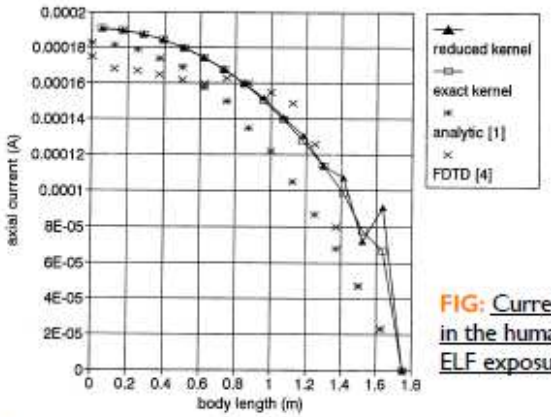

FIG: Current distribution induced in the human body obtained for ELF exposure

Computational examples: LF exposures

The results presented so far are obtained by considering the equivalent antenna of the body with both arms resting close to the sides.

The effects of the arms being raised to various angles to the vertical body axis are also modeled by attaching wires of radius a = 0.05 m and length L = 0.8 m to the cylindrical antenna.

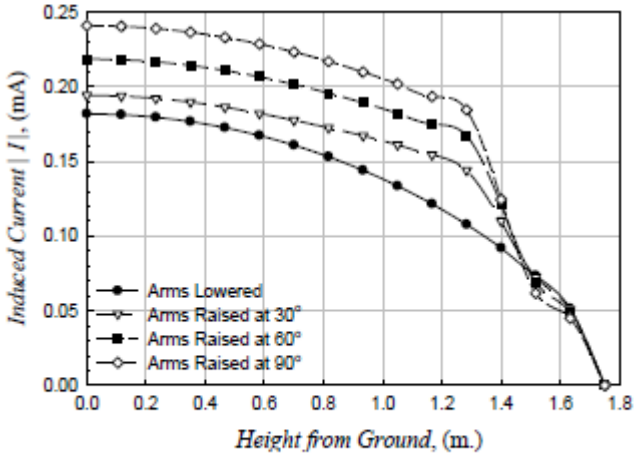

FIG: Current induced with arms stretched out by incident field of 1 kV/m, 60 Hz

Note that the outstretched arms increase the induced current on the body.

INTERNAL FIELD DOSIMETRY PROCEDURES – LF &HF EXPOSURES

Simplified Models

Computational examples: LF exposures

The next example the human body is exposed to electric field of 60 Hz from a power line, E_{inc} = 1081.2 V/m.

Table: Comparison of the analytical and numerical results

Physical parameter	GB-IBEM	Analytical	Discrepancy [%]
I (z=0) [uA]	7.85	8.22	4.5
J (z=0) [uA/m²]	13.08	13.7	4.5
E (z=0) [uV/m]	261.67	274.6	4.7
P (z=0) [nW/m³]	17.12	18.85	9.2

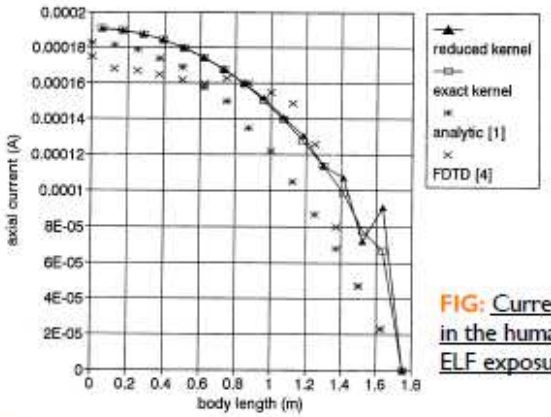

FIG: Current distribution induced in the human body obtained for ELF exposure

Computational examples: LF exposures

The results presented so far are obtained by considering the equivalent antenna of the body with both arms resting close to the sides.

The effects of the arms being raised to various angles to the vertical body axis are also modeled by attaching wires of radius a = 0.05 m and length L = 0.8 m to the cylindrical antenna.

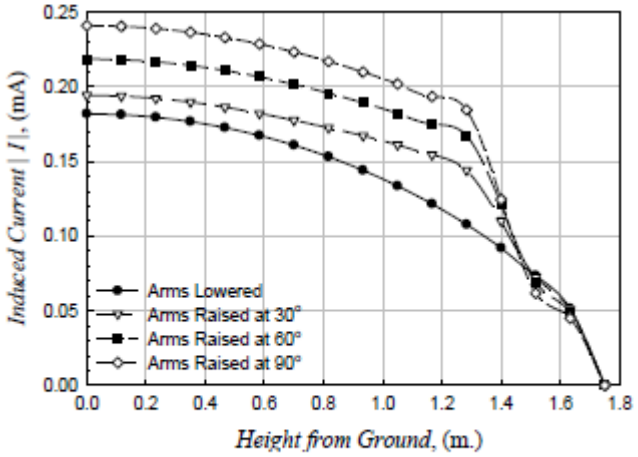

FIG: Current induced with arms stretched out by incident field of 1 kV/m, 60 Hz

Note that the outstretched arms increase the induced current on the body.

INTERNAL FIELD DOSIMETRY PROCEDURES – LF &HF EXPOSURES

Simplified Models

Computational examples: HF exposures

The first example for HF sources deals with the human exposed to a field from a broadcast tower.

A broadcast tower is operating at 700 kHz and the incident field is E_{inc} = 1 V/m.

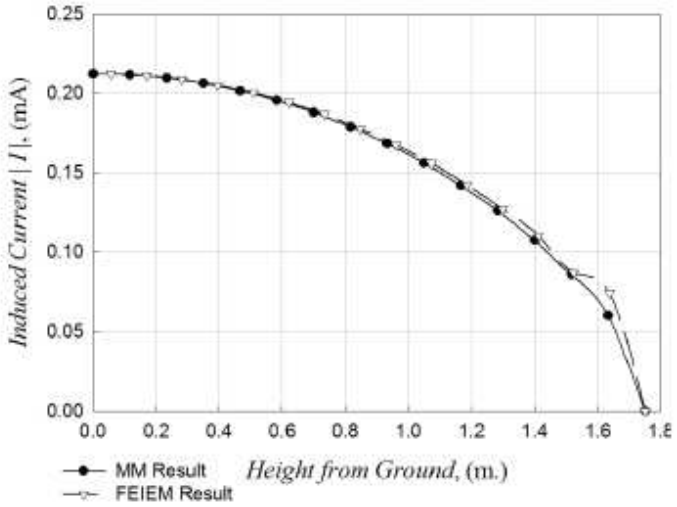

FIG: Current induced by the field in vicinity of broadcast tower

Computational examples: HF exposures

Next example deals with the exposure to a field from missile boat antenna.

The current distribution induced along the body in the vicinity of a monopole antenna on a navy missile boat operating at 5 MHz with the field Einc = 10 V/m is shown:

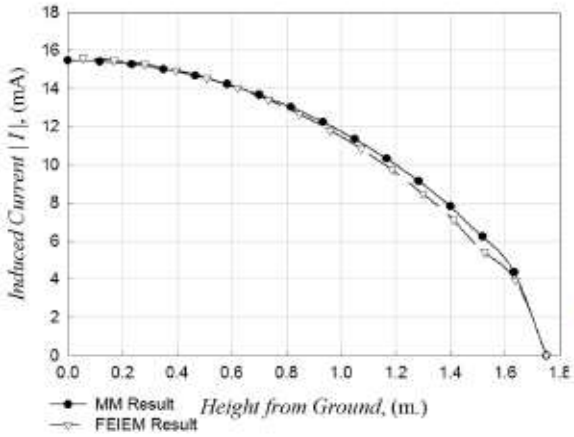

FIG: Current induced by the field in vicinity of a missile boat antenna

The current in this case is about two orders of magnitude larger than that due to the broadcast tower and the power lines.

INTERNAL FIELD DOSIMETRY PROCEDURES – LF &HF EXPOSURES

Simplified Models

Computational examples: HF exposures

The last example in this section is related to the radiation from shipboard antenna system.

Naval personnel standing on the metal deck of the ship are exposed to the near fields of several vertical antennas operating at frequencies from 1–30 MHz. The electromagnetic field close to such an antenna is quite large and the induced current is significant.

The HF transmitter characteristics are: 100 W maximum output power, HF frequency band (3–30 MHz), 5 MHz transmitting frequency during measurement, SSB AM modulation, 6 m long vertical whip antenna located 16.5 m above the deck.

FIG: Measurement points on the ship deck

The shipboard electromagnetic environment consisted of:

- analysed sources antennas;
- other emitters and antennas on the topside;
- metallic (perfectly conductive) objects on the deck
- cabins of different size and shape and other object
- metallic (perfectly conductive) ship hull;
- sea (ground plane).

Computational examples: HF exposures

The vertical component of HF electric field (E_z) was measured at each point.

FIG: Measurement points on the ship deck

The SAR and the current induced in the human body are obtained for the each value of measured electric field E_z.

Calculations of the current distribution and current density and SAR are undertaken at f = 5 MHz, 0.5S/m, ε_r = 50, k_2 = 0.105m^{-1},h = 1.75m, Z_L = 0, a = 0.14 m.

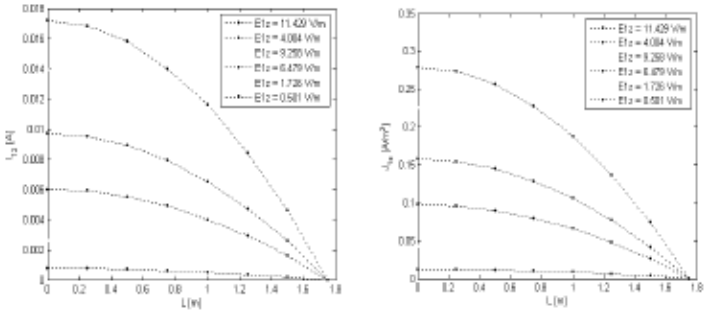

FIG: Axial current (left) and current density distribution (right) along the human body

Maximum value of whole body averaged SAR is SAR_{WB} = 0.079899 mW/kg which is found to be far below 0.08 W/kg (ICNIRP exposure limit for general public).

It is evident that the obtained values of SAR, current density and induced currents in the human body are found to be below appropriate limits.

INTERNAL FIELD DOSIMETRY PROCEDURES – LF &HF EXPOSURES

Simplified Models

Time domain modeling - exposure of humans to transient radiation

The time domain human equivalent antenna model is based on the Hallén integral equation.

A solution of this integral equation can be found using the time domain Galerkin-Bubnov scheme of the boundary element method (GB-BEM).

Once determining the transient response of the human body one can readily calculate a distribution of the average and root mean square values of the space-time varying current flowing through the body as a measure of the transient behavior of the induced current.

The main advantage of the proposed formulation, when compared to a more complex realistic models, is its simplicity and efficiency in getting the rapid estimation of the transient phenomena.

Time domain formulation

The time domain analysis of the transient electromagnetic field illuminating the well-grounded human body standing vertically on the perfectly conducting (PEC) ground, is based on the human equivalent antenna concept.

The dimensions of the human equivalent antenna (L = 1.8 m, a = 5 cm) are within the thin wire approximation and the effective bandwidth of the EMP frequency spectrum is 5 MHz. This bandwidth is also within the frequency range of the human equivalent antenna which is stated to be valid from 50 Hz to 110 MHz.

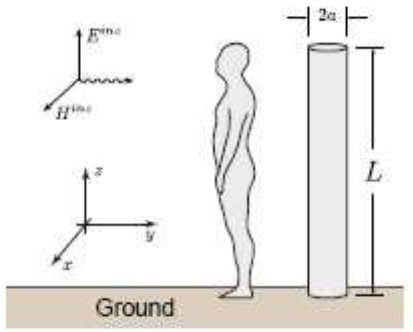

FIG: The equivalent antenna model of the human body

INTERNAL FIELD DOSIMETRY PROCEDURES – LF &HF EXPOSURES

Simplified Models

Time domain formulation

The Hallén integral equation is given by:

$$\int_0^L \frac{I(z',t-R/c)}{4\pi R}\,dz' = F_0\left(t-\frac{z}{c}\right)+F_L\left(t-\frac{L-z}{c}\right)+\frac{1}{2Z_0}\int_0^L E_z^{inc}\left(z',t-\frac{|z-z'|}{c}\right)dz'-$$
$$-\frac{1}{2Z_0}\int_0^L R_L(z')\,I\left(z',t-\frac{|z-z'|}{c}\right)dz'$$

where $I(z_0, t\text{-}R/c)$ is the unknown space-time dependent current to be determined, c is the velocity of light, Z_0 is the wave impedance of a free space, and R_L is the resistance per unit length of the antenna given by:

$$R_L = \frac{1}{a^2\pi\sigma}$$

The unknown functions $F_0(t)$ and $F_L(t)$ account for the multiple reflections of the current wave from the wire ends.

The numerical solution can be sought for using the weighted residual approach.

Measures of the transient response

Once obtaining the transient current flowing through the human body it is possible to calculate additional measures of the body transient response.

Average value of the transient current

$$I_{av} = \frac{1}{T_0}\int_0^{T_0} i(t)\,dt \qquad I_{av}\Big|_{z_i} = \frac{\Delta t}{2T_0}\sum_{k=1}^{N_t}\left[\left(I_i^k\right)+\left(I_i^{k+1}\right)\right]$$

From this parameter one can obtain a rapid estimation of the character of the given transient waveform properties.

Root-Mean-Square value of the transient current

$$I_{rms} = \sqrt{\frac{1}{T_0}\int_0^{T_0} i^2(t)\,dt} \qquad I_{rms}\Big|_{z_i} = \sqrt{\frac{\Delta t}{3T_0}\sum_{k=1}^{N_t}\left[\left(I_i^k\right)^2 + I_i^k\,I_i^{k+1} + \left(I_i^{k+1}\right)^2\right]}$$

The RMS value of the transient current is a more interesting parameter from the bioelectromagnetics point of view as it is directly associated with the thermal effect of a time varying current flowing through a lossy material.

INTERNAL FIELD DOSIMETRY PROCEDURES – LF &HF EXPOSURES

Simplified Models

Measures of the transient response

Instantaneous power

Instantaneous power delivered to a certain resistance R_L or to some resistive medium having equivalent resistance R_L by a transient current is defined by:

$$p(t) = R_L\, i^2(t)$$

On the other hand, the absorbed power in the human body is usually defined as a volume integral over power density, i.e.:

$$p_{rad}(t) = \int_V \sigma \left|\vec{E}(\vec{r},t)\right|^2 dV = \int_V \frac{\left|\vec{J}(\vec{r},t)\right|^2}{\sigma} dV \qquad p_{rad}\Big|_{t_k} = \frac{1}{\sigma S}\frac{\Delta z}{3}\sum_{i=1}^{M}\left[(I_i^k)^2 + I_i^k I_{i+1}^k + (I_{i+1}^k)^2\right]$$

where M denotes the total number of spatial segments along the cylinder.

Total absorbed energy

The total absorbed energy in the resistance or resistive material can be obtained by integrating the instantaneous power

$$W_{tot}(t) = \int_0^t p_{rad}(t)\, dt \qquad W_{tot}\Big|_{t_k} = \frac{\Delta t}{2}\sum_{k=1}^{N_t}\left[(P^k + P^{k+1})\right]$$

Measures of the transient response

The specific absorption

Once calculating the transient current flowing through the human body the specific absorption, a principal measure of this human body transient response, can be also determined in terms of circuit theory concept.

The power dissipated in the human body is usually given by a volume integral over power density P_d:

$$p_{rad}(t) = \int_V \overline{P}_d\, dV \qquad \text{where:} \quad \overline{P}_d = \sigma\left|\vec{E}(\vec{r},t)\right|^2 = \frac{\left|\vec{J}(\vec{r},t)\right|^2}{\sigma}$$

Specific absorption (SA) is defined as a quotient of the incremental energy (dW) absorbed by an incremental mass (dm) contained in the volume (dV) of given density (ρ):

$$SA = \frac{dW}{dm} = \frac{dW}{\rho dV}$$

After combining: $$SA = \int_0^{T_0} \frac{1}{\rho}\frac{\left|\vec{J}(\vec{r},t)\right|^2}{\sigma} dt$$

INTERNAL FIELD DOSIMETRY PROCEDURES – LF &HF EXPOSURES

Simplified Models

Measures of the transient response

The specific absorption

Assuming the transient current distribution to be approximately constant over the cylinder cross-section gives:

$$i(z,t) = J(z,t) \cdot S = J(z,t) \cdot a^2\pi$$

Finally, the SA can be expressed as:

$$SA(z) = \frac{1}{\rho\sigma S^2}\int_0^{T_0} i^2(z,t)\,dt = \frac{1}{\rho\sigma\left(a^2\pi\right)^2}\int_0^{T_0} i^2(z,t)\,dt$$

Once the induced current is known the SA can be represented, using the boundary element formalism, by the following relation:

$$SA = \frac{1}{\rho\sigma\left(a^2\pi\right)^2}\frac{\Delta t}{3}\sum_{k=1}^{N_t}\int_{t_k}^{t_k+\Delta t}\{T\}_k^T\{I\}_k\,dt$$

$$SA = \frac{1}{\rho\sigma\left(a^2\pi\right)^2}\frac{\Delta t}{3}\sum_{k=1}^{N_t}\left[\left(I_i^k\right)^2 + I_i^k I_{i+1}^k + \left(I_{i+1}^k\right.\right.$$

where N_t denotes the total number of time increments and I_i^k denotes the i-th node current at k-th time instant.

Numerical results

Example: Exposure to double-exponential EMP waveform

The transient current induced in the waist due to exposure to the standard double-exponential EMP waveform:

$$E_z^{inc}(t) = E_0\left(e^{-at} - e^{-bt}\right)$$ where: E_0 =1 kV/m, a=4 ·10⁶,b=4.76 ·10⁸.

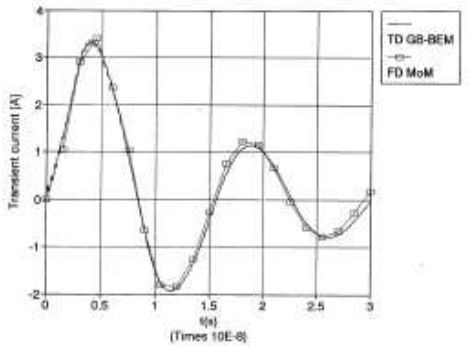

FIG: Transient current induced in the waist exposed to the double-exponential EMP waveform

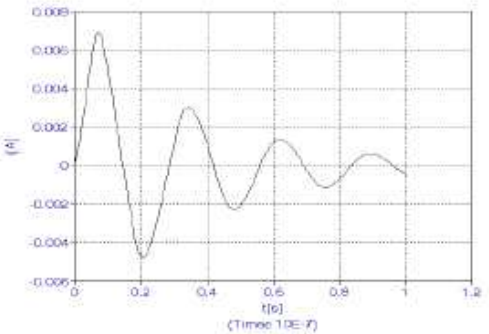

FIG: Transient current induced in the foot exposed to the double-exponential EMP waveform

The results obtained from the time domain simulation are compared with the results calculated by using the frequency domain method of moments code and inverse Fourier transform. The agreement seems to be satisfactory.

INTERNAL FIELD DOSIMETRY PROCEDURES – LF &HF EXPOSURES

Simplified Models

Numerical results

Example: Exposure to double-exponential EMP waveform

The related distribution of the average and rms values along the body.

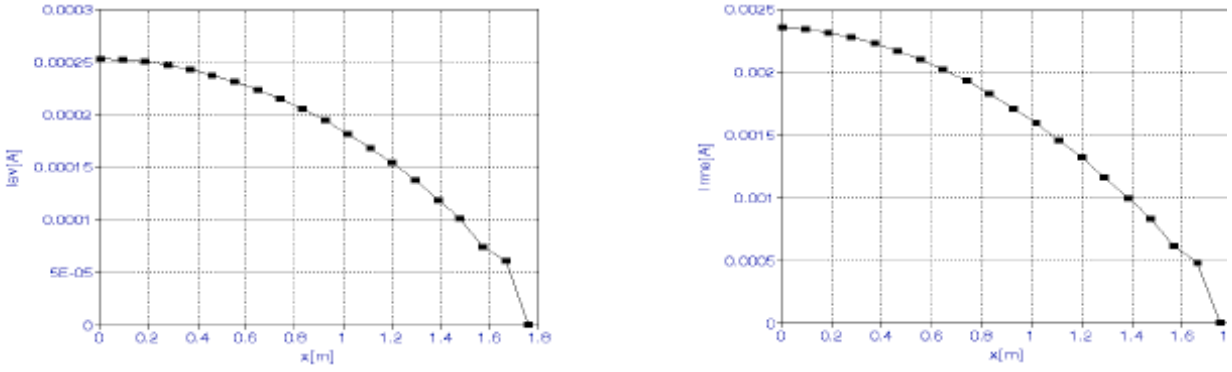

FIG: Spatial distribution of the average values (left) and RMS values (right) along the body for the EMP exposure

Numerical results

Example: Exposure to Gaussian pulse

$$E_z^{inc}(t) = E_0 e^{-g^2(t-t_0)^2}$$

Gaussian pulse parameters: E_0 = 1 V/m, $g = 2 \cdot 10^9$ s^{-1} and t_0 = 2 ns.

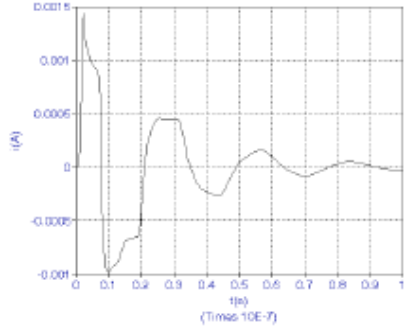

FIG: Transient current induced in the feet due to the Gaussian pulse exposure

As this pulse is a numerical equivalent of Dirac pulse the obtained transient exposure can be regarded as the impulse response of the human body.

Transient response to any other incident waveform then can be computed by performing a simple convolution.

INTERNAL FIELD DOSIMETRY PROCEDURES – LF &HF EXPOSURES

Simplified Models

Numerical results

Example: Exposure to Gaussian pulse

More information regarding the heating effect due to the Gaussian pulse exposure can be obtained from the spatial distribution of the rms values of the transient current:

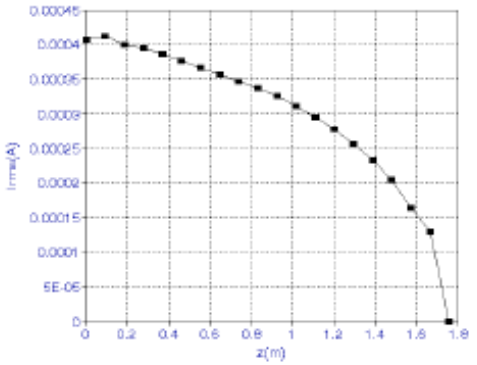

FIG: Spatial distribution of average values of the transient current due to the Gaussian pulse exposure

The Gaussian pulse induces the peak value of current around 1.5 mA in the feet corresponding to the equivalent DC current (approx. 0.4 mA).

Thus, the transient current induced in the feet would produce the same heating effect as the constant DC current of 0.4 mA.

Numerical results

Example: Exposure to Gaussian pulse

The transient behavior of the instantaneous power dissipated in the body is shown next:

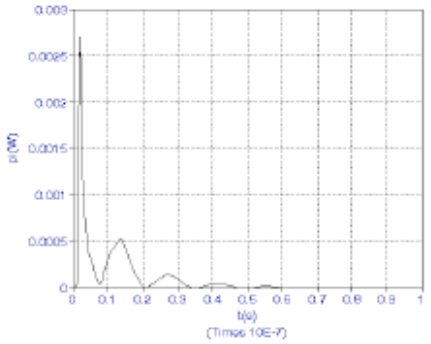

FIG: Instantaneous power dissipated within the body due to the Gaussian pulse exposure

It can be noticed that the power dissipation, with the peak value slightly above 2.5 mW occurs in the early time within the first 50 ns.

The same conclusion from the total energy absorbed in the body versus time.

It is clearly visible that body does not absorb a significant amount of energy after first 50 ns.

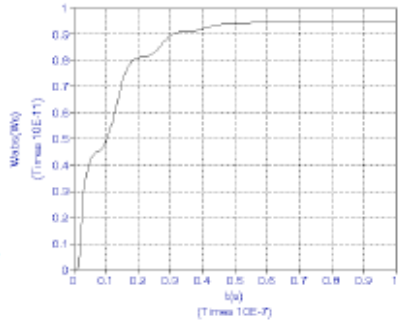

FIG: Total energy absorbed in the body due to the Gaussian pulse exposure

Simplified Models

INTERNAL FIELD DOSIMETRY PROCEDURES – LF &HF EXPOSURES

Numerical results

Example: Exposure to Gaussian pulse

Finally, the corresponding spatial distribution of the specific absorption along the body for the case of Gaussian pulse with: E_0 = 1 V/m, $g = 2 \cdot 10^9$ s^{-1} and t_0 = 2 ns, temporal step being:

$$E_z^{inc}(t) = u(t)$$

where u(t) denotes the unit step.

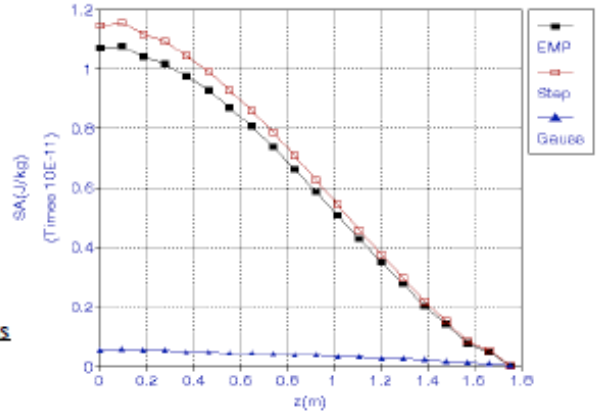

FIG: Specific absorption for various transient exposure waveforms

It is visible that the highest value of SA is achieved in the case of EMP exposure, and the lowest value in the case of Gaussian pulse exposure.

The maximal values of SA (below 12 pJ/kg), compared to the limits of 28.8 J/kg for whole body average, and 576 J/kg for 1-g spatial peak per pulse proposed by an IEEE Standard, stay far below the given threshold.

INTERNAL FIELD DOSIMETRY PROCEDURES – LF &HF EXPOSURES

Simplified Models

Transmission line models of the human body

The representation of the human body in terms of one or more vertical conductors can be formulated via Transmission Line (TL) approach or an enhanced TL theory.

The human body is represented by one or more vertical conductors and modeled via the TL theory in the frequency domain.

The related transient response is computed using the Inverse Fourier Transform (IFT).

Per unit length parameters are calculated for finite heights and the physical characteristics of the human and soil are taken into account.

The assessment of the space-time dependent current distribution induced in the body is carried out in the general case where the human is not directly in contact with the ground.

Transmission line models of the human body

A person standing vertically on the ground and exposed to an incident transient electric field oriented tangential to the body can be represented by multiple imperfectly conducting conductors of length l and radius a.

The calculation of the current distribution within the human body is based following equations:

$$\frac{d\,[U(z,\omega)]}{dz} + [Z(\omega)]\,[I(z,\omega)] = [E_z^e]$$

$$\frac{d\,[I(z,\omega)]}{dz} + [Y(\omega)]\,[U(z,\omega)] = 0$$

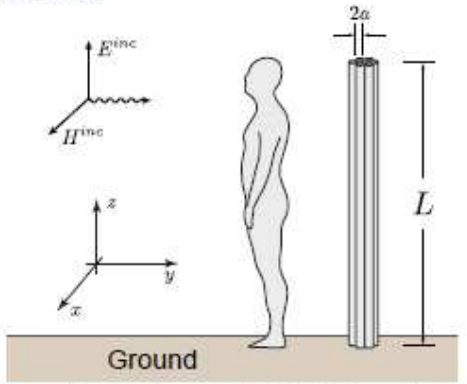

FIG: Multi-conductor model of the human body

where [Z(w)] is the longitudinal per unit length impedance matrix of the vertical multi-conductor system given by:

$$[Z] = j\omega\,[L] + [Z_w] + [Z_g]$$

INTERNAL FIELD DOSIMETRY PROCEDURES – LF &HF EXPOSURES

Simplified Models

Transmission line models of the human body

The equivalent representation with the incident electric field being replaced by two current generators to each conductor's terminations in the frequency domain is shown on figure.

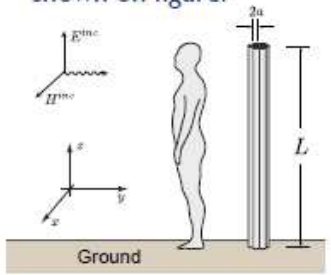

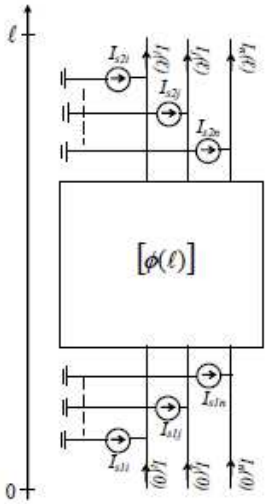

FIG: Equivalent model of a vertical multi-conductor configuration excited by an ex- ternal field

The terminal conditions:

$$U(0) = -Z_0\, I(0)$$
$$U(l) = Z_l\, I(l)$$

The contact of the human body with the ground can be taken into account by means of reactive impedance Z_0:

$$Z_0 = \frac{1}{j\omega C_0}$$

Transmission line models of the human body

The human body in a direct contact with the ground is considered.

The arms are represented by a set of wires attached to the thick cylinder.

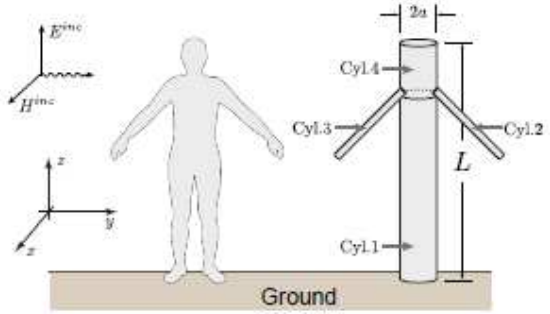

FIG: Model of the human body with arms outstretched

Table: Geometric parameters

	Length L_i [m]	Radius a_i [m]
Cylinder 1 (body)	1.5	0.14
Cylinder 2/3 (arms)	0.5	0.04
Cylinder 4 (head)	0.3	0.14

The set of equations for the coupling between a transmission line (n conductors) and an external electromagnetic field is given by:

$$\frac{d[U(z,\omega)]}{dz} + [Z]\,[I(z,\omega)] = [U_F(z,\omega)] \qquad \frac{d[I(z,\omega)]}{dz} + [Y]\,[U(z,\omega)] = [I_F(z,\omega)]$$

INTERNAL FIELD DOSIMETRY PROCEDURES – LF &HF EXPOSURES

Simplified Models

Computational examples: Single cylinder model

The human body is represented by a cylinder of length L = 1.75 m and radius a = 0.14 m, with the base and the top of the cylinder terminated by impedances Z_L and Z_0.

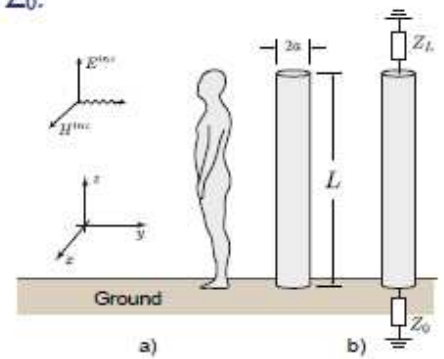

FIG: (a) Cylindrical model of the human body exposed to vertical electric field, (b) impedance Z_L and Z_0 on both ends of the cylinder

The three types of transient electric field excitations are considered: Gaussian pulse, temporal step function and EMP.

EMP pulse: E_0 =1.05V/m, a=4 ·10⁶s⁻¹,4.76 ·10⁸ s⁻¹,

Gaussian pulse: E_0 =1V/m,g=2 ·10⁹ s⁻¹,t_0 =2ns.

Computational examples: Single cylinder model

FIG: Transient current induced in the feet due to EMP exposure (left), temporal time step (middle), and Gaussian pulse exposure (right) obtained using:A) TL model, B) Antenna model.

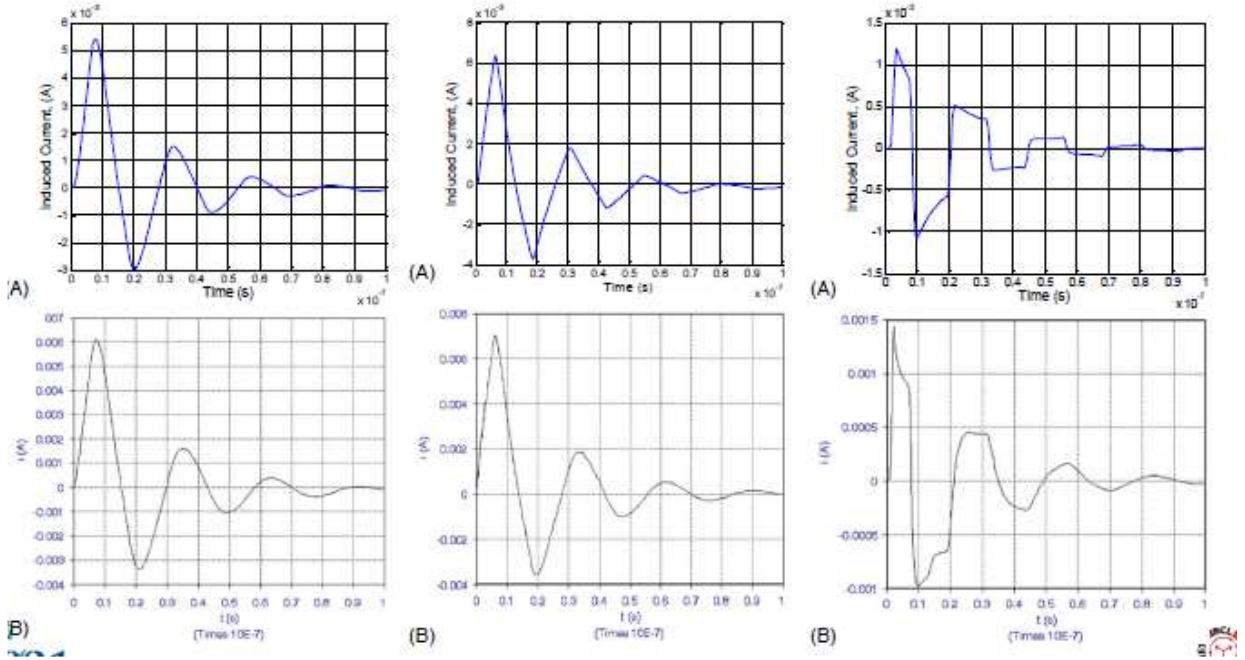

INTERNAL FIELD DOSIMETRY PROCEDURES – LF &HF EXPOSURES

Simplified Models

Computational examples: Single cylinder model

The effects due to the soil conductivity and the capacitance effect are investigated.

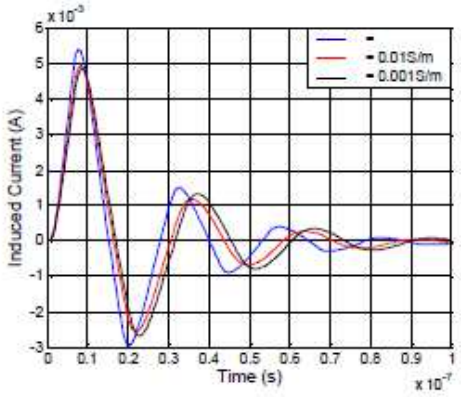

FIG: Transient current induced in the feet due to the double-exponential pulse exposure for different value of conductivity

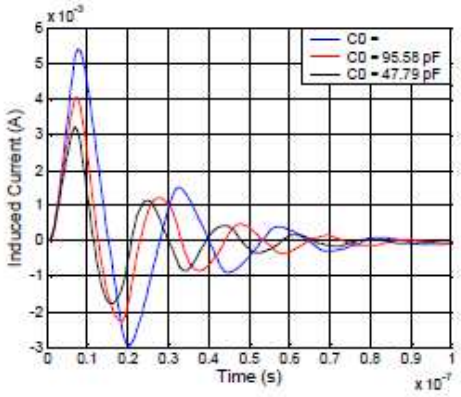

FIG: Transient current induced in the feet of grounde and ungrounded human due to the double exponentia pulse exposure for different value of capacitance

It can be seen that certain differences occur especially if the perfect conductivity of the body is assumed.

The assumption of direct contact of the body with the earth implies the higher values of the induced transient current. Thus, the transient response of the body is more affected by the capacitance than by soil conductivity.

Computational examples: Human body with the arms outstretched

The human body with the arms outstretched is exposed to the double exponential pulse and to transient electric field in the form of Gaussian pulse with: E_0 =1V/m, $g=2 \cdot 10^9 s^{-1}$, t_0 =2ns.

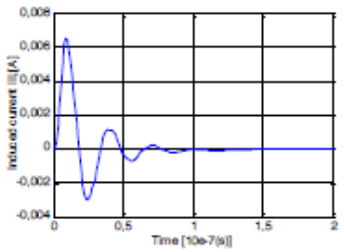

FIG: Transient current induced in the feet due to the EMP exposure

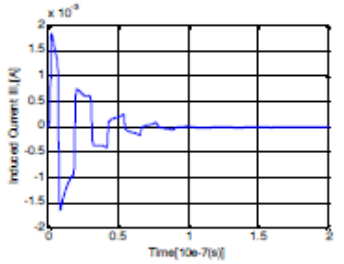

FIG: Transient current induced in the feet due to the Gaussian pulse

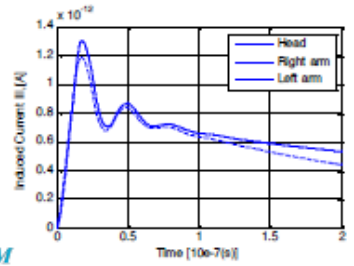

FIG: Transient current induced in the right arm, left arm and head due to the EMP exposure

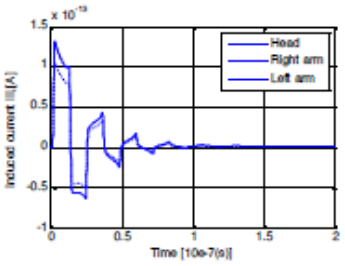

FIG: Transient current induced in the right arm, left arm and head due to the Gaussian pulse

INTERNAL FIELD DOSIMETRY PROCEDURES – LF &HF EXPOSURES

Simplified Models

Computational examples: Human exposure to HF radiation

The SAR (W/kg) is defined as: $$SAR = \frac{\sigma |E|^2}{2\rho}$$

The current density induced in the body can be expressed in terms of the axial current I_z as follow:

$$J_z(r,z) = \frac{I_z(z)}{a^2\pi}\left(\frac{ka}{2}\right)\frac{J_0(j^{-1/2}k \cdot r)}{J_1(j^{-1/2}k \cdot a)}$$

where J_0 and J_1 are the Bessel functions, k is the free space phase constant.

The induced electrical field is given by: $$E_z(z) = \frac{J_z(r,z)}{\sigma + j\omega\varepsilon}$$

The human with arms in contact of the sides, exposed to HF radiation (1 V/m, 30 MHz), is represented by a cylinder (length L, radius a).

The average value of the conductivity and permittivity of the human body, respectively, are assumed to be: 0.6 S/m, ε_r = 60.

Computational examples: Human exposure to HF radiation

The worst conditions are assumed, i.e. the maximum coupling conditions (uniform field along the body) and hence the maximum perturbation induced in the human body.

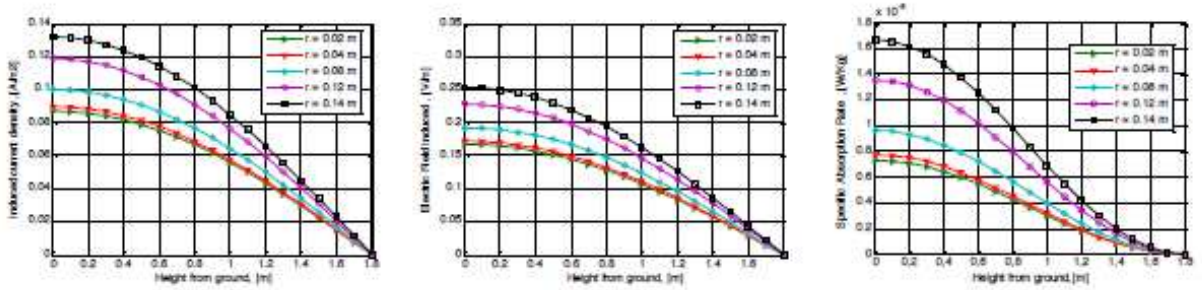

FIG: Current density (left), electric field (middle), and calculated specific absorption rate (right) (SAR) inside the human body, E_z = 1 V/m, f = 30 MHz

Table: The maximum values obtained

	$J_z(a,0)$	$E_z(z=0)$	SAR(z=0)
	[A/m²]	[V/m]	[W/kg]
f=30 MHz, a=0.14 m	0.1318	0.2534	1.67×10^{-5}

Simplified Models

INTERNAL FIELD DOSIMETRY PROCEDURES – LF &HF EXPOSURES

Computational examples:
Human exposure to HF radiation

The obtained results are compared to the exposure limits proposed by ICNIRP (SAR = 0.4 W/kg for general population, SAR = 0.08 W/kg for occupational).

The SAR values do not exceed the basic restrictions (SARmax = $1.6693 \cdot 10^{5}$ W/Kg) and as such, any heating effect is negligible.

Table: Electrical parameters for a few

Frequency [MHz]	σ [S/m]	ε_r
5	0.54	150
15	0.56	100
20	0.57	80
30	0.6	60
35	0.66	53
40	0.7	50

Table: Maximum values of the SAR inside the human body

Frequency [MHz]	SAR_{max} [W/kg] for J (r=a,0)
5	$6.03 \cdot 10^{-10}$
15	$9.01 \cdot 10^{-8}$
20	$4.34 \cdot 10^{-7}$
30	$1.67 \cdot 10^{-5}$
35	$2.46 \cdot 10^{-4}$
40	$2.42 \cdot 10^{-3}$

The specific absorption rate (SAR) inside the human body increases rapidly with frequency, while SAR_{max} for different frequency never exceeds the limit of 0.08 W/kg defined by ICNIRP.

Simplified Models

INTERNAL FIELD DOSIMETRY PROCEDURES – LF &HF EXPOSURES

Assessment of circular current density induced in the body

- Internal dosimetry of human exposure ELF fields deals with internal electric and fields and current densities, respectively.
- According to ICNIRP 1998 basic restrictions pertain to axial currents when human is exposed to electric field and circular current densities when the body is exposed to magnetic field.
- On the other hand, ICNIRP 2010 [9] proposes induced electric field instead of the induced axial current density.
- The internal circular current density due to the existence of the normal component of the magnetic flux density is presented here.

INTERNAL FIELD DOSIMETRY PROCEDURES – LF &HF EXPOSURES

Simplified Models

Assessment of circular current density induced in the body

- The internal current density can be assessed by using the disk model of the human body.
- These analytical models of the body provide rapid estimation of the human exposure to ELF magnetic field.

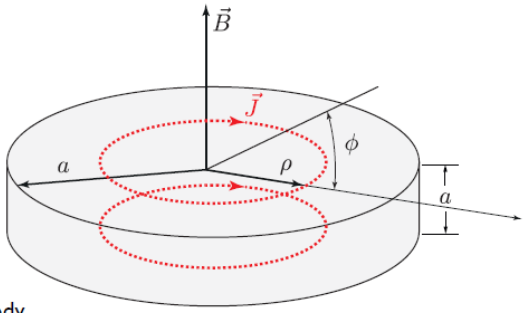

FIG: Disk model of the human body

- Starting from the Faraday's law:

$$\nabla \times \vec{E} = -\frac{\partial \vec{B}}{\partial t}$$

- and using the constitutive relation:

$$\vec{J} = \sigma \vec{E}$$

Assessment of circular current density induced in the body

- Taking into account the rotational symmetry the analytical integration simply yields the following simple expression for the induced current density inside the disk:

$$|J_\phi| = \sigma \pi \rho f \cdot B_z$$

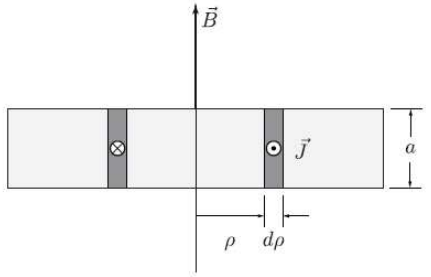

FIG: Integration over the disk cross-section

- The total current flowing through the disk can be calculated using:

$$I = \int_S \vec{J}\, d\vec{S} = \int_0^a \int_0^{2\pi} \sigma \pi f B_z \rho \, d\rho \, dz = \sigma \pi f B_z \int_0^a \int_0^{2\pi} \rho \, d\rho \, dz = \sigma \pi f B_z \frac{a^3}{2}$$

Table: Maximal values of magnetic flux density and related internal current densities

Domain	Magnetic flux density B [uT]	Current density J [uA/m²]	Axial current I [uA]
1	2.701	29.7	0.29
2	0.945	10.39	0.102
3	3.344	36.77	0.36
4	2.552	28.06	0.275
5	0.747	8.21	0.085

Table: ICNIRP Guidelines

Occupational exposure	General population
500 uT	100 uT
10 mA/m²	2 mA/m²

INTERNAL FIELD DOSIMETRY PROCEDURES – LF &HF EXPOSURES

Simplified Models

Assesment of SAR in a Simplified Body Model due to Hertz Dipole Exposure

SPECIFIC ABSORPTION RATE $\left[\frac{W}{kg}\right]$

$$SAR = \frac{d}{dt}\left(\frac{dW}{dm}\right) = \frac{d}{dt}\left(\frac{dW}{\rho dV}\right)$$

$$SAR = \sigma\frac{|\vec{E}|^2}{\rho}$$

$$SAR = C\frac{dT}{dt}$$

$$SAR_V = \frac{\int_V \sigma|\vec{E}|^2 dV}{\int_V \rho dV}$$

σ – tissue conductivity [S/m]
ρ – tissue density [kg/m^3]
C – specific heat capacity [J/(kg ^{0}C)]

V – volume of a given mass

Whole body, WB — 10 g

ABSORBED POWER DENSITY $\left[\frac{W}{m^2}\right]$

$$S_{ab} = \frac{\iint_A dxdy \int_{z=0}^{Z_{max}} \rho(x,y,z)\cdot SAR(x,y,z)dz}{A}$$

$$S_{ab} = \frac{\iint_A Re[\vec{E}\times\vec{H}^*]d\vec{s}}{A}$$

$z = 0$ is body surface
Z_{max} is depth of the body at the corresponding region

$A = 4\ cm^2$
$A = 1\ cm^2$

4
1

INTERNAL FIELD DOSIMETRY PROCEDURES – LF &HF EXPOSURES

Simplified Models

Assesment of SAR in a Simplified Body Model due to Hertz Dipole Exposure

Model geometry

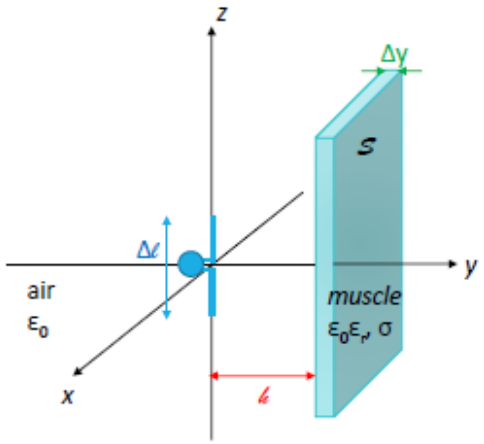

A Hertz dipole

- The simplest linear antenna
- Non-efficient radiator
- Mathematically well described
- A building block for modelling complex antenna structures

Parallelepiled body model

- Constant surface, ***S***
- Constant thickness, Δy
- Homogeneous medium – muscle tissue: frequency dependent electric permittivity and conductivity, ε_r, σ

Formulation

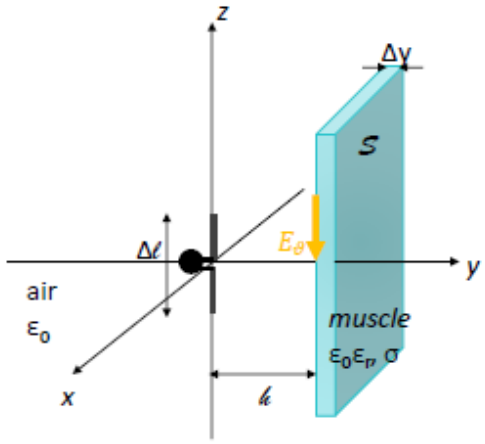

Field incident to body surface:

$$E_\vartheta(r,\vartheta) = jZ_0 \frac{kI_0\Delta l}{4\pi r}\left(1+\frac{1}{jkr}-\frac{1}{(kr)^2}\right)e^{-jkr}\sin\vartheta$$

$k^2 = \omega^2\mu_0\varepsilon_0$ ... *free space constant*

$Z_0 = 377\ \Omega$ ... *free space impedance*

r ...distance between antenna and observation point

INTERNAL FIELD DOSIMETRY PROCEDURES – LF &HF EXPOSURES

Simplified Models

Assesment of SAR in a Simplified Body Model due to Hertz Dipole Exposure

Formulation

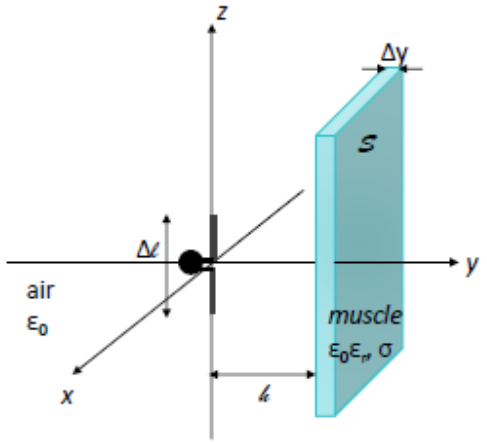

I_0 *... current exciting the antenna*

1) A constant value

2) Computed from expression:

$$P_{rad} = \frac{1}{3} Z_0 \pi I_0^2 \left(\frac{\Delta l}{\lambda}\right)^2$$

P_{rad} *... Power radiated by Hertz dipole*

Formulation

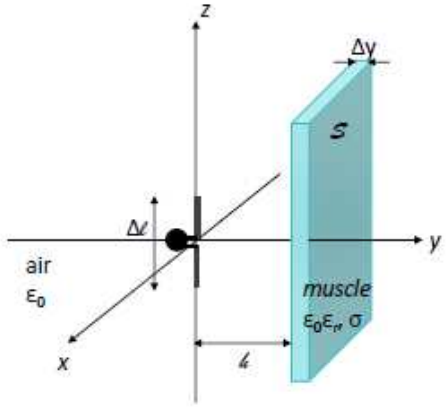

The SAR averaged over the whole body:

$$SAR_{WB} = \frac{1}{V} \int_V SAR_{muscle} dV$$

$$SAR_{muscle} = \frac{1}{2} \frac{\sigma}{\rho} |E_{muscle}|^2$$

$$V = S \cdot \Delta y$$

σ ... tissue conductivity
ρ ... tissue density

INTERNAL FIELD DOSIMETRY PROCEDURES – LF &HF EXPOSURES

Simplified Models

Assesment of SAR in a Simplified Body Model due to Hertz Dipole Exposure

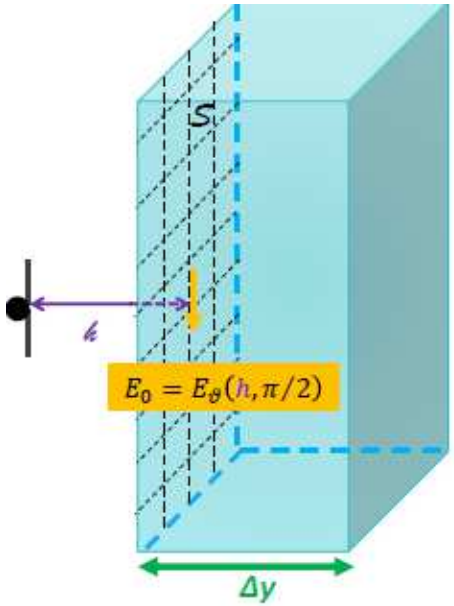

$$SAR_{muscle} = \frac{1}{2}\frac{\sigma}{\rho}|E_{muscle}|^2$$

$$E_{muscle}(y) = E_0 \cdot e^{-\alpha y} \cdot \Gamma_{tr}$$

$$E_0 = E_\vartheta(r = h, \vartheta = \pi/2)$$

$$\alpha = Re(\gamma_{muscle}) \approx \sqrt{\frac{\omega\mu\sigma}{2}}$$

$$\delta = \sqrt{2/\omega\mu\sigma} \quad \rightarrow \text{skin dept}$$

$$SAR_{muscle} = \frac{1}{2}\frac{\sigma}{\rho}|\Gamma_{tr}|^2|E_0|^2 e^{\frac{-2y}{\delta}}$$

FRESNEL'S COEFFICIENT APPROXIMATION

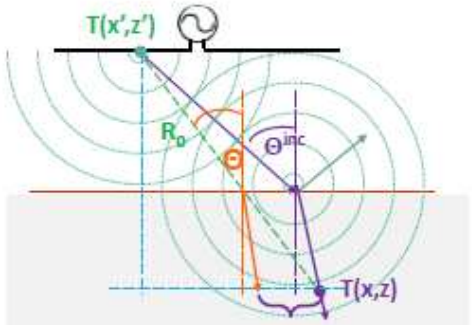

$$\Gamma_{tr} = \frac{2\sqrt{n}\cos\Theta}{n\cos\Theta + \sqrt{n - (\sin\Theta)^2}}$$

$$tg\,\Theta = \frac{x - x'}{z - z'}$$

MODIFIED IMAGE THEORY APPROACH

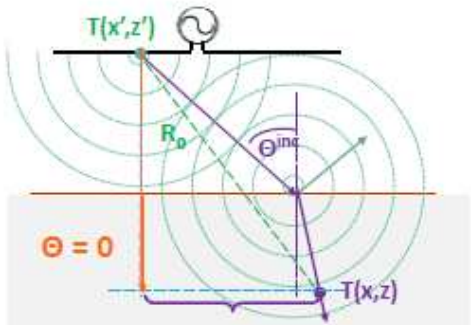

$$\Gamma_{tr} = \frac{2n}{n+1}$$

$$n = \varepsilon_r - j\frac{\sigma}{\omega\varepsilon_0}$$

$$\Theta = 0$$

INTERNAL FIELD DOSIMETRY PROCEDURES – LF &HF EXPOSURES

Simplified Models

Assesment of SAR in a Simplified Body Model due to Hertz Dipole Exposure

Formulation

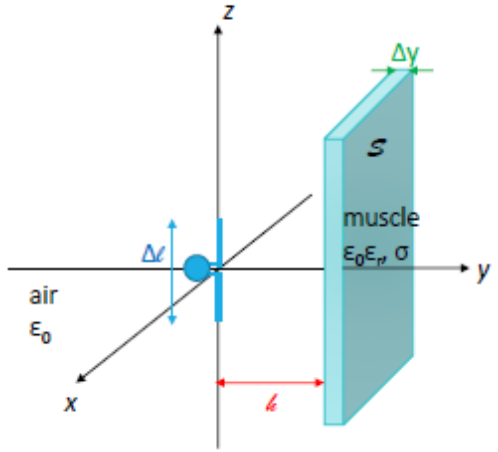

The whole body averaged SAR:

$$SAR_{WB} = \frac{1}{V}\int_V SAR_{muscle}\,dV$$

$$SAR_{muscle} = \frac{1}{2}\frac{\sigma}{\rho}|E_{muscle}|^2$$

(...)

$$SAR_{WB} = \frac{1}{2}\frac{\sigma}{\rho}|\Gamma_{tr}|^2|E_0|^2\frac{\delta}{2\Delta y}\left(1-e^{-\frac{2\Delta y}{\delta}}\right)$$

RESULTS #1

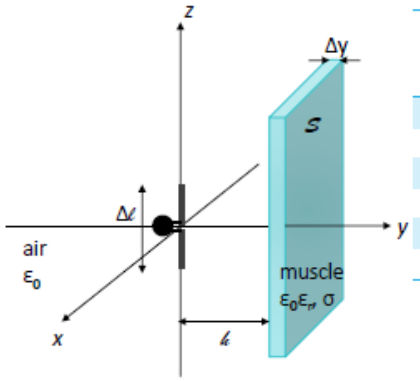

Muscle properties:

Frequency f[GHz]	Wavelength λ[m]	Permitivitty ε_r	Conductivity σ[S/m]
0.1	3	66	0.708
0.3	1	58.2	0.771
1	0.3	54.8	0.978
3	0.1	52.1	2.14
6	0.05	48.2	5.2
10	0.03	42.8	10.6

Antenna length: Δl = 1 cm
Radiated power: P_{rad} = 10 mW
Distance h: from 10 cm to 2 m
Density of muscle tissue: ρ = 1090 kg/m³

INTERNAL FIELD DOSIMETRY PROCEDURES – LF &HF EXPOSURES

Simplified Models

Assesment of SAR in a Simplified Body Model due to Hertz Dipole Exposure

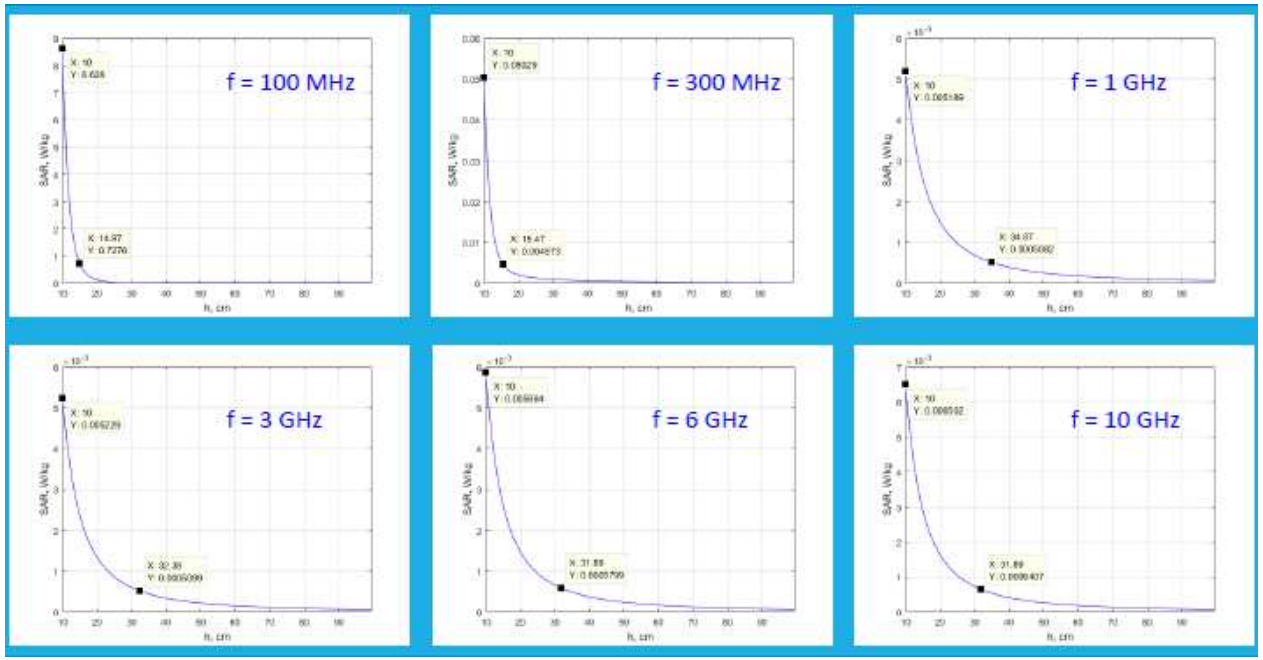

RESULTS #1

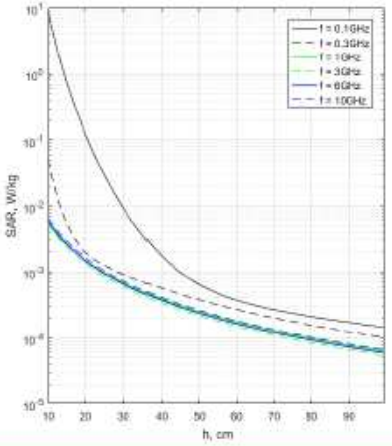

f (GHz)	0.1	0.3	1	3	6	10
I_0 [A]	1.5099	0.5033	0.1510	0.0503	0.0252	0.0151
$\Delta l/\lambda$	1/30	1/10	1/3	1	10/5	10/3

Antenna length: Δl = 1 cm
Radiated power: P_{rad} = 10 mW
Distance h: from 10 cm to 2 m
Density of muscle tissue: ρ = 1090 kg/m³

INTERNAL FIELD DOSIMETRY PROCEDURES – LF &HF EXPOSURES

Simplified Models

Assesment of SAR in a Simplified Body Model due to Hertz Dipole Exposure

RESULTS #2

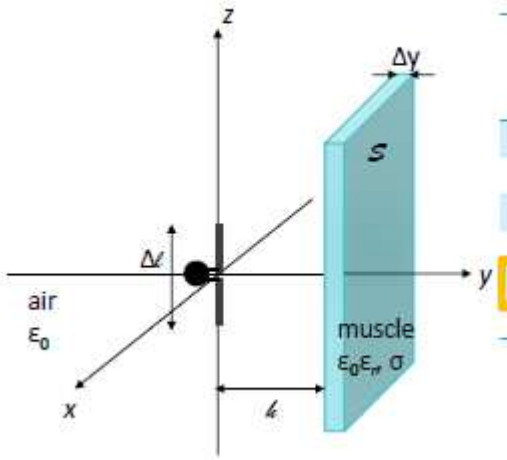

Muscle properties:

Frequency f[GHz]	Wavelength λ[m]	Permitivitty ε_r	Conductivity σ[S/m]
0.1	3	66	0.708
0.3	1	58.2	0.771
1	0.3	54.8	0.978
3	0.1	52.1	2.14
6	0.05	48.2	5.2
10	0.03	42.8	10.6

Frequency: f = 6 GHz
Current: I = 50 mA
Distance h: from 10 cm to 2 m
Density of muscle tissue: ρ = 1090 kg/m³

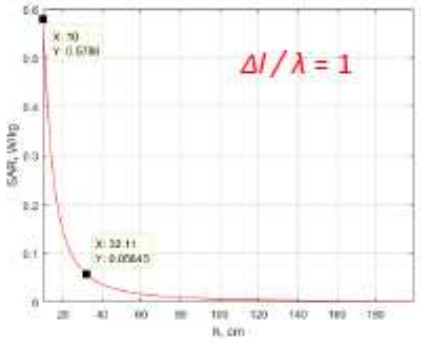

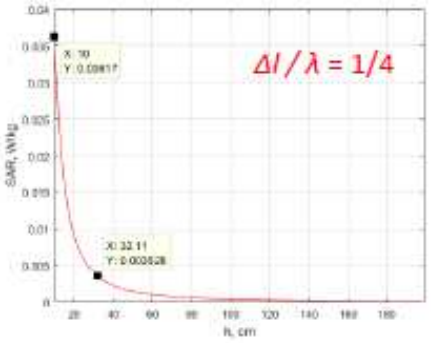

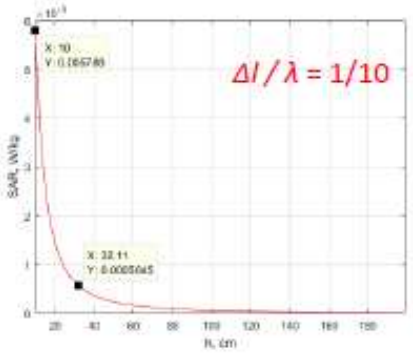

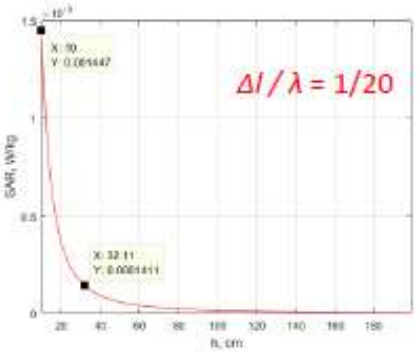

INTERNAL FIELD DOSIMETRY PROCEDURES – LF &HF EXPOSURES

Simplified Models

Assesment of SAR in a Simplified Body Model due to Hertz Dipole Exposure

RESULTS #2

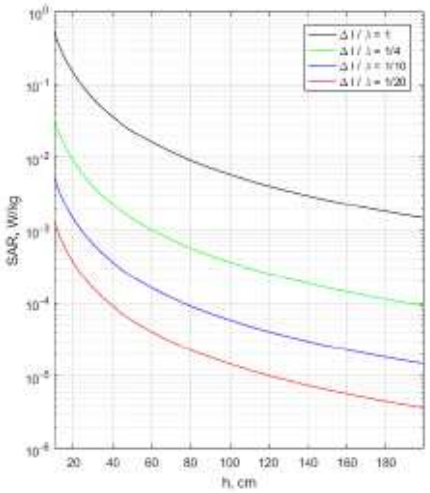

Δl	λ	$\lambda/4$	$\lambda/10$	$\lambda/20$
P_{rad} [W]	6.2832	0.3927	0.0628	0.0157

Frequency: f = 6 GHz
Current: I = 50 mA
Distance h: from 10 cm to 2 m
Density of muscle tissue: ρ = 1090 kg/m³

Closure

An efficient analytical approach to the assessment of a specific absorption rate (SAR) in simplified body model exposed to incident electric field in GHz frequency range corresponding to forthcoming 5G systems is presented.

The radiation source is represented by **Hertz dipole**.

Body is represented as **parallellepiped**.

The effect of the air-body interface is taken into account via the **transmission coefficient** arising from the **modified image theory (MIT)** approach.

Some illustrative results for the whole body average SAR pertaining to several frequencies, antenna lengths and antenna-body distances are presented in the paper thus enabling:

- a rapid assessment of values of interest
- a benchmark for more complicated numerical approaches
- a didactic value for all newcomers to the field

INTERNAL FIELD DOSIMETRY PROCEDURES – LF &HF EXPOSURES

COMPUTATIONAL EXAMPLES

Analysis of human exposure to WPT systems

HUMAN EXPOSURE TO FIELDS GENERATED FROM WPT SYSTEMS – Internal Field Dosimetry

Table 4. *Characteristics of human muscle tissue at different frequencies [9]*

Frequency f (Hz)	ε_r	σ (S/m)
13.56 M	92	0.419
6.78 M	210	0.391
100 k	8020	0.362

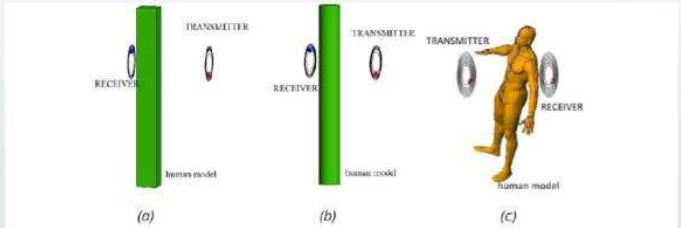

Fig. 3 *Simplified (a) parallelepiped, (b) cylinder human body model and (c) realistic human body model positioned between antennas*

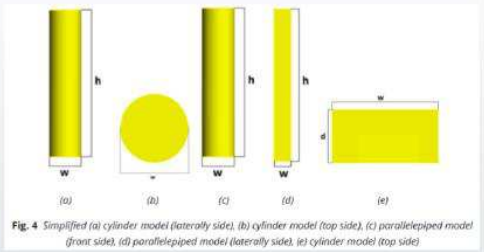

Fig. 4 *Simplified (a) cylinder model (laterally side), (b) cylinder model (top side), (c) parallelepiped model (front side), (d) parallelepiped model (laterally side), (e) cylinder model (top side)*

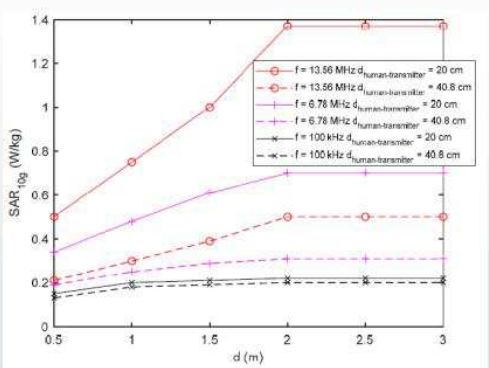

Fig. 8 *SAR_{10g} of WPT systems with parallelepiped human model*

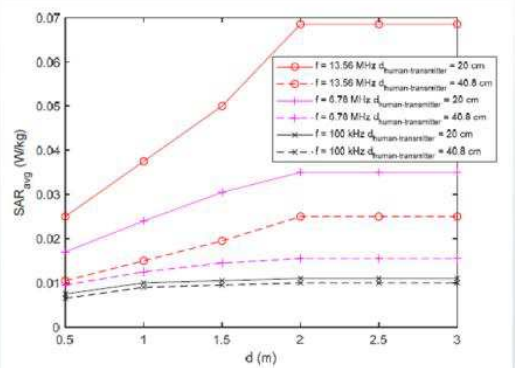

Fig. 9 *SAR_{avg} of WPT systems with parallelepiped human model*

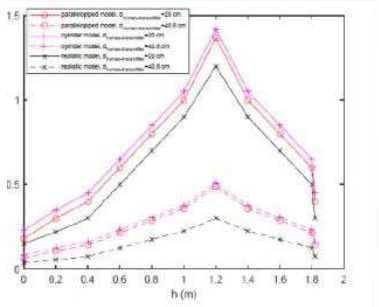

14 *SAR_{10g} distribution along the different human body models at f = 13.56 MHz*

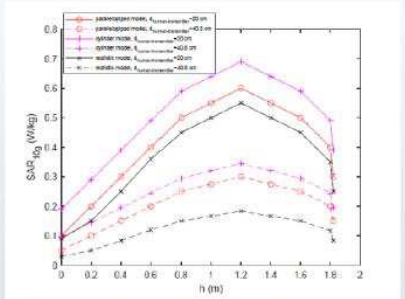

Fig. 15 *SAR_{10g} distribution along the different human body models at f = 6.78 MHz*

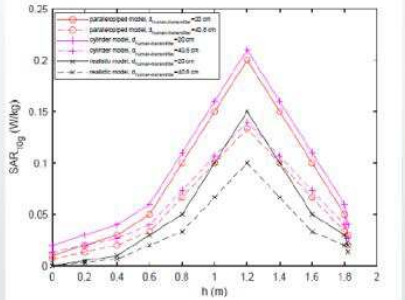

Fig. 16 *SAR_{10g} distribution along the different human body models at f = 100 kHz*

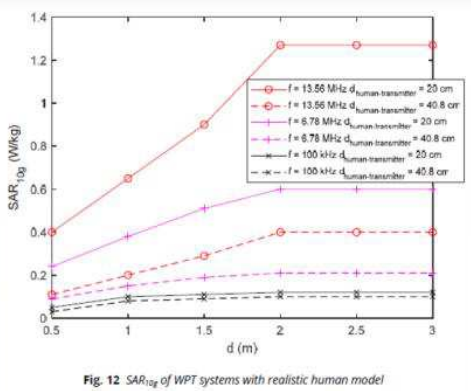

Fig. 12 *SAR_{10g} of WPT systems with realistic human model*

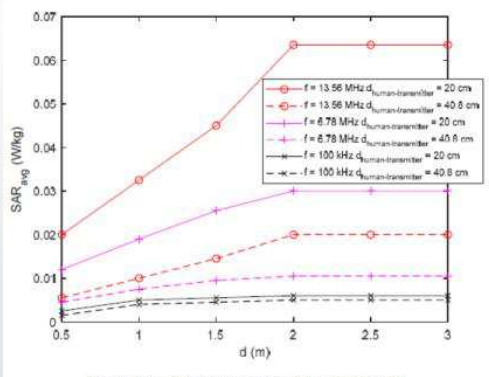

Fig. 13 *SAR_{avg} of WPT systems with realistic human model*

INTERNAL FIELD DOSIMETRY PROCEDURES – LF &HF EXPOSURES

Realistic Models – LF Exposures

- Realistic models of the body exposed to static and low frequency (LF) fields.
- The human head models exposed to static electric field is handled via finite element method (FEM) and boundary element method (BEM), respectively.
- Whole body exposure to LF fields is analyzed by using the quasistatic formulation and BEM.
- Realistic body models with organs included are presented.
- Examples: human head exposed to electrostatic field from video display unit; whole body and pregnant woman/foetus exposed to high voltage extremely low frequency (ELF) electric fields generated by overhead power lines; human inside transformer substation.

Realistic Models – LF Exposures

INTERNAL FIELD DOSIMETRY PROCEDURES – LF &HF EXPOSURES

FORMULATION: Laplace equation

3D electrostatic field distribution between a VDU and the head is governed by the Laplace equation for electric potential φ:

$$\nabla^2 \varphi = 0$$

Boundary conditions:

$\varphi = \varphi_s$ on the display

$\varphi = \varphi_h$ on the head

$\nabla \varphi \cdot \hat{n} = 0$ on the far field boundaries

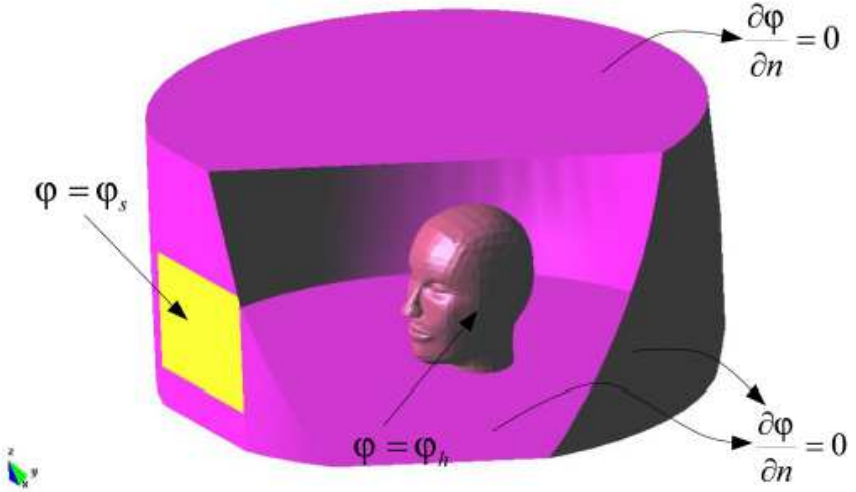

FIG: 3D head model in front of VDU

Realistic Models – LF Exposures

INTERNAL FIELD DOSIMETRY PROCEDURES – LF &HF EXPOSURES

Dosimetry: Exposure to static fields - FEM SOLUTION

Applying the weighted residual approach to Laplace equation yields:

$$\int_{\Omega} \nabla^2 \varphi W_j \, d\Omega = 0$$

Performing some mathematical manipulations gives:

The Galerkin-Bubnov procedure (W_j=f_j) it follows:

$$\int_{\Omega} \nabla\varphi \cdot \nabla f_j \, d\Omega = \int_{\Gamma} \frac{\partial \varphi}{\partial n} f_j \, d\Gamma$$

Neumann condition:

$$\int_{\Omega} \nabla\varphi \cdot \nabla f_j \, d\Omega = 0$$

The unknown potential over an element is expressed by shape functions:

$$\varphi^e = \sum_{i=1}^{4} \alpha_i f_i$$

The global matrix system:

$$[a]\{\alpha\} = \{Q\}$$

The shape functions:

$$f_i(x,y,z) = \frac{1}{D}\left(V_i + a_i x + b_i y + c_i z\right), \quad i = 1,2,3,4$$

The electrostatic field

$$\vec{E} = -\nabla\varphi$$

Realistic Models – LF Exposures

INTERNAL FIELD DOSIMETRY PROCEDURES – LF &HF EXPOSURES

Dosimetry: Exposure to static fields - Computational examples

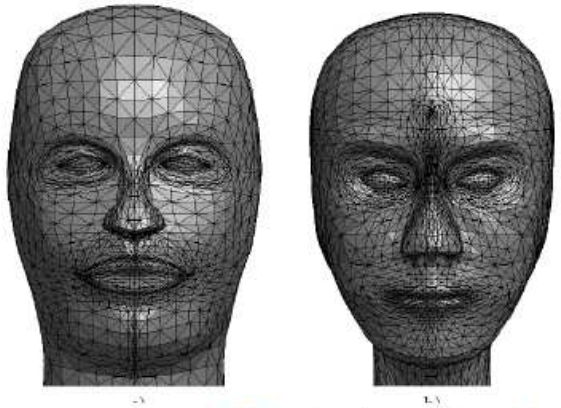

The parameters:

l_s=40 cm, d_s=17", φ s=15 kV and φ h = 0 kV.

The monitor is 4:3 format; 34.3 cm by 25.7 cm.

FIG: Head models with finite element mesh: a) Person 1 b) Person 2

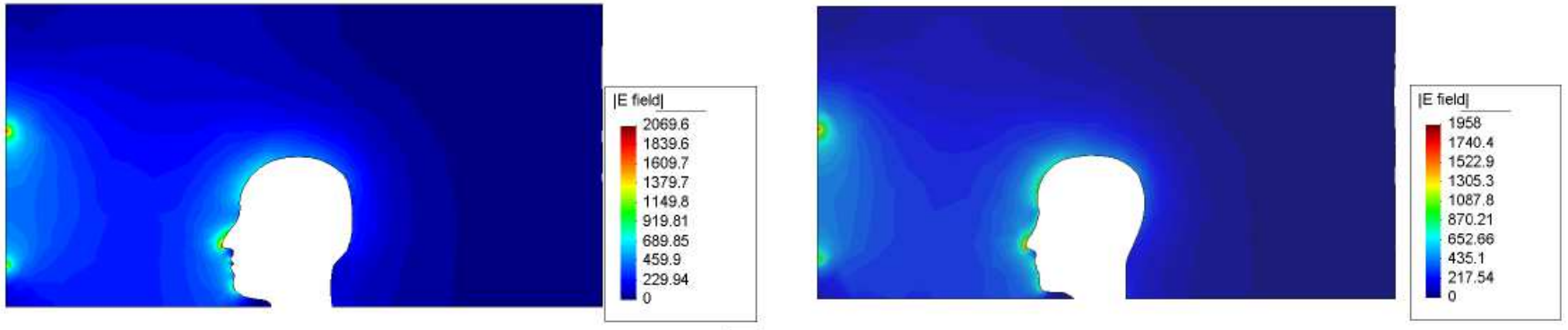

FIG: Electrostatic field in the mid-face symmetry for person 1 (left) and person 2 (right)

Realistic Models – LF Exposures

INTERNAL FIELD DOSIMETRY PROCEDURES – LF &HF EXPOSURES

Dosimetry: Exposure to static fields - Computational examples

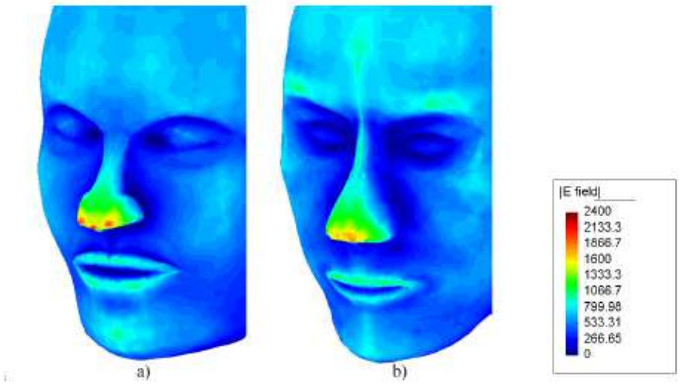

FIG: Electrostatic field strength [V/cm] around the nose and eye a) Person 1; b) Person 2

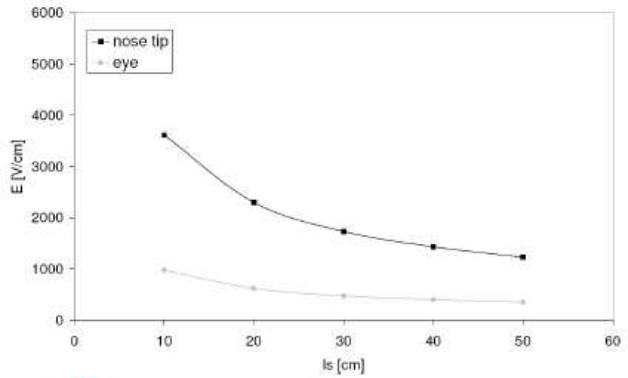

FIG: Electrostatic field on the nose tip and eyes vs distance between display and head for 17" VDU

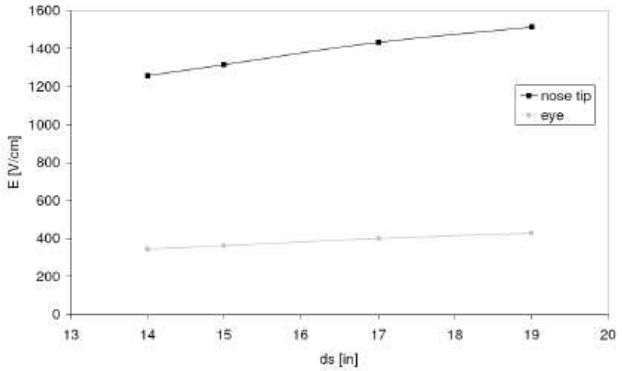

FIG: Electrostatic field in the nose tip and eyes vs display size for 40 cm distance between display and head

INTERNAL FIELD DOSIMETRY PROCEDURES – LF &HF EXPOSURES

Realistic Models – LF Exposures

Realistic approach: anatomically based body models

FORMULATION:
The equation of continuity

$$\nabla \vec{J} + \frac{\partial \rho}{\partial t} = 0$$

$$\vec{J} = -\sigma \nabla \varphi \qquad \nabla (\varepsilon \nabla \varphi) = -\rho$$

For the time-harmonic ELF exposures it follows:

$$\nabla \left[(\sigma + j\omega\varepsilon) \nabla \varphi \right] = 0$$

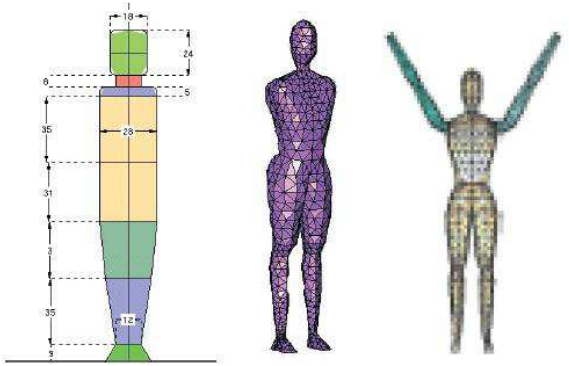

FIG: Several multi-domain models of the body and conducting properties of different parts at ELF exposures

The air-body interface conditions:

$$\hat{n} \times (\nabla \varphi_b - \nabla \varphi_a) = 0 \qquad \varepsilon_0 \hat{n} \nabla \varphi_a = \rho_s$$

$$\sigma_b \hat{n} \nabla \varphi_b = -j\omega \rho_s$$

Numerical method: The Boundary Element Method

The beauty of BEM...

- BEM tends to avoid volume meshes for large-scale problems.
- BEM formulation is based on the fundamental solution of the leading operator for the governing equation thus being competitive with other well-established methods, such as FEM or FDM, in terms of accuracy and efficiency.

The problem consists of finding the solution of the Laplace equation in a non-homogenous media with prescribed boundary conditions

$$\nabla \cdot (\sigma \nabla \varphi) = 0 \text{ on } \Omega$$

$$\varphi = \bar{\varphi} \text{ on } \Gamma_1$$

$$\frac{\partial \varphi}{\partial x_j} \hat{n}_j = \frac{\partial \bar{\varphi}}{\partial n_j} \text{ on } \Gamma_2$$

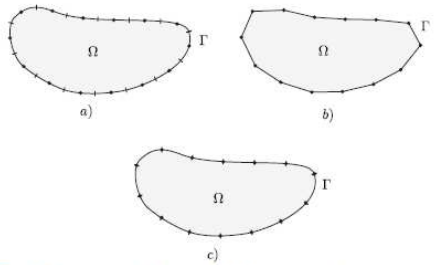

FIG: a) Constant element, b) Linear element, and c) Quadratic element approximations

The integration domain is considered piecewise homogeneous, so it can be decomposed into an assembly of N homogeneous subdomains Ω_k (k = 1, m).

INTERNAL FIELD DOSIMETRY PROCEDURES – LF &HF EXPOSURES

Realistic Models – LF Exposures

Green's theorem yields the integral representation for a subdomain:

$$c_i\varphi_i = \int_\Gamma \Psi \frac{\partial \varphi}{\partial n} d\Gamma - \int_\Gamma \varphi \frac{\partial \Psi}{\partial n} d\Gamma \qquad c_i = \begin{cases} 1, & i \in \Omega \\ \frac{1}{2}, & i \in \Gamma \quad \text{(smooth boundary)} \end{cases}$$

where Ψ is the 3D fundamental solution of Laplace equation,

Discretization to N_k elements leads to an integral relation:

$$c_i u_i = \sum_{j=1}^{N_e} \int_{\Gamma_j} \psi \frac{\partial \varphi}{\partial n} d\Gamma - \sum_{j=1}^{N_e} \int_{\Gamma_j} \varphi \frac{\partial \psi}{\partial n} d\Gamma$$

Potential and its normal derivative can be written by means of the interpolation functions ϕ_a

$$\varphi(\xi) = \sum_{k=1}^{N_{fn}} \Phi_k(\xi)\, \varphi_k$$

$$\frac{\partial \varphi(\xi)}{\partial n} = \sum_{k=1}^{N_{fn}} \Phi_k(\xi)\, \left.\frac{\partial \varphi}{\partial n}\right|_k$$

The system of equations for each subdomain can be written as:

$$[\mathbf{H}]\{\phi\} - [\mathbf{G}]\left\{\frac{\partial \phi}{\partial n}\right\} = 0$$

where H and G are matrices defined by:

$$[\mathbf{H}] = h_{ij}^a = \int_{\Gamma_{k,j}} \psi_a \left(\frac{\partial \phi^*}{\partial n}\right)_j d\Gamma \qquad [\mathbf{G}] = g_{ij}^a = \int_{\Gamma_{k,j}} \psi_a \ \phi^* d\Gamma$$

The matching between two subdomains can be established through their sharing nodes:

$$\phi_{jA}^\alpha = \phi_{jB}^\alpha$$

$$\left(-\tau_A \left.\frac{\partial \phi}{\partial n}\right|_j^\alpha\right)_A = \left(\tau_A \left.\frac{\partial \phi}{\partial n}\right|_j^\alpha\right)_B$$

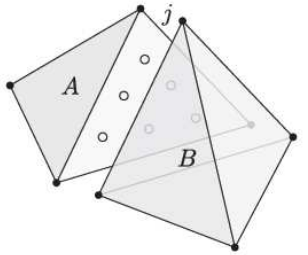

FIG: Assembly of subdomains A and B by imposing continuity of potentials and fluxes at the common interface j

INTERNAL FIELD DOSIMETRY PROCEDURES – LF &HF EXPOSURES

Realistic Models – LF Exposures

Computational examples: Exposure to power lines

The multidomain body of revolution model

The well-grounded body of 175cm height exposed to the10kV/m/60Hz power line E-field. The height of the power line is 10m above ground.

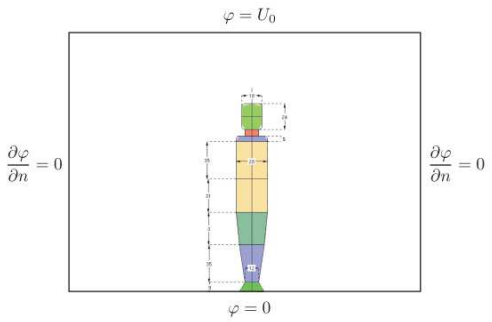

IG: Calculation domain with the prescribed B.C.'s

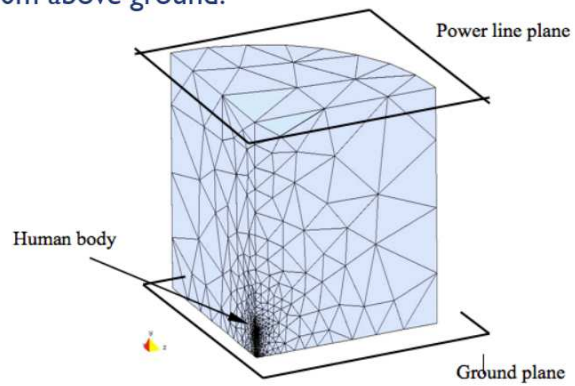

FIG: The boundary element mesh

Table: Conductivities of different body compartments

Body part	Head	Neck	Shoulders	Thorax	Pelvis	Knee	Ankle	Foot
Region	I,II	III	IV	V	VI	VII	VIII	IX
σ [S/m]	0.12	0.6	0.04	0.11	0.11	0.52	0.04	0.11

Computational examples: Exposure to power lines

The current density values increase at narrow sections such as ankle and neck

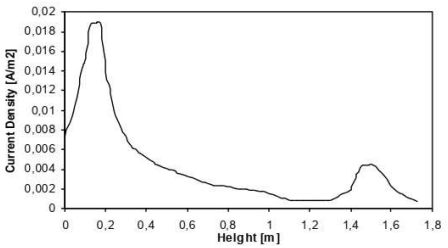

FIG: The current density distribution inside the human body

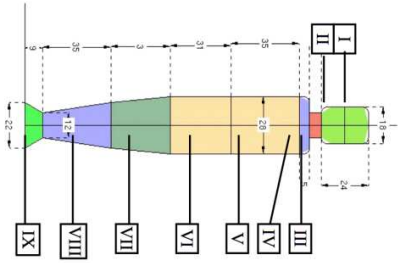

Table: Comparison between the BEM, FEM and experimental results for the induced current density at various body portions, expressed in [nA/cm²]

Body part	BEM	FEM	Experiment
Neck	452	462	466
Pelvis	232	227	225
Ankle	1891	1916	1866

The calculated results via BEM agree well with FEM and measurements.

The main difference is in the area of ankles and neck. The peak values of J in those parts maintain the continuity of the axial current throughout the body.

Exposure scenario	Current density J [mA/m²]
ICNIRP guidelines for occupational exposure	10
ICNIRP guidelines for general public exposure	2
J_{zmax} (cylinder on earth)	3
J_{zmax} (body of revolution model)	19

INTERNAL FIELD DOSIMETRY PROCEDURES – LF &HF EXPOSURES

Realistic Models – LF Exposures

Computational examples: Exposure to power lines

The realistic models of the human body

The electric field in the air begins to sense the presence of the grounded body at around 5m above ground level

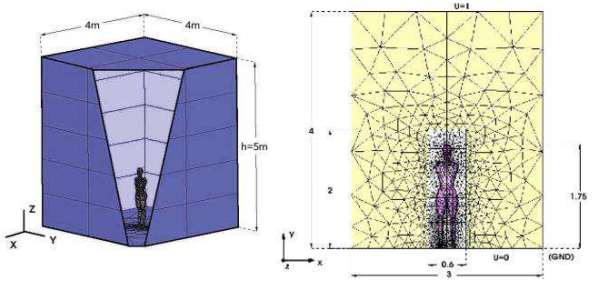

FIG: Calculation domain: a) A plan view of the integration domain, b) BEM mesh

BEM with domain decomposition and triangular elements (40 000) is used.

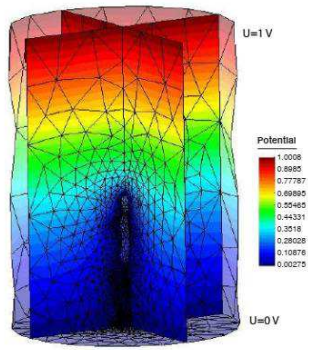

FIG: Scalar potential lines in air

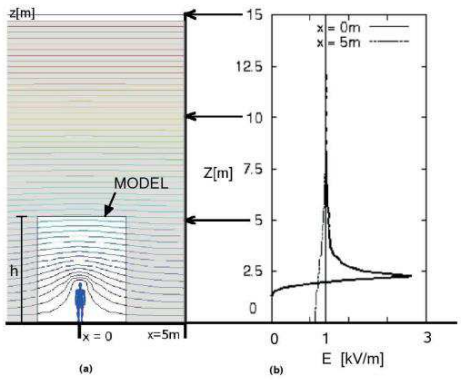

FIG: Electric field in the air near the human body

Computational examples: Exposure to power lines

The realistic models of the human body

Front and side view of equipotential lines in air are presented.

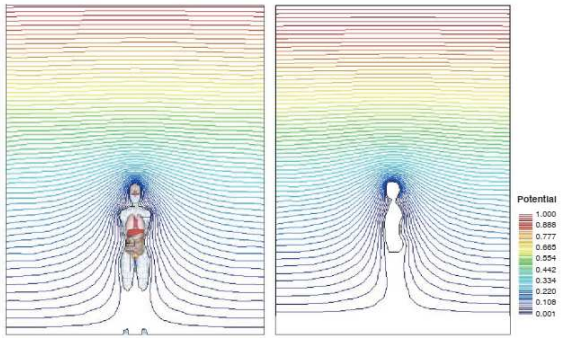

FIG: Equipotentials around the body (near field) plane x y view

An oversimplified cylindrical representation of the body is unable to capture the current density peaks in the regions with narrow cross section.

The presence of peaks in current density values corresponds to the position of the ankle and the neck.

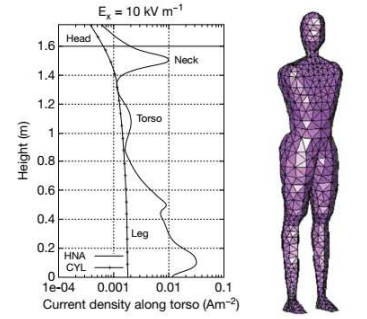

FIG: Current density distribution

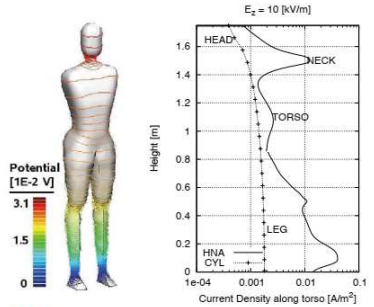

FIG: Induced current density along the body

INTERNAL FIELD DOSIMETRY PROCEDURES – LF &HF EXPOSURES

Realistic Models – LF Exposures

Computational examples: Exposure to power lines

The realistic models of the human body

The mesh and scalar potential for the body model with arms up is presented.

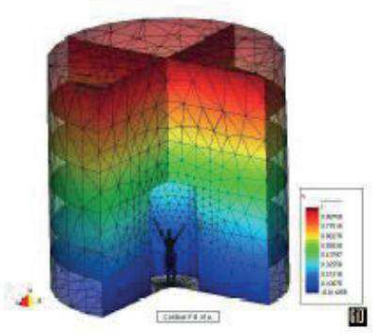

FIG: Meshing for the realistic model of the body with arms up

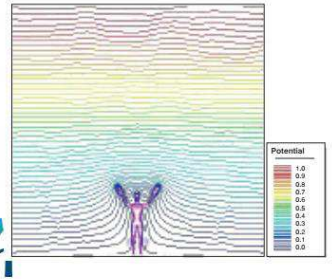

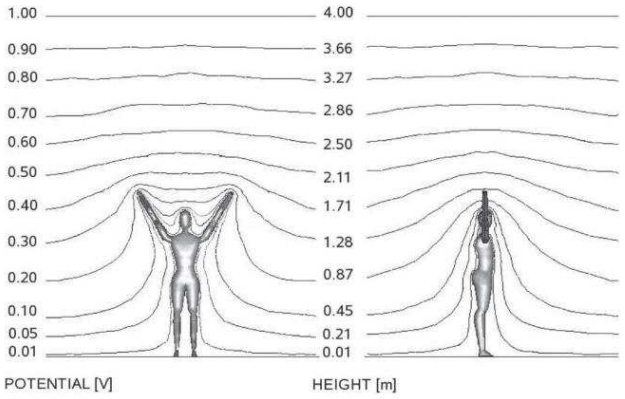

FIG: Front and lateral view of equipotential surfaces for the HAU model exposed to a reference incident field Ez = 0.25 V/m.

The numbers on the left indicate voltage, while the numbers on the right indicate height of the equipotentials taken at 2.5m away from the subject, i.e. when equipotential surface become parallel to the ground.

Computational examples: Exposure to power lines

The realistic models of the human body

Distribution of axial current density along the torso and head in function of the height for the HAU, HAO, HAD and HNA models.

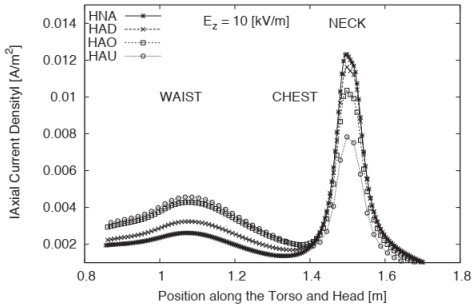

FIG: Induced current density distribution for the various body models

HAU - Human with arms up
HAO - Human with arms open
HAD - Human with arms down
HNA - Human model without arms

Table: ICNIRP Safety Standard	Current density J [mA/m²]
Occupational exposure	10
General public exposure	2

Table: Peak values of the current density in the ankle for some typical values of electric field near ground under power lines.

E [kV/m]	J [mA/m²]
1	2
5	10
10	19

Realistic Models – LF Exposures

INTERNAL FIELD DOSIMETRY PROCEDURES – LF &HF EXPOSURES

Computational examples: Human inside a substation

The realistic model of the human body

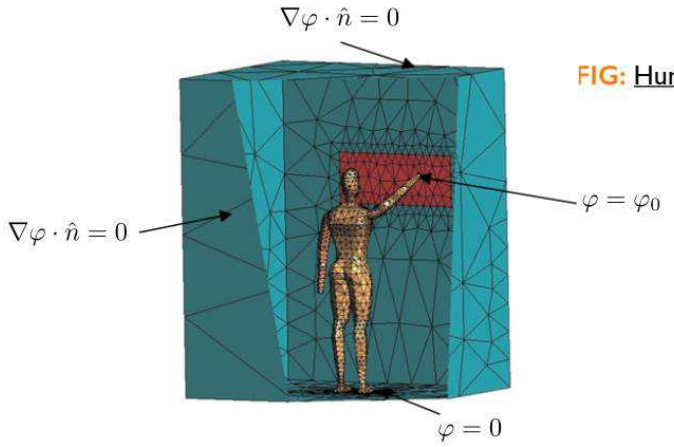

FIG: Human inside a substation touching a control panel

Realistic 1.75 m tall human body inside a transformer substation room (2.5 m x1.6 m x 2 m) touching a control panel (1m x 2m) at the potential φ_0 = 400 V.

Two scenarios for dry-air between worker's hand and panel are considered: d = 0.016m and d = 0.116m.

The floor is kept grounded and all other surfaces of the room are considered with Neumann adiabatic type conditions.

In this case, for both scenarios, the values of internal current density do not exceed ICNIRP basic restrictions.

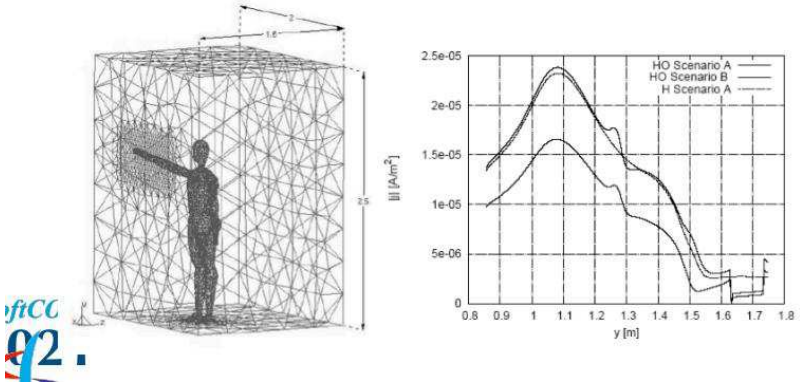

FIG: The conceptual model and the results: a) BEM mesh, b) Internal current density for different scenarios

INTERNAL FIELD DOSIMETRY PROCEDURES – LF &HF EXPOSURES

Realistic Models – LF Exposures

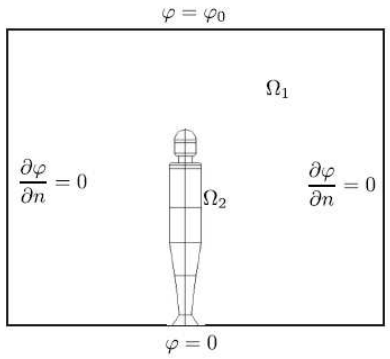

Table: Three different conductivity scenarios considered

Scenario	[S/m]	Week 8	Week 13	Week 26	Week 38
1	σ_f	0.23	0.23	0.23	0.23
	σ_{AF}	1.28	1.28	1.27	1.10
	σ_m	0.20	0.20	0.20	0.20
2	σ_f	0.996	0.996	0.574	0.574
	σ_{AF}	1.70	1.70	1.64	1.64
	σ_m	0.52	0.52	0.52	0.52
3	σ_f	0.732	0.732	0.396	0.396
	σ_{AF}	1.70	1.70	1.64	1.64
	σ_m	0.17	0.17	0.17	0.17

Computational examples: Pregnant woman exposure

The realistic models of the human body

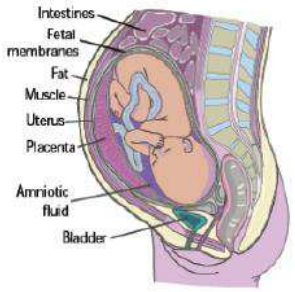

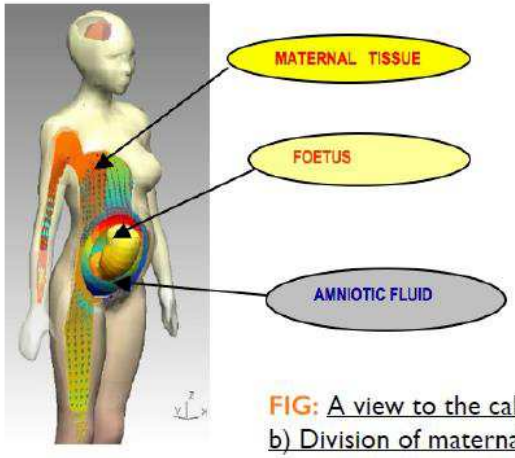

FIG: A view to the calculation domain: a) Different tissues, b) Division of maternal abdomen into equivalent subdomains

Realistic, anatomically based, model of pregnant woman/foetus uses a quasi-static approximation based on the Laplace equation formulation and a solution via three dimensional multi-domain BEM.

The model accounts for variations in geometry, body mass, fat and overall chemical composition in the female body.

Realistic Models – LF Exposures

INTERNAL FIELD DOSIMETRY PROCEDURES – LF &HF EXPOSURES

Computational examples: Pregnant woman exposure

The realistic models of the human body

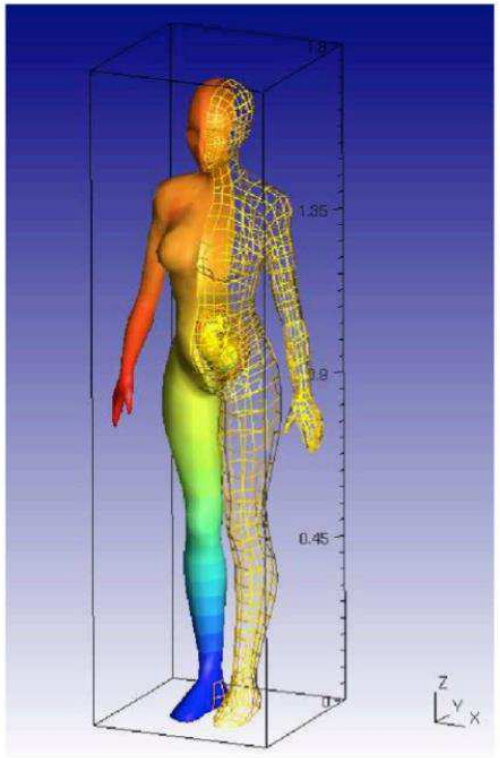

FIG: A 3D view of the model at 26th week of pregnancy (cephalic presentation)

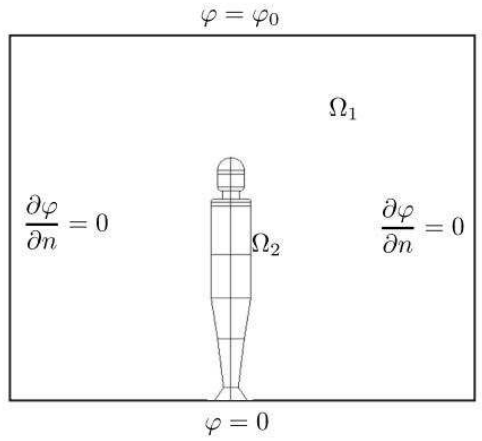

FIG: The calculation domain with the associated boundary conditions

Table: Three different conductivity scenarios considered

Scenario	[S/m]	Week 8	Week 13	Week 26	Week 38
1	σ_f	0.23	0.23	0.23	0.23
	σ_{AF}	1.28	1.28	1.27	1.10
	σ_m	0.20	0.20	0.20	0.20
2	σ_f	0.996	0.996	0.574	0.574
	σ_{AF}	1.70	1.70	1.64	1.64
	σ_m	0.52	0.52	0.52	0.52
3	σ_f	0.732	0.732	0.396	0.396
	σ_{AF}	1.70	1.70	1.64	1.64
	σ_m	0.17	0.17	0.17	0.17

INTERNAL FIELD DOSIMETRY PROCEDURES – LF &HF EXPOSURES

Realistic Models – LF Exposures

Computational examples: Pregnant woman exposure

The realistic models of the human body

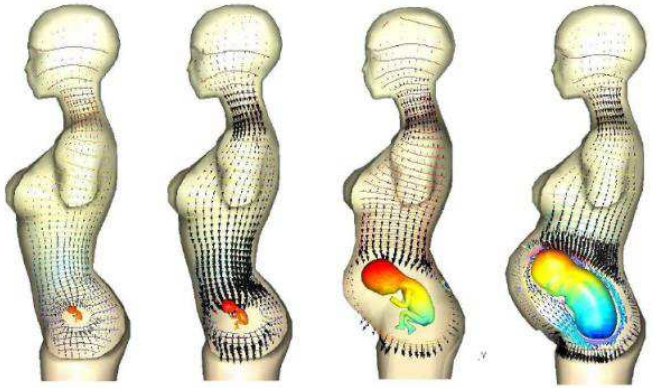

FIG: Lateral view of the pregnant woman at 8th, 13th, 26th and 38th gestational week (breech presentation); E- field and scalar potential.

Uterus, due to its higher conductivity comparing to the maternal tissue, tends to concentrate the field lines.

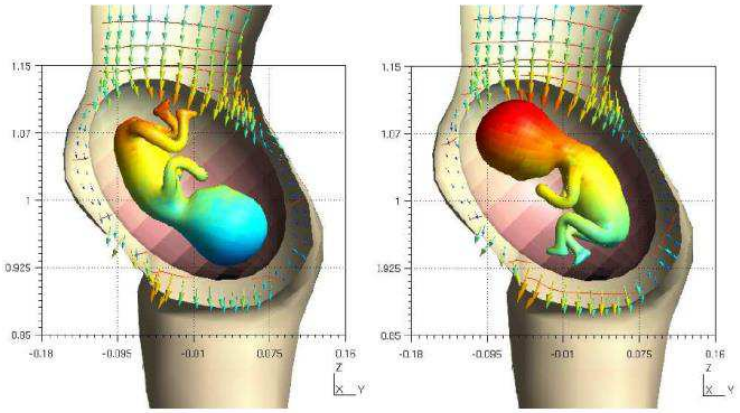

FIG: Lateral view of the pregnant woman at 26th gestational week: a) foetus in the cephalic presentation, b) foetus in the breach presentation

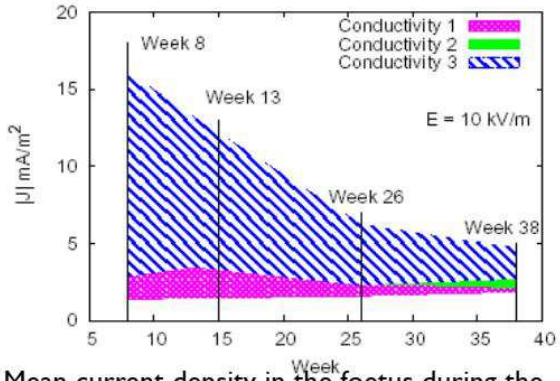

FIG: Mean current density in the foetus during the pregnancy for different conductivity scenarios

INTERNAL FIELD DOSIMETRY PROCEDURES – LF &HF EXPOSURES

Realistic Models – HF Exposures

- Examples of realistic models of the human head, eye, brain, and the complete body exposed to high-frequency electromagnetic radiation are given.
- Integral methods for electromagnetics dosimetry based on
  - Surface Integral Equation (SIE) and Method of Moments (MoM),
  - tensor volume integral equation (VIE),
  - hybrid BEM/FEM.
- The thermal dosimetry are models based on the use of Pennes' bioheat transfer equation (PBHE)

Realistic Models – HF Exposures

Internal Electromagnetic Field Dosimetry Methods

INTERNAL FIELD DOSIMETRY PROCEDURES – LF &HF EXPOSURES

- **The main dosimetric quantity for HF fields is the specific absorption rate (SAR) defined as the rate of energy W absorbed by, or dissipated in the unit body mass m:**

$$\mathrm{SAR} = \frac{dP}{dm} = \frac{d}{dm}\frac{dW}{dt} = C\frac{dT}{dt}$$

- **where C is the specific heat capacity of tissue, T is the temperature and t denotes time.**

- **Also, SAR is proportional to the square of the internal electric field:**

$$\mathrm{SAR} = \frac{dP}{dm} = \frac{dP}{\rho dV} = \frac{\sigma}{2\rho}|E|^2 = \frac{\sigma}{\rho}|E_{rms}|^2$$

INTERNAL FIELD DOSIMETRY PROCEDURES – LF &HF EXPOSURES

Realistic Models – HF Exposures

In the GHz frequency (f>6GHz) range one has:

- Absorbed power density (S_{ab})

$$S_{av} = \frac{1}{2A_{av}} \int_{A_{av}} \mathrm{Re}\left(\vec{E} \times \vec{H}^{*}\right) d\vec{A}$$

... defined at the surface of the body.

E ... the peak value of the electric field
H... the peak value of the magnetic field
A_{av} ... the averaging area

INTERNAL FIELD DOSIMETRY PROCEDURES – LF &HF EXPOSURES

SURFACE INTEGRAL EQUATION Formulation

- **Problem formulated as EM scattering problem** *[Cvetkovic&Poljak EMCEurope 2014]*
- Brain as a lossy homogeneous dielectric body of arbitrary shape *S* placed in free space

$$\varepsilon_{eff} = \varepsilon_0 \varepsilon_r - j\frac{\sigma}{\omega}$$

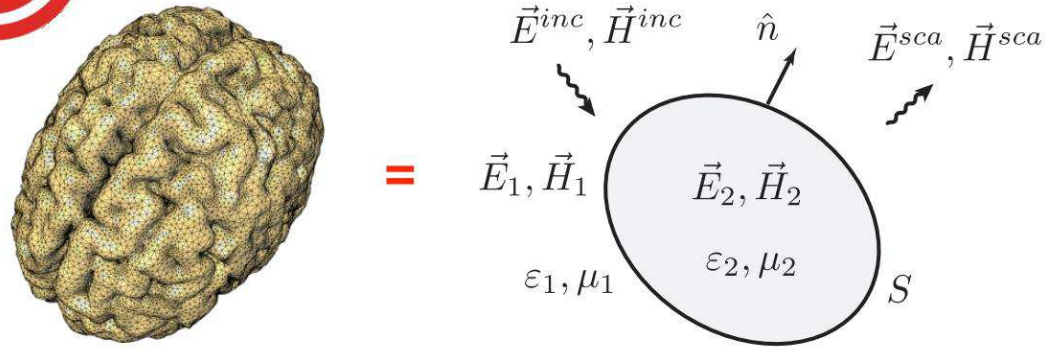

- Surface integral equation (SIE) formulation
- Equivalence theorem - two equivalent problems

Surface Integral Equation Formulation

EFIE (electric field integral equation) **- frequency domain formulation for dielectric**

$$\left[-\vec{E}_n^{sca}(\vec{J},\vec{M})\right]_{tan} = \begin{cases} \left[\vec{E}^{inc}\right]_{tan}, & n=1 \\ 0, & n=2 \end{cases}$$

$$\vec{E}_1^{inc} = j\omega\mu_1 \iint_S \vec{J}(\vec{r}\,')G_1(\vec{r},\vec{r}\,')\,\mathrm{d}S' - \\ -\frac{j}{\omega\varepsilon_1}\nabla\iint_S \nabla'_S\cdot\vec{J}(\vec{r}\,')G_1(\vec{r},\vec{r}\,')\,\mathrm{d}S' + \nabla\times\iint_S \vec{M}(\vec{r}\,')G_1(\vec{r},\vec{r}\,')\,\mathrm{d}S'$$

$$0 = j\omega\mu_2 \iint_S \vec{J}(\vec{r}\,')G_2(\vec{r},\vec{r}\,')\,\mathrm{d}S' - \\ -\frac{j}{\omega\varepsilon_2}\nabla\iint_S \nabla'_S\cdot\vec{J}(\vec{r}\,')G_2(\vec{r},\vec{r}\,')\,\mathrm{d}S' + \nabla\times\iint_S \vec{M}(\vec{r}\,')G_2(\vec{r},\vec{r}\,')\,\mathrm{d}S'$$

- E^{inc} known, J and M unknowns

INTERNAL FIELD DOSIMETRY PROCEDURES – LF &HF EXPOSURES

Realistic Models – HF Exposures

Plane wave illuminating the human head - an **unbounded scattering problem** formulated by the **Stratton-Chu integral relation** and **Helmholtz equation**.

The **domain exterior** to the head is expressed via the boundary integral equation

$$\alpha E'_{ext} = E'_{inc} - j\omega\mu \iint_{\partial V} (\vec{n}\times H_{ext}) G(\vec{r},\vec{r}')\,dS + \iint_{\partial V} \left[(\vec{n}\times E_{ext}) \times \nabla G(\vec{r},\vec{r}') - \frac{\nabla_s \cdot (\vec{n}\times H_{ext})}{\sigma + j\omega\mu} \nabla G(\vec{r},\vec{r}') \right] dS$$

$\vec{n}$ ... outer normal to surface bounding the volume ∂V

α ... solid angle subtended at the observation point

$\vec{E}'_{ext}$ $\vec{E}'_{inc}$ ... the total and the incident electric field, respectively

$$G(\vec{r},\vec{r}') = \frac{e^{-jk|\vec{r}-\vec{r}'|}}{4\pi|\vec{r}-\vec{r}'|}$$

... the Green's function

The behaviour of the field in an **interior region** is governed by partial differential equation

$$\nabla \times \left(\frac{j}{\omega\mu} \nabla \times \vec{E}_{\text{int}} \right) - (\sigma + j\omega\varepsilon)\vec{E}_{\text{int}} = 0$$

INTERNAL FIELD DOSIMETRY PROCEDURES – LF &HF EXPOSURES

Realistic Models – HF Exposures

Numerical procedure: hybrid FEM/BEM

Unknown electric and magnetic fields are approximated in terms of edge elements preserving the tangential continuity of the fields on the boundary:

$$\vec{E} = \sum_{i=1}^{n} \delta_i \vec{w}_i e_i \qquad \vec{H} = \sum_{i=1}^{n} \delta_i \vec{w}_i h_i$$

According to the weighted residual approach it can be written:

$$\int_V \left[\nabla \times \left(\frac{j}{\omega\mu} \nabla \times \vec{E}_{\text{int}} \right) - (\sigma + j\omega\varepsilon) \vec{E}_{\text{int}} \right] \delta_i \vec{w}_i dV = 0$$

Having applied some standard vector identities, followed by the divergence theorem, the weak formulation is obtained:

$$\int_V \left[\nabla \times \delta_i \vec{w}_i \cdot \vec{E}_{\text{int}} - (\sigma + j\omega\varepsilon) \delta_i \vec{w}_i \cdot \vec{E}_{\text{int}} \right]_i dV = \oint_{\partial V} \delta_i \vec{w}_i \cdot d\vec{S} \times \vec{H}_{\text{int}}$$

INTERNAL FIELD DOSIMETRY PROCEDURES – LF &HF EXPOSURES

Realistic Models – HF Exposures

Numerical procedure: hybrid FEM/BEM

Now FEM/BEM coupling can be undertaken by forcing the tangential components of electric and magnetic fields to be continuous across the surface ∂V

$$\oint_{\partial V} \delta_i \vec{w}_i \cdot d\vec{S} \times \vec{E}'_{\text{int}} = \oint_{\partial V} \delta_i \vec{w}_i \cdot d\vec{S} \times \vec{E}'_{ext}$$

Substituting E_{ext} and H_{ext} in Stratton-Chu IE with E_{int} and H_{int}, respectively, it follows:

$$\oint_{\partial V} \delta_i \vec{w}_i \cdot d\vec{S} \times \alpha_i \vec{E}'_{ext} =$$

[redacted]

$$-\frac{1}{\sigma + j\omega\mu} \oint_{\partial V} \delta_i \vec{w}_i \cdot d\vec{S} \times \oint_{\partial V} \nabla_s \cdot \left(\vec{n} \times \vec{H}_{ext}\right) \times \nabla G\left(\vec{r}, \vec{r}'\right) d\vec{S}$$

FEM/BEM procedure results in the following system of equations:

$$[E_{BEM}]\{e_{BEM}\} = \{e_{inc}\} + [H_{BEM}]\{h_{BEM}\}$$

$$[E_{FEM}]\{e_{FEM}\} = [H_{FEM}]\{h_{FEM}\}$$

INTERNAL FIELD DOSIMETRY PROCEDURES – LF &HF EXPOSURES

Realistic Models – HF Exposures

TENSOR VOLUME INTEGRAL Equation

The electric field induced inside the body illuminated by the incident field E_{inc} is governed by the tensor VIE given by:

$$\left[1+\frac{\tau(\vec{r})}{3j\omega\varepsilon_0}\right]\vec{E}(\vec{r})-\mathrm{PV}\int_v \tau(\vec{r}')\vec{E}(\vec{r})\cdot\underline{G}(\vec{r},\vec{r}')dv'=\vec{E}^{inc}(\vec{r})$$

where properties of biological body denoted by:

$$\tau(\vec{r})=\sigma(\vec{r})+j\omega\left[\varepsilon(\vec{r})-\varepsilon_0\right]$$

are known quantitites, while the total electric field inside the biological body is unknown to be determined.

The inner product can be expressed as:

$$\vec{E}(\vec{r})\cdot\underline{G}(\vec{r},\vec{r}')=\begin{bmatrix}\vec{G}_{xx}(\vec{r},\vec{r}') & \vec{G}_{xy}(\vec{r},\vec{r}') & \vec{G}_{xz}(\vec{r},\vec{r}')\\ \vec{G}_{yx}(\vec{r},\vec{r}') & \vec{G}_{yy}(\vec{r},\vec{r}') & \vec{G}_{yz}(\vec{r},\vec{r}')\\ \vec{G}_{zx}(\vec{r},\vec{r}') & \vec{G}_{zy}(\vec{r},\vec{r}') & \vec{G}_{zz}(\vec{r},\vec{r}')\end{bmatrix}\cdot\begin{bmatrix}E_x(\vec{r}')\\ E_y(\vec{r}')\\ E_z(\vec{r}')\end{bmatrix}$$

Numerical Solution using Method of Moments

Each element can be written in the following form

$$G_{x_px_q}(\vec{r},\vec{r}')=-j\omega\mu_0\left[\delta_{pq}+\frac{1}{k_0^2}\frac{\partial^2}{\partial x_p\partial x_q}\right]G_0(\vec{r},\vec{r}'),\quad p,q=1,2,3$$

representing the tensor Green function, where m, n= 1, 2, ..., N, and p, q= 1, 2, 3.

VIE is solved via MoM by discretizing the body into N subvolumes V_m. Each scalar component at the center of the m-th cell satisfies:

$$\left[1+\frac{\tau(\vec{r})}{3j\omega\varepsilon_0}\right]E_{x_p}(r_m)-\sum_{q=1}^{3}\left[\sum_{n=1}^{N}\tau(\vec{r})\,\mathrm{PV}\int_{V_m}G_{x_px_q}(\vec{r}_m,\vec{r}')dv'\right]E_{x_q}(\vec{r}_n)=E_{x_p}^{inc}(\vec{r}_m)$$

3N simultaneous equations for Ex, Ey, and Ez at the centers of N cells are obtained, and matrix system can be written as:

$$[G]\,[E]=-\left[E^{inc}\right]$$

where [G] is 3N x 3N matrix, while [E] and [E_{inc}] are 3N column matrices.

INTERNAL FIELD DOSIMETRY PROCEDURES – LF &HF EXPOSURES

Realistic Models – HF Exposures

The **temperature increase** can be obtained by solving the **bio-heat equation**

$$\nabla \cdot \left(k \nabla T \right) + \rho_b c_b w \left(T_a - T \right) + Q_m + Q_{EM} = 0$$

The boundary condition at the interface between skin and air is given in terms of the heat flux density:

$$\lambda \frac{\partial T}{\partial n} = -H \left(T_s - T_a \right)$$

Symbol	Description
k	heat conduction
ρ_b	blood mass density
c_b	specific heat capacity of blood
w	perfusion rate
T_a	arterial temperature
Q_m	tissue dependent heat source due to metabolic processes

Symbol	Description
λ	thermal conductivity
H	convection coefficient
T_s	temperature of the skin
T_a	temperature of the air
	volumetric heat source due to external field

INTERNAL FIELD DOSIMETRY PROCEDURES – LF &HF EXPOSURES

Realistic Models – HF Exposures

Numerical procedure: FEM

The integral formulation convenient for FEM solution:

$$\int_{V'}\left[\lambda\nabla f_j\cdot\nabla T+\rho_b c_b w\cdot T\cdot f_j\right]dV'=\int_{V'}\left(\rho_b c_b w\cdot T_a+Q_m+Q_{EM}\right)\cdot f_j dV'+\oint_{\partial V'}\lambda\frac{\partial T}{\partial n}f_j\vec{n}\cdot d\vec{S}'$$

FEM matrices:

$$[K]\{T\}=\{M\}+\{P\}$$

$$K_{ji}=\int_{\Omega_e}\nabla f_j(\lambda\nabla f_i)d\Omega_e+\int_{\Omega_e}W_b C_{pb}f_j f_i d\Omega_e$$

$$P_j=\int_{\Omega_e}\left(W_b C_{pb}T_a+Q_m+Q_{EM}\right)\cdot f_j d\Omega_e$$

$$M_j=\int_{\Gamma_e}\lambda\frac{\partial T}{\partial n}f_j d\Omega_e$$

INTERNAL FIELD DOSIMETRY PROCEDURES – LF &HF EXPOSURES

Realistic Models – HF Exposures

HF EXPOSURES – Computational Examples

Computational model of the human head including various head and eye tissues constructed from the magnetic resonance imaging (MRI) of a 24-year old male →

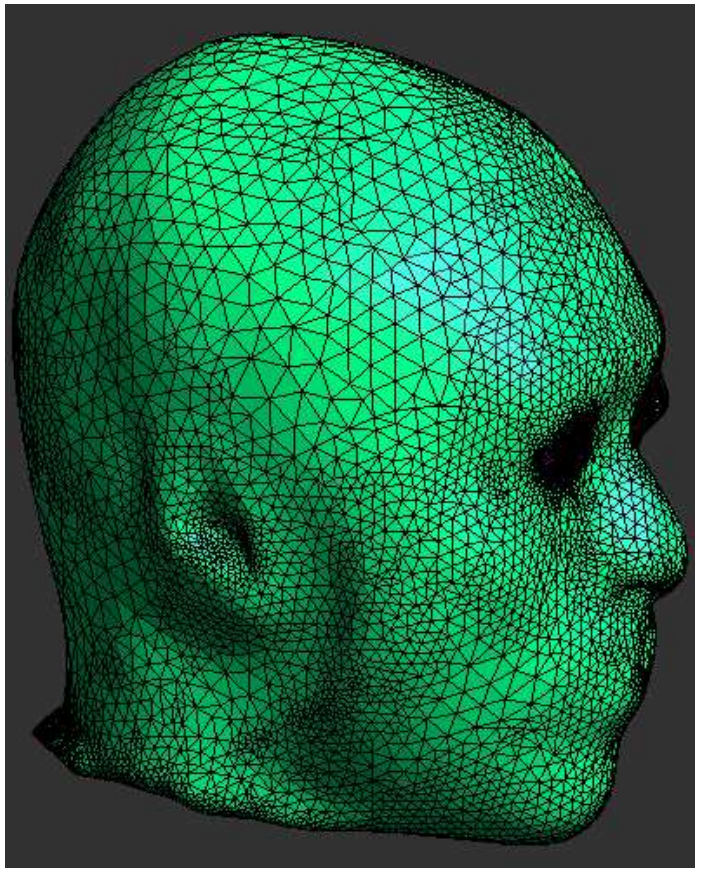

Head is exposed to vertically polarized plane wave at ***f*=1.8GHz** (1V/m amplitude) incident on the anterior side.

INTERNAL FIELD DOSIMETRY PROCEDURES – LF &HF EXPOSURES

HF EXPOSURES – Computational Examples

Realistic Models – HF Exposures

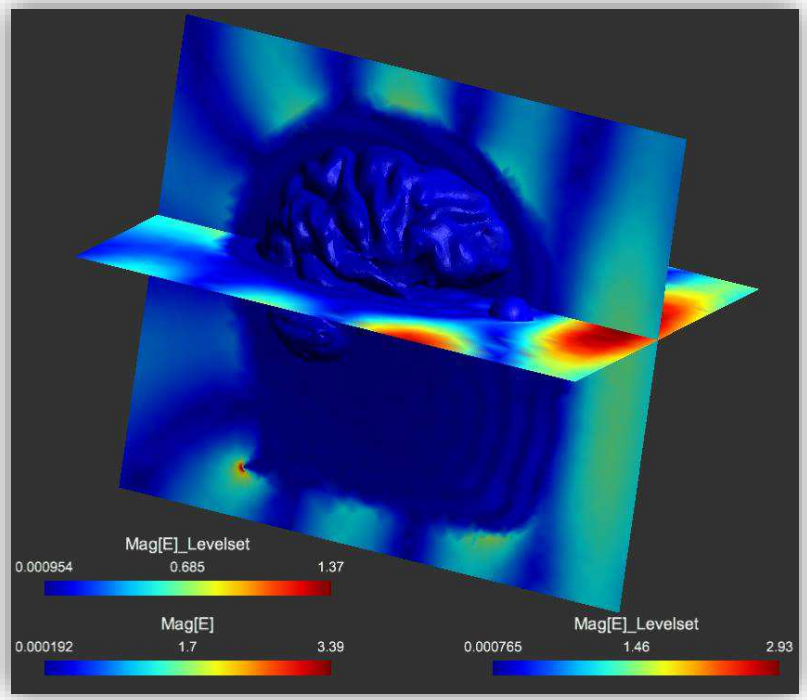

induced electric field

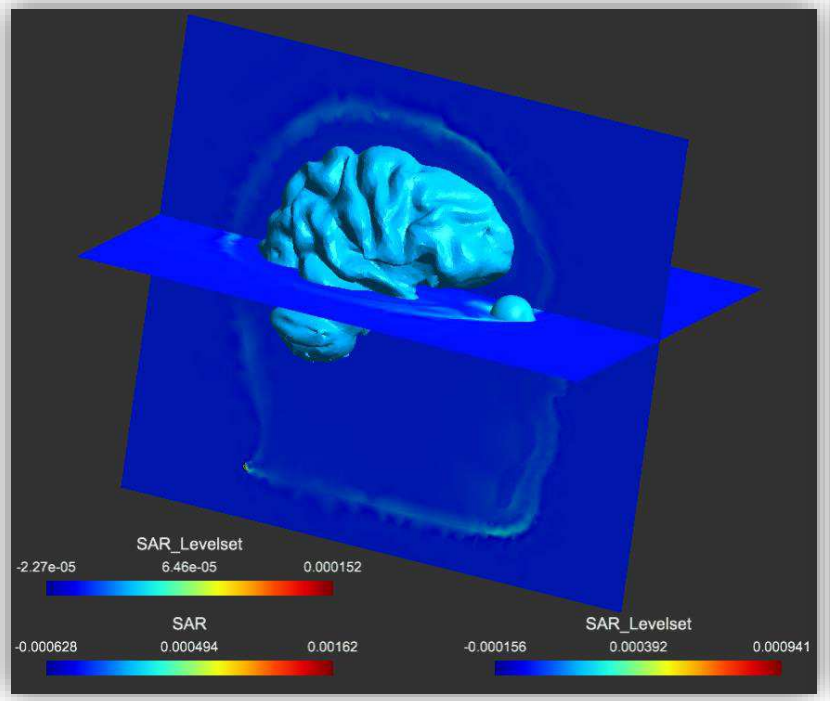

specific absorption rate (SAR)

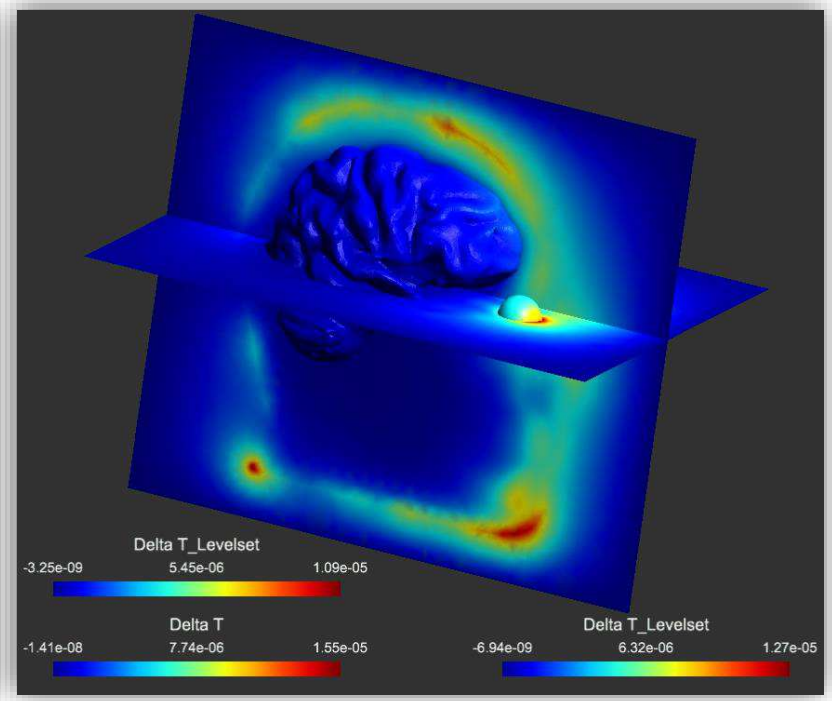

temperature increase

Head is exposed to vertically polarized plane wave at ***f*=1.8GHz** (1V/m amplitude) incident on the anterior side.

INTERNAL FIELD DOSIMETRY PROCEDURES – LF &HF EXPOSURES

Realistic Models – HF Exposures

HF EXPOSURES – Computational Examples

SAR and temperature increase in the eye due to the exposure to the plane wave at ***f*=1GHz** and ***f*=1.8GHz**

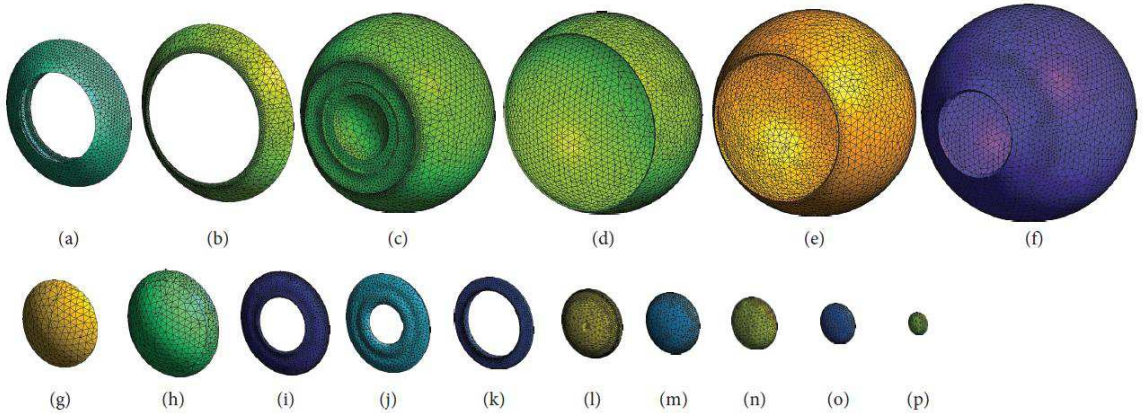

FIGURE 1: Modeled tissues from the extracted and the compound eye models (from [15]). (a) Ciliary body. (b) Ora serrata. (c) Vitreous humour. (d) Retina. (e) Choroid. (f) Sclera. (g) Cornea. (h) Aqueous humour. (i) Posterior ligaments. (j) Iris. (k) Ligaments. (l) Lens-I. (m) Lens-II. (n) Lens-III. (o) Lens-IV. (p) Lens-V.

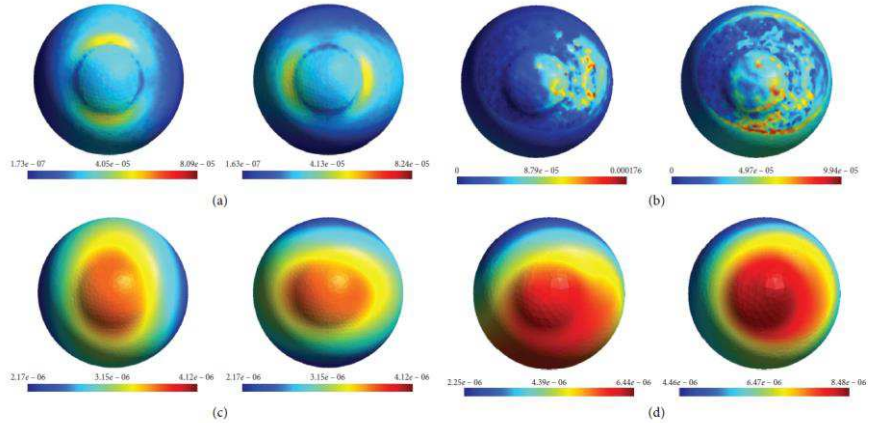

FIGURE 3: Surface distribution of SAR (in W/kg) (a, b) and temperature increase (in °C) (c, d) due to 1 GHz EM wave. Results obtained using the extracted eye model are in the top row and the compound eye model are in the bottom row. In each figure, the results on the left are due to horizontal polarization and on the right are due to vertical polarization.

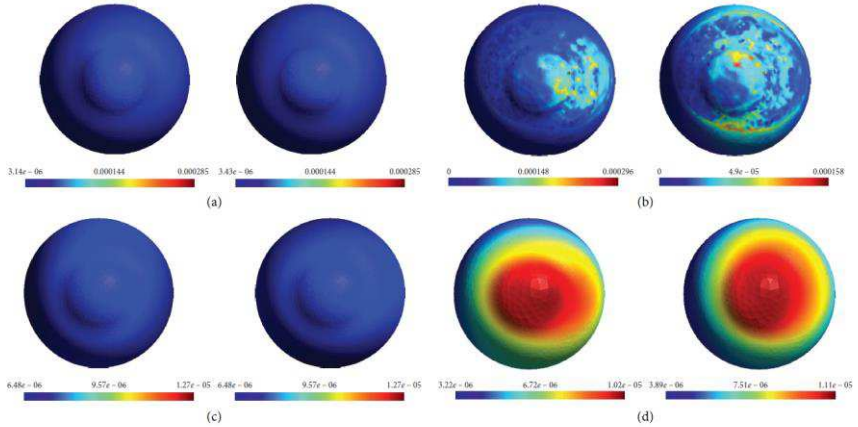

FIGURE 4: Surface distribution of SAR (in W/kg) (a, b), and temperature increase (in °C) (c, d) due to 1.8 GHz EM wave. Results obtained using the extracted eye model are in the top row and the compound eye model are in the bottom row. In each figure, the results on the left are due to horizontal polarization and on the right are due to vertical polarization.

INTERNAL FIELD DOSIMETRY PROCEDURES – LF &HF EXPOSURES

Realistic Models – HF Exposures

HF EXPOSURES – Computational Examples

Human Head Exposure

- **Hybrid FEM/BEM formulation**
- Head model from the MRI of a 24-year old male, 7 tissues, 16 ocular tissues, 4-Cole-Cole for tissue parameters, *[Laakso, Brain stimulation 8(5), pp. 906-813, 2015.]*

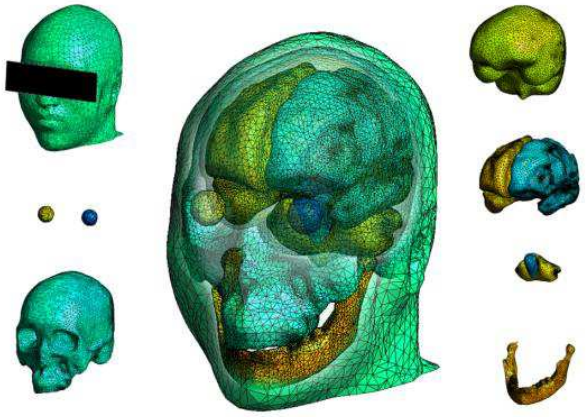

- Boundary surface 6.838 triangular elements
- Interior domain 1.034.641 tetrahedral elements

Table 1: Tissue dielectric parameters according to the 4-Cole-Cole Model described in [14]

	900 MHz		1800 MHz	
Tissue	σ (S/m)	ε (-)	σ (S/m)	ε (-)
Brainstem	0.591	38.886	0.915	37.011
Cerebellum	1.263	49.444	1.709	46.114
Eye (vitreous)	1.636	68.902	2.032	68.573
Head skin	0.867	41.405	1.185	38.872
Skull and mandible	0.339	20.788	0.588	19.343
Grey matter	0.942	52.725	1.391	50.079
Muscle tissue	0.943	55.032	1.341	53.549

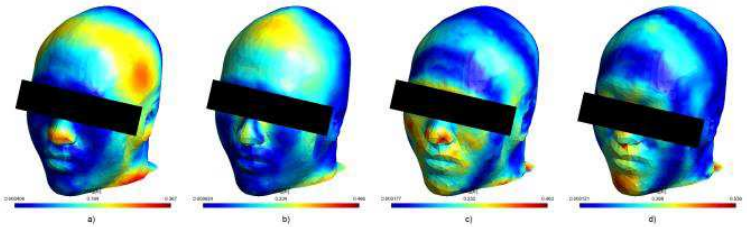

FIG: Induced electric field at head surface due to 900MHz/ 1800MHz, Vpol, Hpol, plane wave

INTERNAL FIELD DOSIMETRY PROCEDURES – LF &HF EXPOSURES

Realistic Models – HF Exposures

HF EXPOSURES – Computational Examples

Human Head Exposure

- **Hybrid FEM/BEM formulation**

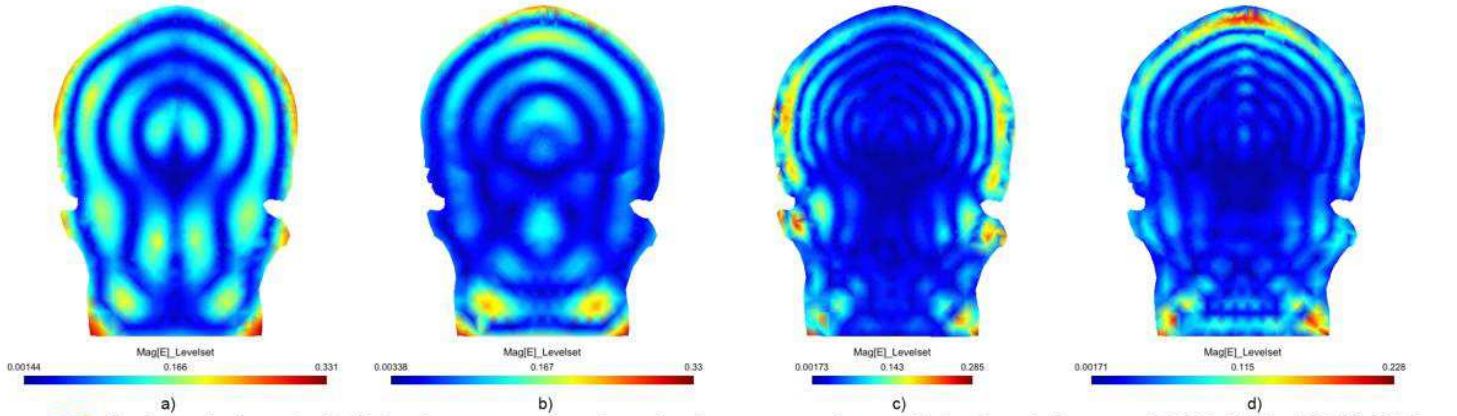

FIG: Induced electric field in the coronal and sagittal cross-sections of the head due to: a) 900 MHz HP, b) 900 MHz VP, c) 1800 MHz HP, d) 1800 MHz VP.

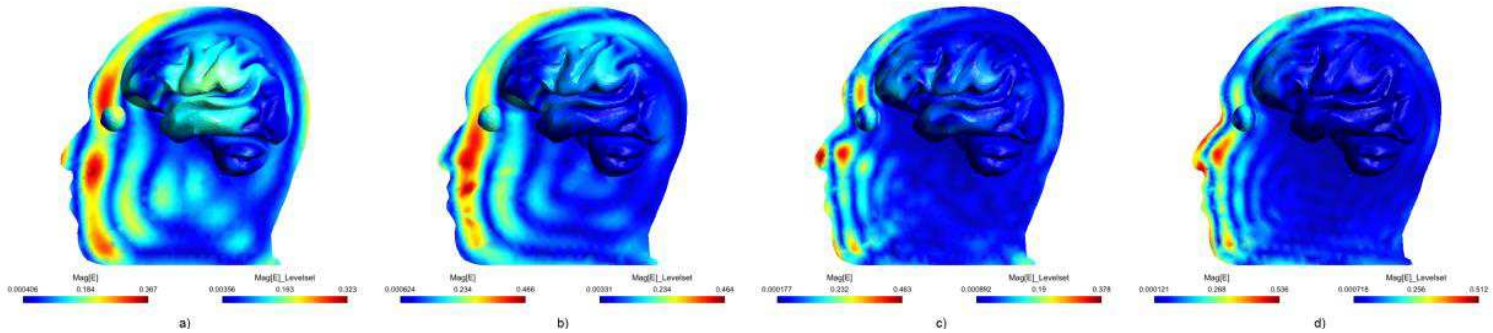

INTERNAL FIELD DOSIMETRY PROCEDURES – LF &HF EXPOSURES

Realistic Models – HF Exposures

HF EXPOSURES – Computational Examples

The Whole Body Exposure

The electric field induced inside the human body exposed to the plane wave incident field can be evaluated using the tensor volume integral equation.

The computational example: whole body exposure to base station antenna system mounted on the building roof at the height h=15 m.

The assessment is carried out for two frequency carriers, from the GSM (936 MHz) and UMTS downlink bands (2140 MHz).

Table: The electric field obtained by narrowband measurements and the related calculated whole-body SAR

Frequency [MHz]	E_{inc} [V/m]	SAR_{avg} [uW/kg]
936	0.141	0.0251
2140	14.87	267.5

Table: Electrical properties of the human body

Frequency [MHz]	ε_r [-]	σ [S/m]
936	55	1.4
2140	53.11	1.54

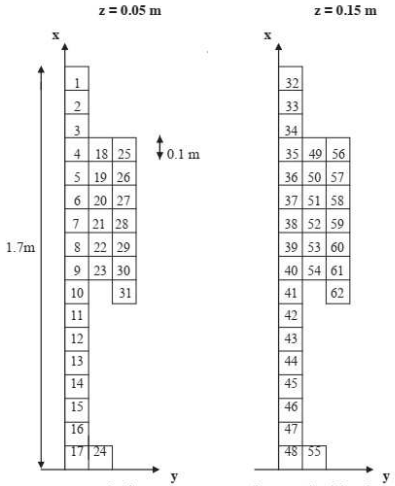

FIG: Geometry and dimensions of one half of the human body model constructed from 62 cells

The Whole Body Exposure

Whole-body average SAR is far below the ICNIRP exposure limit (0.08 W/kg).

Local SAR in any cube is also below the exposure limits.

Therefore the corresponding heating effects are negligible.

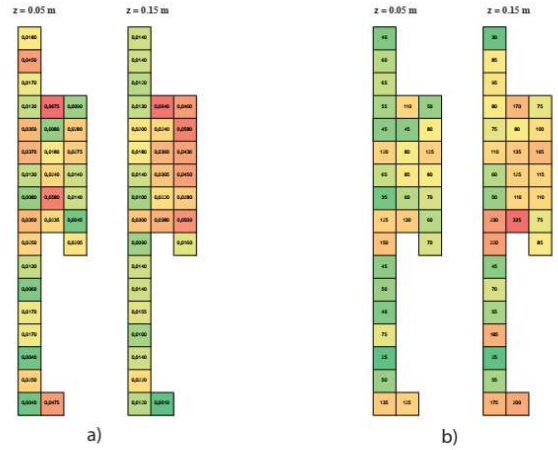

FIG: Specific absorption rate [μW/kg] in the human body model determined at z = 0.05 m and z = 0.15 m due to incident field at: a) 936 MHz, b) 2140 MHz

Table: Comparison of MoM results with the results obtained by measurements

Frequency	SAR_{avg}, measured	SAR_{avg}, MoM	SAR_{max}, MoM
MHz	[uW/kg]	[uW/kg]	[uW/kg]
936	0.0251	0.0212	0.064
2140	267.5	82.47	314.38

The numerical results and the measurement results are shown to be in a very good agreement.

INTERNAL FIELD DOSIMETRY PROCEDURES – LF &HF EXPOSURES

Realistic Models – HF Exposures

Uncertainty Quantification(UQ) & Sensitivity Analysis (SA)

- Uncertainties deal with **physics** of the problem of interest not to the errors in the mathematical description/solution...

Uncertainty Quantification

- Uncertainty quantification (UQ) - **quantitative characterization** and **reduction** of uncertainties in both computational and real world applications aiming to determine **how likely certain outcomes are** if some aspects of the system are not exactly known.

Sensitivity Analysis

- The study of how the uncertainty in the **output** of a mathematical model or a system (numerical or otherwise) can be apportioned to different sources of uncertainty in its **inputs**.

INTERNAL FIELD DOSIMETRY PROCEDURES – LF &HF EXPOSURES

Realistic Models – HF Exposures

Uncertainty Quantification(UQ) & Sensitivity Analysis (SA)

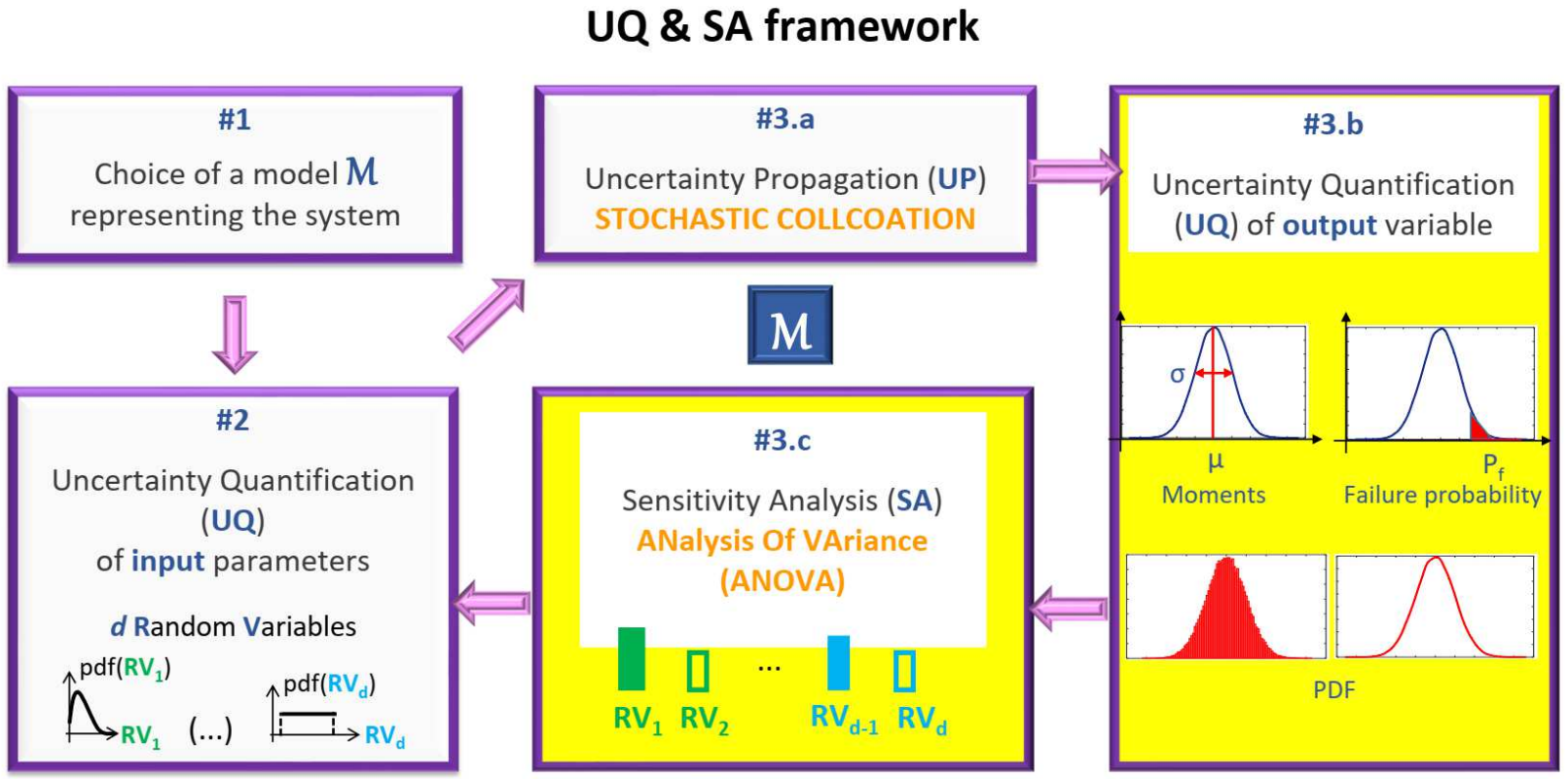

Realistic Models – HF Exposures

INTERNAL FIELD DOSIMETRY PROCEDURES – LF &HF EXPOSURES

UQ & SA

3 Compartment Electromagnetic Head Model

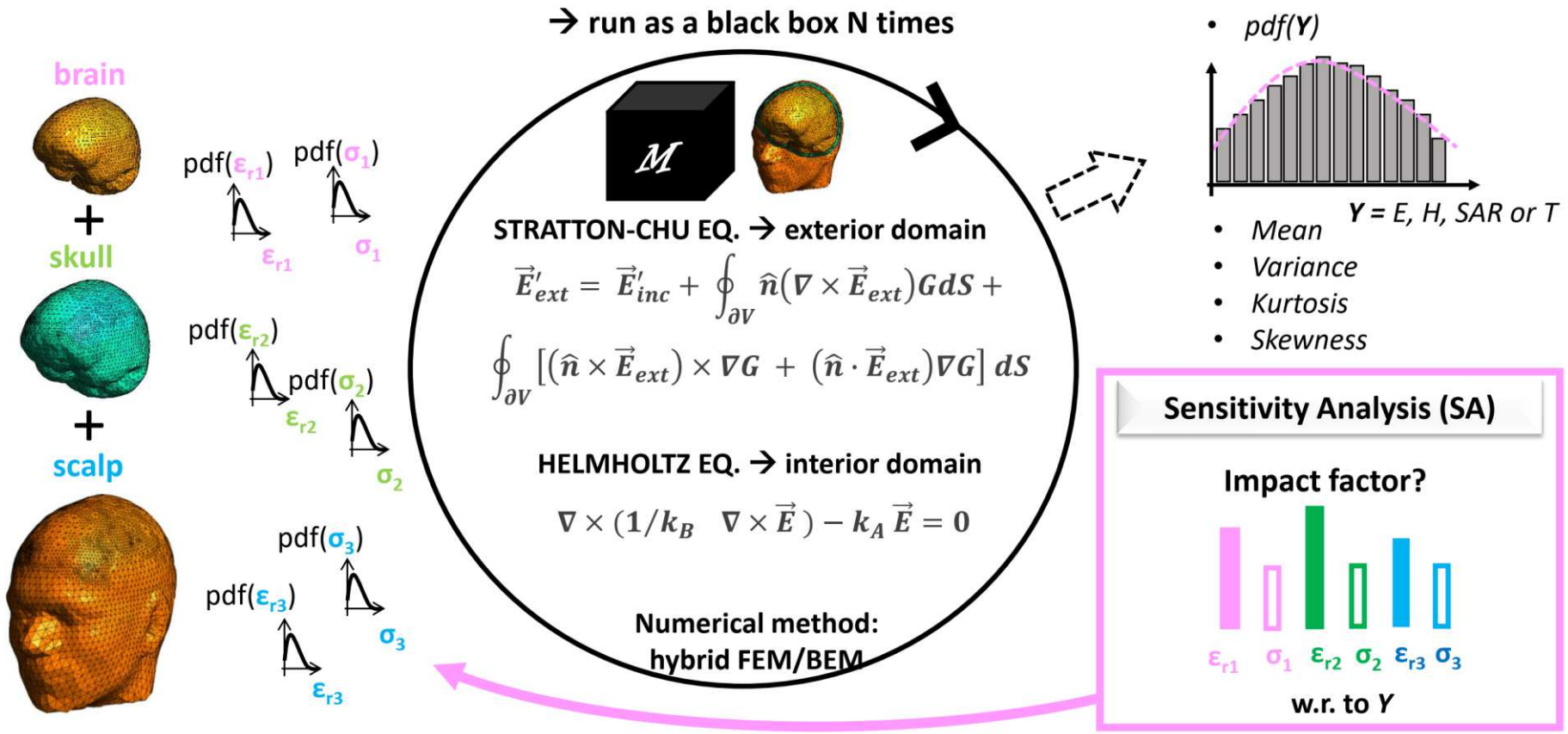

Realistic Models – HF Exposures

INTERNAL FIELD DOSIMETRY PROCEDURES – LF &HF EXPOSURES

UQ & SA

OUTLINE ON STOCHASTIC MODELING

- Heuristic
  - Instead of considering the random output Y = M(X) through samples, Y is represented by a series expansion

$$Y = \sum_{j=0}^{+\infty} y_j \, Z_j$$

where:

Sudret, *PCE Theory, Numerical Methods & Applications Parts I & II*, MNMUQ, 2014

  - $\{Z_j\}_{j=0}^{+\infty}$ is a numerable set of random variables that forms a basis of a suitable space $\mathcal{H} \supset Y$
  - $\{y_j\}_{j=0}^{+\infty}$ is the set of coordinates of Y in this basis

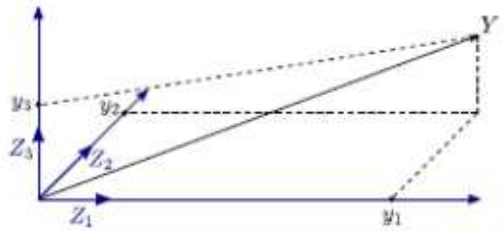

- Actually
  - Truncated series expansion
  - EMC illustration: Y = current *I*

Random N-vector: $\mathbf{X} = (X_1, X_2, \ldots, X_N)$

Polynomial basis: $\Phi^u(\mathbf{X})$ function of $\mathbf{X}$

$$[I]_u(\mathbf{X}) \approx \sum_{v_1=0}^{n_1} \cdots \sum_{v_N=0}^{n_N} \eta_w^{v_1 \ldots v_N} \Phi^u(\mathbf{X})$$

Expansion coefficient: $\eta_w^{v_1 \ldots v_N}$

Realistic Models – HF Exposures

INTERNAL FIELD DOSIMETRY PROCEDURES – LF &HF EXPOSURES

UQ & SA

OUTLINE ON STOCHASTIC MODELING

Basic idea: close to PCE (spectral method) → choice of polynomial basis

Finding a polynomial approximation of the function of a real variable

$$f(x)=\frac{1}{1+x^2}$$

Lagrange polynomials

$$f(x)\approx\sum_{i=0}^{n} f_i L_i(x)$$

$\{L_i(x)\}_{0\le i\le n}$ nth order polynomial basis

$$L_i(x)=\prod_{\substack{j=0\\ j\neq i}}^{n}\frac{x-x_j}{x_i-x_j}$$

We can demonstrate:

$$f_i=f(x_i)$$

Finding a polynomial approximation of the function of a random variable:

$$f(X)=\frac{1}{1+X^2}$$

Lagrange polynomials

$$f(X)\approx\sum_{i=0}^{n} f_i L_i(X)$$

Stochastic collocation method

Problem:

$$p(x)=\frac{1}{\sqrt{2\pi}}e^{-\frac{x^2}{2}}$$

$$Y=f(X)$$

Realistic Models – HF Exposures

INTERNAL FIELD DOSIMETRY PROCEDURES – LF &HF EXPOSURES

UQ & SA

OUTLINE ON STOCHASTIC MODELING

$\{x_j\}_{0\le j\le n}$ defined by the Gauss quadrature rule

$$I=\int_{-\infty}^{+\infty}\frac{1}{\sqrt{2\pi}}e^{\frac{-x^2}{2}}f(x)dx\approx\sum_{j=0}^{n}\omega_j f(x_j)$$

Mean value assessment

$$<Y>=<f(X)>=\int_{-\infty}^{+\infty}\frac{1}{\sqrt{2\pi}}e^{\frac{-x^2}{2}}f(x)dx$$

Replacing f(x) by its expansion

$$\omega_i=\int_{-\infty}^{+\infty}\frac{1}{\sqrt{2\pi}}e^{\frac{-x^2}{2}}L_i(x)dx$$

$$<Y>=\int_{-\infty}^{+\infty}\frac{1}{\sqrt{2\pi}}e^{\frac{-x^2}{2}}\left(\sum_{i=0}^{n}f_iL_i(x)\right)dx=\sum_{i=0}^{n}f_i\int_{-\infty}^{+\infty}\frac{1}{\sqrt{2\pi}}e^{\frac{-x^2}{2}}L_i(x)dx \Rightarrow I_i=\sum_{j=0}^{n}\omega_jL_i(x_j)$$

$L_i(x_j)=\delta_{ij}$ ⟹ All the terms are equal to 0 except at its particular collocation point i:

$$<Y>\approx\sum_{i=0}^{n}\omega_i f_i$$

Variance assessment

$$\mathrm{var}(Y)=\sum_{k=0}^{n}\omega_k(f_k)^2-<Y>^2$$

Realistic Models – HF Exposures

INTERNAL FIELD DOSIMETRY PROCEDURES – LF &HF EXPOSURES

UQ & SA

OUTLINE ON STOCHASTIC MODELING

Derivation of statisctical moments:

$$E(Z^0;t)=\sum_{i=0}^{n}E_i(Z^0)L_i(t) \qquad L_i(t_j)=\delta_{ij} \qquad E_i(Z^0)=E(Z^0;t_i) \qquad \int_D pdf(u)f(u)du=\sum_{i=0}^{n}\omega_i f(t_i)$$

Mean value derivation

$$\left\langle E(Z^0;t)\right\rangle=\int_D E(Z^0;u)\,pdf(u)du \qquad \left\langle E(Z^0;t)\right\rangle=\sum_{i=0}^{n}E_i\left(Z^0\right)\int_D L_i(u)\,pdf(u)du=\sum_{i=0}^{n}\omega_i E_i\left(Z^0\right)$$

Variance derivation

$$\sigma^2=\int_D\left[E(Z^0;u)-\left\langle E(Z^0;t)\right\rangle\right]^2 pdf(u)du \qquad \sigma^2=\int_D\left[\sum_{i=0}^{n}E_i(Z^0)L_i(u)-\sum_{i=0}^{n}\omega_i E_i(Z^0)\right]^2 pdf(u)du$$

$$\sigma^2=\int_D E^2(Z^0,u)\,pdf(u)du-2\int_D E(Z^0,u)\left\langle E(Z^0,t)\right\rangle pdf(u)du+\left\langle E(Z^0,t)\right\rangle^2\int_D pdf(u)du$$

$$\sigma^2=\int_D E^2(Z^0,u)\,pdf(u)du-2\left\langle E(Z^0,t)\right\rangle\int_D E(Z^0,u)\,pdf(u)du+\left\langle E(Z^0,t)\right\rangle^2$$

$$\sigma^2=\int_D E^2(Z^0,u)\,pdf(u)du-\left\langle E(Z^0,t)\right\rangle^2=\left\langle E^2(Z^0,t)\right\rangle-\left\langle E(Z^0,t)\right\rangle^2$$

$$\sigma^2=\sum_{i=0}^{n}\omega_i E_i^2(Z^0)-\left(\sum_{i=0}^{n}\omega_i E_i(Z^0)\right)^2 \qquad \sigma^2=\left\langle E^2(Z^0,t)\right\rangle-\left\langle E(Z^0,t)\right\rangle^2$$

Realistic Models – HF Exposures

INTERNAL FIELD DOSIMETRY PROCEDURES – LF &HF EXPOSURES

UQ & SA

OUTLINE ON STOCHASTIC MODELING

- Determination of weights w_i and points x_i
- Computation of the system response

$$f_i = f(x_i) = \frac{1}{1 + x_i^2}$$

- Mean value and variance assessment methods are given by:

$$< f(X) >= \sum_{i=0}^{n} \omega_i f_i$$

$$\mathrm{var}(f) = \sum_{i=0}^{n} \omega_i f_i^2 - < f(X) >^2$$

Small number N of collocation points !

N=n+1	Weights	Points
2	0.5000 0.5000	1 -1
3	0.1667 0.6667 0.1667	1.7321 0 -1.7321
4	0.0459 0.4541 0.4541 0.0459	2.3344 0.7420 -0.7420 -2.3344
5	0.0113 0.2221 0.5333 0.2221 0.0113	2.8570 1.3556 0 -1.3556 -2.8570

Normal distribution (Gauss-Hermite)

General approach

Realistic Models – HF Exposures

INTERNAL FIELD DOSIMETRY PROCEDURES – LF &HF EXPOSURES

UQ & SA

OUTLINE ON STOCHASTIC MODELING

- Random parameter: $Z \equiv \hat{u} = Z^0 + \hat{u}^0$
  Z^0 central value, $\hat{u}^0$ Random Variable (RV) arbitrarily given
- Uniform, normal, exponential ... laws ($\hat{u}$)
- Stat. moments from output I computed from "$n+1$ well chosen" weighted (ω_i) points I_i [3]

Mean $\langle I \rangle = \sum_{i=0}^{n} \omega_i I_i$	Variance $\sigma_I^2 = \sum_{i=0}^{n} \omega_i I_i^2 - \langle I \rangle^2$

Extension to multi-RV

Statistical moment	Computation
1st	$mean(I) = \sum_{i=0}^{n1} \sum_{j=0}^{n2} \omega_i^s \omega_j^t I_{ij}$
2nd	$variance(I) = \sum_{i=0}^{n1} \sum_{j=0}^{n2} \omega_i^s \omega_j^t I_{ij}^2 - [mean(I)]^2$
3rd	$skewness(I) = \sum_{i=0}^{n1} \sum_{j=0}^{n2} \frac{[\omega_i^s \omega_j^t I_{ij} - mean(I)]^3}{[variance(I)]^{\frac{3}{2}}}$
4th	$kurtosis(I) = \sum_{i=0}^{n1} \sum_{j=0}^{n2} \frac{[\omega_i^s \omega_j^t I_{ij} - mean(I)]^4}{[variance(I)]^2}$

Modeling « Uncertainties »

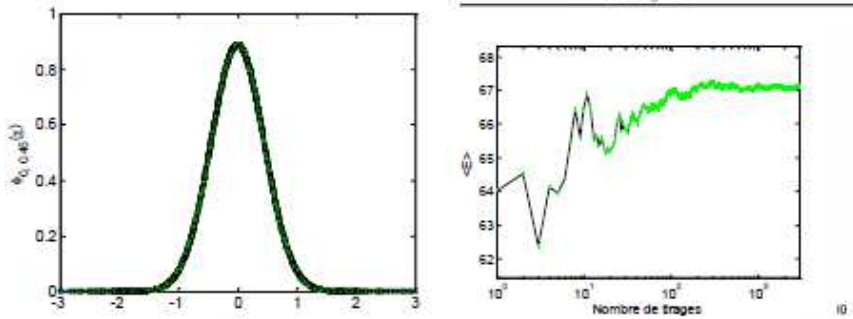

Validation

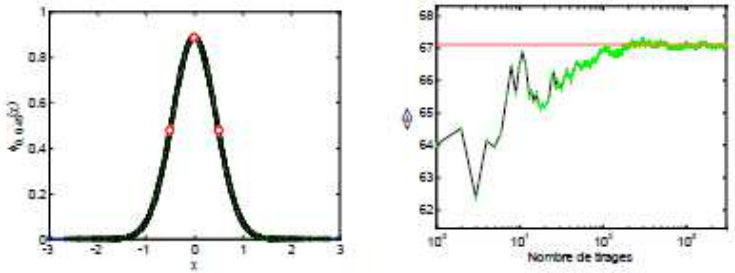

SC ≈ smart MC

Realistic Models – HF Exposures

INTERNAL FIELD DOSIMETRY PROCEDURES – LF &HF EXPOSURES

UQ & SA

Stochastic moments of the induced electric field in the surface of the tissues

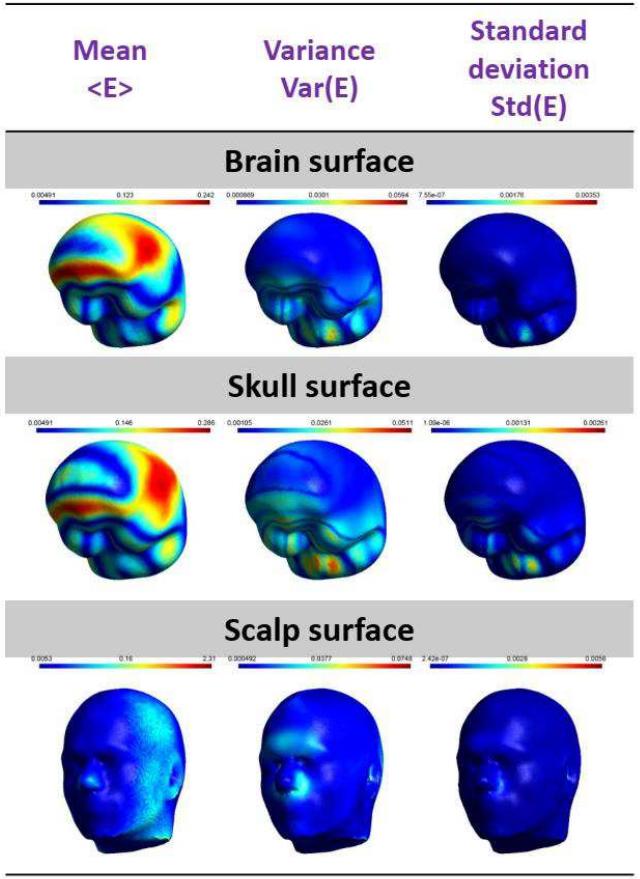

The impact of input variables on induced electric field along the sagittal axis of the head

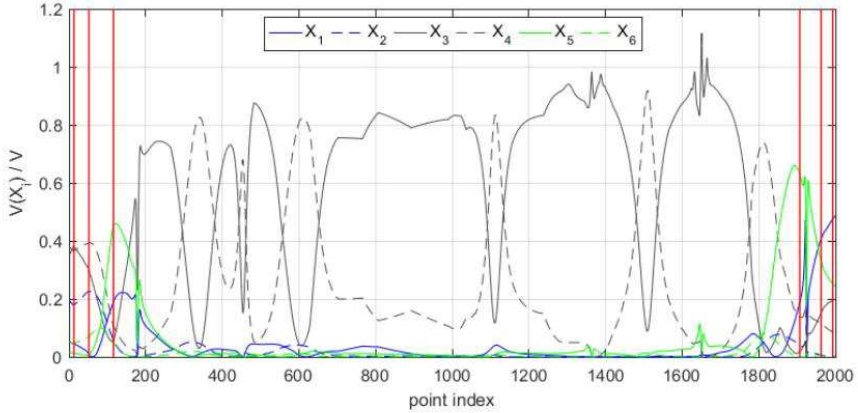

The impact factor of input variables on induced electric field on the surface of the tissues

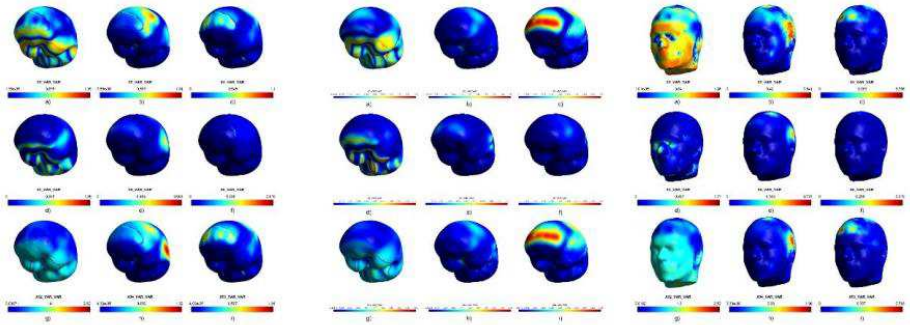

Biomedical Applications

Transcranial Magnetic Stimulation (TMS)

UNDERLYING PRINCIPLES

- TMS (transcranial magnetic stimulation):
  - very important in diagnostic and therapeutic purposes,
  - in studying functional mechanism and role of specific cortical regions,
  - in preoperative mapping in patients undergoing awake brain surgery,
  - etc.
- Basically:
  - brief current pulse (5-10 kA)
  - generates changing magnetic field (1-5 T),
  - the induced electric field (5 V/cm), that in turn,
  - depolarization or hyperpolarization of neurons
  - causes activation of action potential if certain threshold value is achieved
  - TMS requires (**focused**) stimulation of specific regions while minimizing stimulation elsewhere

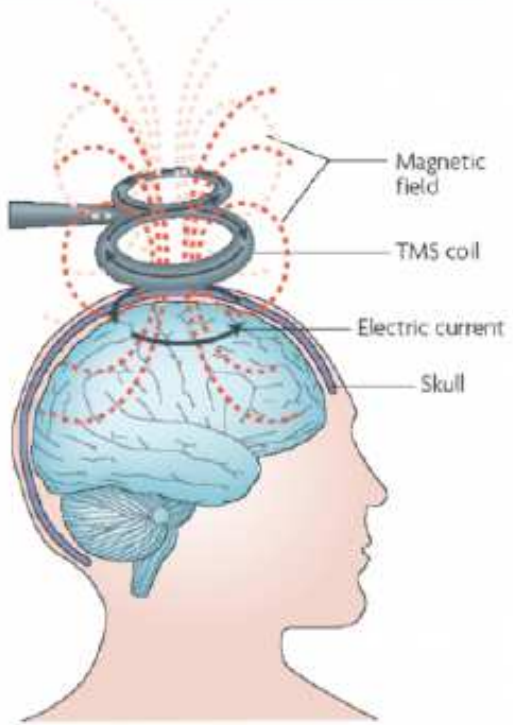

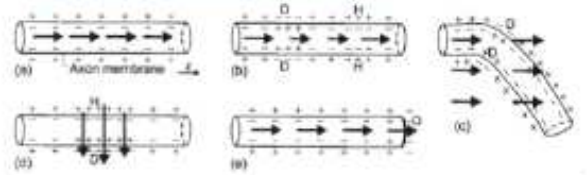

- Neuron activation by electric field

Biomedical Applications

Transcranial Magnetic Stimulation (TMS)

Typical TMS coils

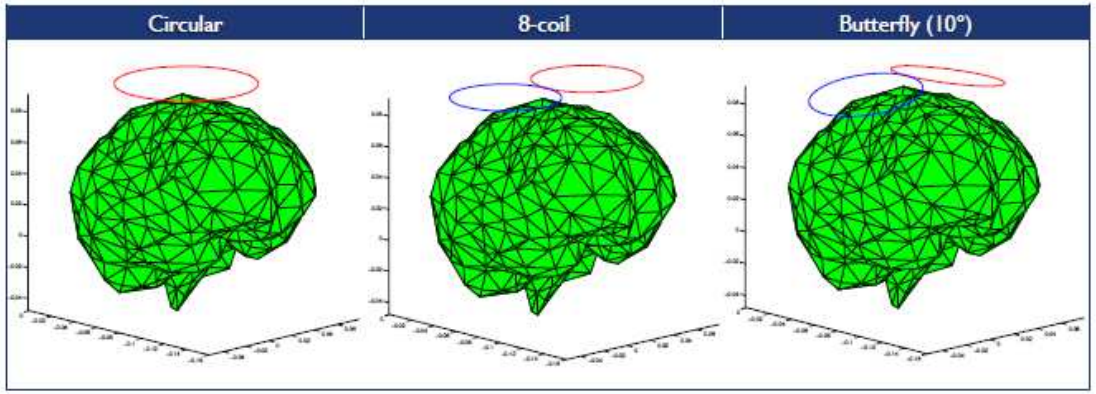

Table: TMS coils parameters			
	Circular	8-coil	Butterfly (10°)
Frequency	2.44 kHz	2.44 kHz	2.44 kHz
Coil radius	4.5 cm	3.5 cm	3.5 cm
Number of turns	14	15	15
Coil current (max)	2843 A (8000 A)	2843 A (8000 A)	2843 A (8000 A)

FIG: Magstim coils

MODELING TMS

- Problem formulated as EM **scattering** problem *[Cvetkovic&Poljak EMCEurope 2014]*
- Brain as a lossy homogeneous dielectric body of arbitrary shape S placed in free space

$$\varepsilon_{eff} = \varepsilon_0 \varepsilon_r - j\frac{\sigma}{\omega}$$

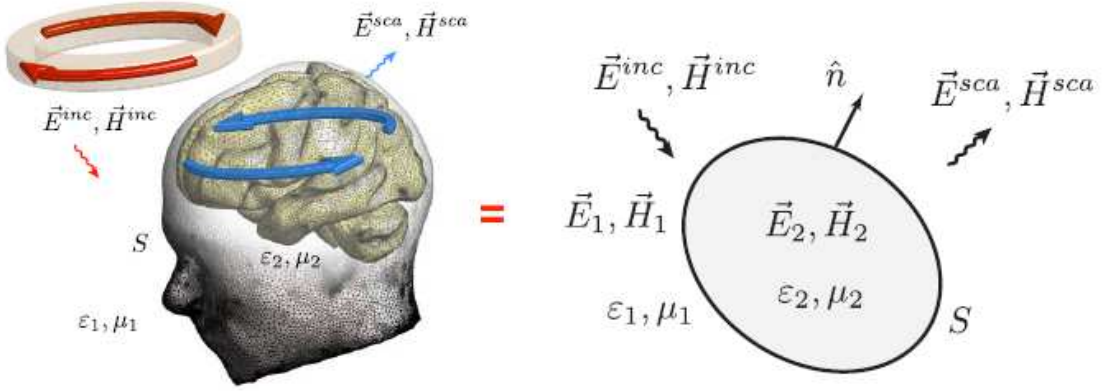

- Surface integral equation (SIE) formulation
- Equivalence theorem - two equivalent problems

Biomedical Applications

Transcranial Magnetic Stimulation (TMS)

MODELING TMS

- Fields due to these equivalent sources placed in homogeneous space

$$\vec{E}_n^{sca}(\vec{J},\vec{M}) = -j\omega\vec{A}_n - \nabla\varphi_n - \frac{1}{\varepsilon_n}\nabla\times\vec{F}_n$$

$$\vec{H}_n^{sca}(\vec{J},\vec{M}) = -j\omega\vec{F}_n - \nabla\psi_n + \frac{1}{\mu_n}\nabla\times\vec{A}_n$$

- n=1,2; index of the region

$$\vec{A}_n(\vec{r}) = \mu_n\int_S \vec{J}(\vec{r}')G_n(\vec{r},\vec{r}')\,\mathrm{d}S' \qquad \varphi_n(\vec{r}) = \frac{j}{\omega\varepsilon_n}\int_S \nabla'_S\cdot\vec{J}(\vec{r}')G_n(\vec{r},\vec{r}')\,\mathrm{d}S'$$

$$\vec{F}_n(\vec{r}) = \varepsilon_n\int_S \vec{M}(\vec{r}')G_n(\vec{r},\vec{r}')\,\mathrm{d}S' \qquad \psi_n(\vec{r}) = \frac{j}{\omega\mu_n}\int_S \nabla'_S\cdot\vec{M}(\vec{r}')G_n(\vec{r},\vec{r}')\,\mathrm{d}S'$$

- Green's fn. for homogeneous region n

$$G_n(\vec{r},\vec{r}') = \frac{e^{-jk_nR}}{4\pi R};\ R = |\vec{r}-\vec{r}'|$$

k_n - wave number in medium n

MODELING TMS

- Scattered field in terms of two equivalent surface currents (fictitious)
- Coupled integro-differential equation set

$$\left[-\vec{E}_1^{sca}(\vec{J},\vec{M})\right]_{tan} = \left[\vec{E}^{inc}\right]_{tan}$$

$$\left[-\vec{H}_1^{sca}(\vec{J},\vec{M})\right]_{tan} = \left[\vec{H}^{inc}\right]_{tan}$$

$$\left[-\vec{E}_2^{sca}(\vec{J},\vec{M})\right]_{tan} = 0$$

$$\left[-\vec{H}_2^{sca}(\vec{J},\vec{M})\right]_{tan} = 0$$

- Choosing the two b.c. for electric field >> frequency domain integral formulation for dielectric object

EFIE (electric field integral equation): (other possible formulations MFIE, CFIE, PMCWHT, Muller)

$$\left[-\vec{E}_n^{sca}(\vec{J},\vec{M})\right]_{tan} = \begin{cases}\left[\vec{E}^{inc}\right]_{tan}, & n=1\\ 0, & n=2\end{cases}$$

$$\vec{E}_1^{inc} = j\omega\mu_1\iint_S \vec{J}(\vec{r}')G_1(\vec{r},\vec{r}')\,\mathrm{d}S' - \\ -\frac{j}{\omega\varepsilon_1}\nabla\iint_S \nabla'_S\cdot\vec{J}(\vec{r}')G_1(\vec{r},\vec{r}')\,\mathrm{d}S' + \nabla\times\iint_S \vec{M}(\vec{r}')G_1(\vec{r},\vec{r}')\,\mathrm{d}S'$$

$$0 = j\omega\mu_2\iint_S \vec{J}(\vec{r}')G_2(\vec{r},\vec{r}')\,\mathrm{d}S' - \\ -\frac{j}{\omega\varepsilon_2}\nabla\iint_S \nabla'_S\cdot\vec{J}(\vec{r}')G_2(\vec{r},\vec{r}')\,\mathrm{d}S' + \nabla\times\iint_S \vec{M}(\vec{r}')G_2(\vec{r},\vec{r}')\,\mathrm{d}S'$$

- E^{inc} known, J and M unknowns

Biomedical Applications

Transcranial Magnetic Stimulation (TMS)

Computational example: distribution of induced fields

Distribution of E and B fields on brain surface

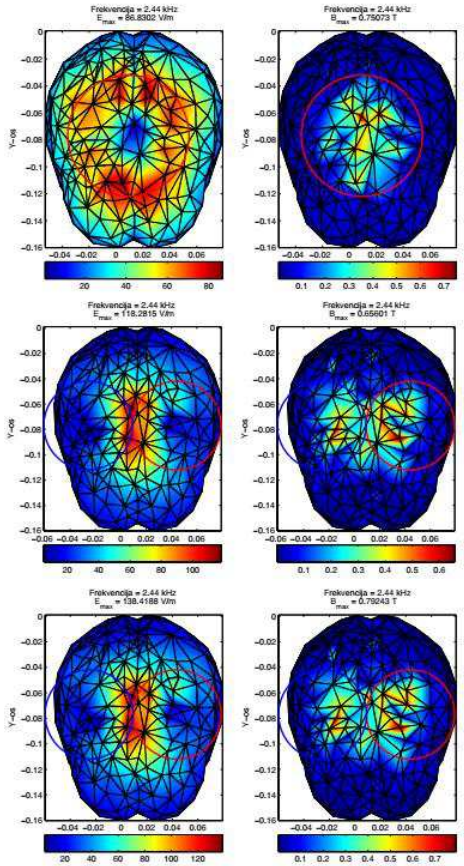

Electric field versus distance from the brain surface, under the coil geometric center

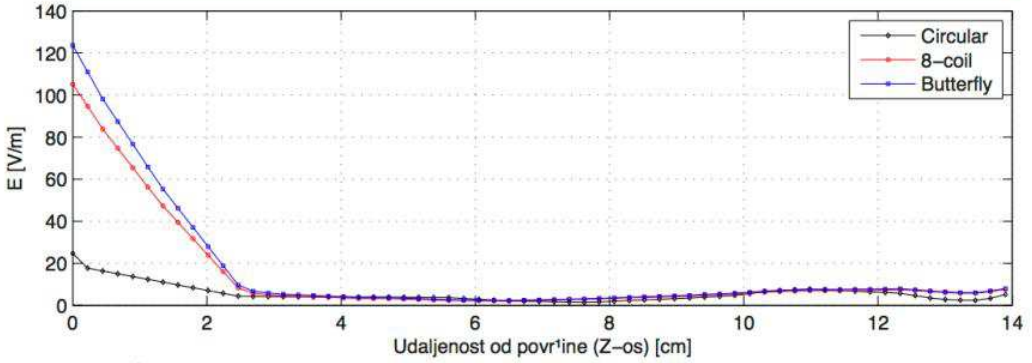

CVETKOVIĆ *et al.*: ANALYSIS OF TRANSCRANIAL MAGNETIC STIMULATION BASED ON THE SURFACE INTEGRAL EQUATION 1541

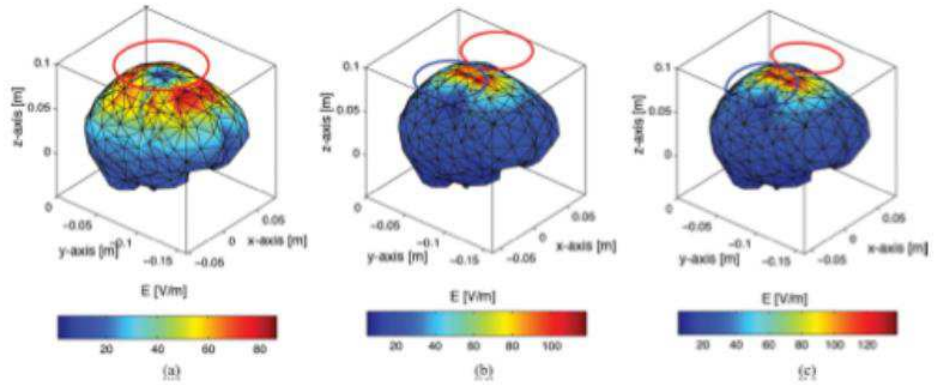

Fig. 4. Induced electric field on the brain surface due to: (a) Circular coil, (b) 8-coil, and (c) butterfly coil. All coils are placed 1 cm over the primary motor cortex.

[Cvetković, Poljak, Haueisen, IEEE Trans BME, June 2015.]

Biomedical Applications

Transcranial Electric Stimulation (TES)

Transcranial Electric Stimulation (TES)

- The technique of **transcranial electric stimulation (TES)** involves an application of the electrical current through two or more electrodes placed on the scalp.
- Its principal mechanism of action is a subthreshold modulation of neurona membrane potentials, which alters cortical excitability and activity dependent on the current flow direction through the target neurons.
- It is reported to play an important role in the treatment of various neurological and psychiatric disorders such as *depression*, *anxiety* and *Parkinson's disease*.

- *S. Bai, C. Loo and S. Dokos, "A review of computational models of transcranial electrical stimulation," Crit Rev Biomed Eng, vol. 41, no. 1, pp. 21-35., 2013.*
- *G. M. Noetscher, J. Yanamadala, S. N. Makarov and A. Pascual-Leone, "Comparison of cephalic and extracephalic montages for transcranial direct current stimulation--a numerical study," IEEE Trans Biomed Eng., vol. 61, no. 9, pp. 2488-2498, 2014.*

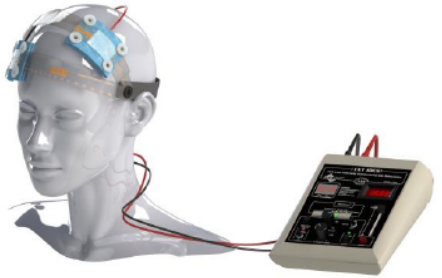

Biomedical Applications

Transcranial Electric Stimulation (TES)

MODELS

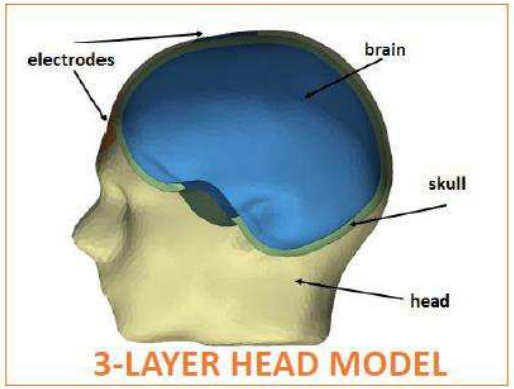

3-LAYER HEAD MODEL

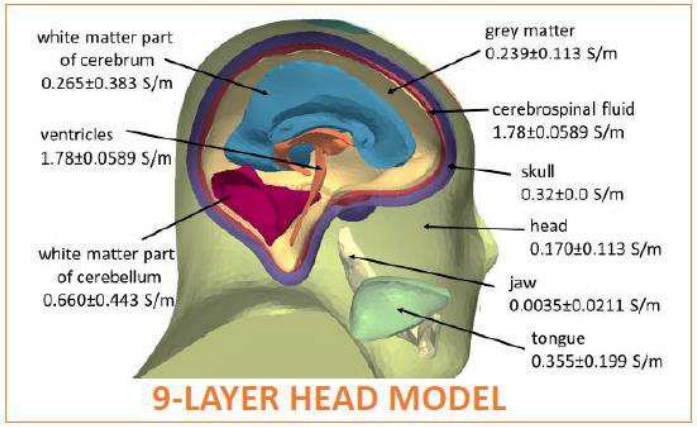

9-LAYER HEAD MODEL

FORMULATION

POISSON'S PARTIAL DIFFERENTIAL EQUATION FOR QUASI-STATIC APPROXIMATION

$$\nabla \cdot (-\sigma \nabla \varphi) = I$$

The boundary conditions:

$\varphi = \pm 1\ V$ at the circular area of the electrodes

$J = -\sigma \frac{\partial \varphi}{\partial n}$ at the rest of the domain

Biomedical Applications

Transcranial Electric Stimulation (TES)

Boundary-integral method

The boundary integral representation of:

$$\nabla^2\varphi = 0$$

is:

$$e(\vec{\xi})u(\vec{\xi}) + \int_\Gamma \varphi\vec{\nabla}u^* \cdot \vec{n}d\Gamma = \int_\Gamma u^* \cdot (\vec{n} \cdot \vec{\nabla}\varphi)d\Gamma$$

where:

Γ .... boundary of the cylinder
$\vec{\xi}$ ... source point
c ... free coefficient

$u^* = 1/4\pi|\vec{r} - \vec{\xi}|$ ... fundamental solution of the Laplace operator.
φ ... potential & flux $= \vec{n} \cdot \vec{\nabla}\vec{r}$).

Stochastic moments

- We are interested in computing the stochastic moments of the output value of interest, $Y(\boldsymbol{\xi})$. From the statistics the formulas for the mean and variance are as follows:

$$\mu(Y(\boldsymbol{\xi})) = \int_D Y(\boldsymbol{\xi})p(\boldsymbol{\xi})d\boldsymbol{\xi}$$

$$Var(Y(\boldsymbol{\xi})) = \int_D \left(Y(\boldsymbol{\xi}) - \mu(Y(\boldsymbol{\xi}))\right)^2 p(\boldsymbol{\xi})d\boldsymbol{\xi}$$

$\boldsymbol{D}$ ... probability space for the input vector $\boldsymbol{\xi}^{(i)} = \left[\xi_1^{(i)}, \xi_2^{(i)}, \dots, \xi_d^{(i)}\right]$

$p(\boldsymbol{\xi}) = \prod_{i=1}^{d} p(\xi_i)$ ... joint probability density function

Biomedical Applications

Transcranial Electric Stimulation (TES)

The on going activity is modelling of the realistic human head with **three tissues** whose respective conductivities are modelled as random variables.

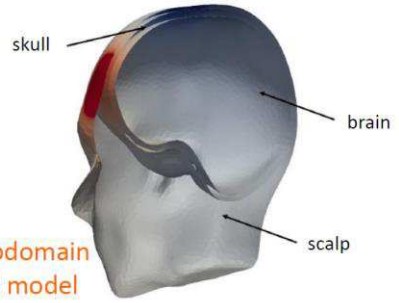

3 subdomain head model

Tissue	Average conductivity (S/m)	Minimum conductivity (S/m)	Maximum conductivity (S/m)
Scalp	0,17	0,09	0,25
Skull	0,32	0,256	0,384
Brain	0,6722	0,0644	1,28

https://itis.swiss/virtual-population/tissue-properties/database/low-frequency-conductivity/

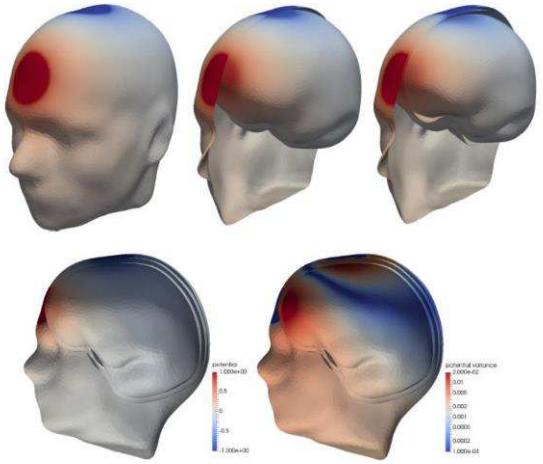

Potential at scalp (left), skull (centre) and brain (right) in a 3-subdomain head model

Left: Mean potential

Right: Potential variance

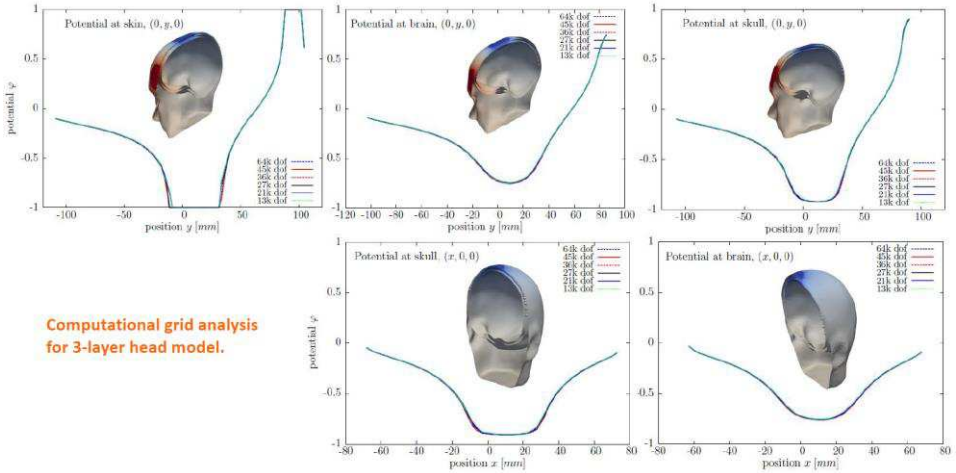

Computational grid analysis for 3-layer head model.

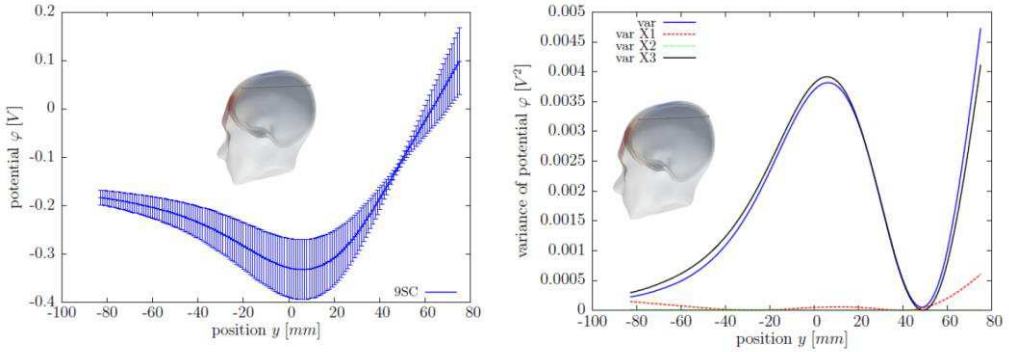

Domain profiles (0mm;y; 90mm) obtained using the 3-subdomain head model

CONCLUSIONS

- Some incident and internal dosimetry procedures for the assessment of human exposure to EM fields have been discussed.
- Different EMI sources and human body models have been addressed.
- Some illustrative results have been presented throughout the course.

Concluding remarks

- The fundamentals of interaction of electromagnetic fields with materials were known by late nineteenth century in the form of Maxwell equations.
- However, the implementation of these basic laws of electromagnetics to living systems is an extremely difficult task due to the tremendously high complexity and multiple organizational levels of biological systems.
- As experiments on humans in the high dose range or for long-term exposures is not possible, irradiation experiments can be performed only on phantoms, tissue probes, and laboratory animals.

Concluding remarks

- Theoretical models are then needed to interpret and confirm an experiment and to offer an extrapolation procedure, and thereby establish proper safety guidelines and corresponding exposure limits for humans.
- The mathematical complexity of the problem has led researchers to investigate simple canonical representations such as plane slabs, cylinders, homogeneous and layered spheres, and prolate spheroids.
- Spherical models are still being used to study the power deposition characteristics of the heads of humans and animals.
- On the other hand, sophisticated numerical modeling is required to successfully predict distribution of internal fields.

Concluding remarks

- Majority of contemporary realistic, anatomically based, computational models comprising of cubical cells mostly use finite-difference time domain (FDTD) method schemes.
- However, though robust, FDTD suffers from stair-casing approximation error. Thus, recently the finite element method (FEM) is used in dosimetry as the method is considered to be more accurate than the FDTD, and a more sophisticated and versatile tool as well, particularly for the treatment of non-homogeneous irregular or curved shape domains.
- Recent research has also demonstrated that the use of the boundary element method (BEM), Method of Moments (MoM), fast multipole techniques, and wavelet techniques can be used to reduce the computational task.

Concluding remarks

- All computational models used in electromagnetic-thermal dosimetry suffer from serious drawbacks pertaining to uncertainties in input data propagated to the response of interest such as SAR, or temperature increase due to HF exposures.
- In the last few years some deterministic models are accompanied with stochastic analysis to partly overcome these difficulties.
- Furthermore, instead of using a robust Monte Carlo Method (MCM), with rather slow convergence rate, the implementation of Stochastic Collocation Method (SCM) has been reported due to its nonintrusive nature and the polynomial representation of the stochastic output, thus significantly reducing the number of simulations.
- The stochastic methods applied to assessment of human exposure to radio-frequency fields is currently a hot topic and subject of an ongoing investigation.

Thank you very much for your kind attention!